

การพัฒนาเทคนิคการถ่ายภาพด้วยรังสีเอกซ์สำหรับคัดกรอง
ของเหลวตามสนามบิน

นางสาวนอร์ฮานี สุไลมาน

จุฬาลงกรณ์มหาวิทยาลัย
CHULALONGKORN UNIVERSITY

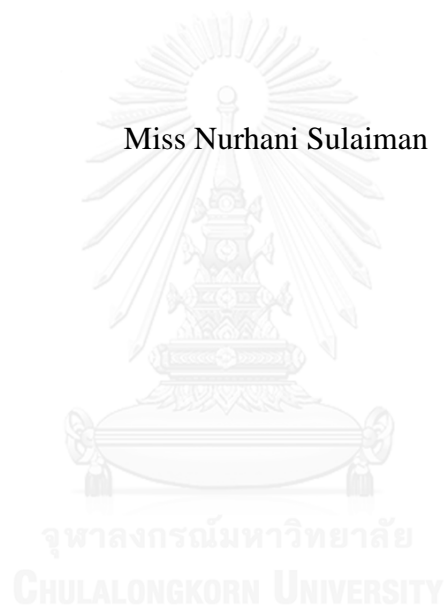
บทคัดย่อและแฟ้มข้อมูลฉบับเต็มของวิทยานิพนธ์ตั้งแต่ปีการศึกษา 2554 ที่ให้บริการในคลังปัญญาจุฬาฯ (CUIR)
เป็นแฟ้มข้อมูลของนิสิตเจ้าของวิทยานิพนธ์ ที่ส่งผ่านทางบัณฑิตวิทยาลัย

The abstract and full text of theses from the academic year 2011 in Chulalongkorn University Intellectual Repository (CUIR)
are the thesis authors' files submitted through the University Graduate School.

วิทยานิพนธ์นี้เป็นส่วนหนึ่งของการศึกษาตามหลักสูตรปริญญา
วิทยาศาสตรมหาบัณฑิต
สาขาวิชานิวเคลียร์เทคโนโลยี ภาควิชาวิศวกรรมนิวเคลียร์
คณะวิศวกรรมศาสตร์ จุฬาลงกรณ์มหาวิทยาลัย
ปีการศึกษา 2558
ลิขสิทธิ์ของจุฬาลงกรณ์มหาวิทยาลัย

Development of X-ray Imaging Technique for Liquid Screening at Airport

Miss Nurhani Sulaiman



A Thesis Submitted in Partial Fulfillment of the Requirements
for the Degree of Master of Science Program in Nuclear Technology
Department of Nuclear Engineering
Faculty of Engineering
Chulalongkorn University
Academic Year 2015
Copyright of Chulalongkorn University

นอร์ฮานี สุไลมาน : การพัฒนาเทคนิคการถ่ายภาพด้วยรังสีเอกซ์สำหรับคัดกรองของเหลวตามสนามบิน (Development of X-ray Imaging Technique for Liquid Screening at Airport) อ.ที่ปรึกษาวิทยานิพนธ์หลัก: สมยศ ศรีสถิตย์, 105 หน้า.

เทคโนโลยีการถ่ายภาพด้วยรังสีเอกซ์ทำให้ทราบได้ว่า ของเหลวที่ตรวจสอบนั้นเป็นสารติดไฟได้หรือไม่ ซึ่งเป็นวัตถุประสงค์ของความมั่นคงปลอดภัย ในการศึกษาวิจัยนี้ได้ประยุกต์ใช้เทคนิคการถ่ายภาพด้วยรังสีเอกซ์ โดยการรับภาพจากแผ่นเรืองรังสีชนิดแกโดลิเนียมออกซีสัลไฟด์ (gadolinium oxysulfide, GOS) ด้วยกล้องถ่ายภาพดิจิทัล ซึ่งควบคุมการเก็บข้อมูลภาพโดยใช้โปรแกรมสำเร็จรูปผ่านสายเคเบิลยูเอสบี (USB cable) ภาพถ่ายรังสีที่ได้จะถูกนำมาวิเคราะห์จากการอ่านข้อมูลระดับสีเทา ด้วยโปรแกรมที่พัฒนาขึ้นจากไมโครซอฟท์วิซวลเบสิก (Microsoft Visual Basic 6) ข้อมูลดังกล่าวได้จากการถ่ายภาพรังสีของตัวอย่างของเหลวที่มีความหนาแน่นระหว่าง 0.7 ถึง 1.4 กรัม/ซม³ บรรจุในขวดพลาสติกบางเส้นผ่านศูนย์กลาง 4.5, 6.0 และ 7.5 ซม และค่าความต่างศักย์ไฟฟ้าตั้งแต่ 70 ถึง 200 kVp ในการตรวจสอบนั้นได้สร้างกราฟเปรียบเทียบจากการเก็บข้อมูลที่ทราบคุณสมบัติครบถ้วนและใช้ของเหลวบางชนิดเพื่อทดสอบความถูกต้อง ดังนั้นระบบที่พัฒนาขึ้นนี้จึงมีความสะดวกรวดเร็วและถูกต้อง เหมาะสำหรับการคัดกรองของเหลวชนิดที่อาจก่อให้เกิดอันตรายและไม่มีอันตรายเพื่อความมั่นคงปลอดภัย



5670579521 : MAJOR NUCLEAR TECHNOLOGY

KEYWORDS: X-RAY IMAGING / SECURITY / LIQUID SCREENING / AIRPORT

NURHANI SULAIMAN: Development of X-ray Imaging Technique for Liquid Screening at Airport. ADVISOR:
ASSOC. PROF. SOMYOT SRISATIT, 105 pp.

X-ray imaging technology is a viable option to recognize flammable liquids for the purposes of aviation security. In this study, an X-ray imaging technology was developed whereby, the image viewing system was built with the use of a digital camera coupled with a gadolinium oxysulfide (GOS) fluorescent screen. The camera was equipped with a software for remote control setting of the camera via a USB cable which allows the images to be captured. The image was analysed to determine the average grey level using a software designed by Microsoft Visual Basic 6.0. The data was obtained for various densities of liquid between 0.7 to 1.4 g/cm³ contained in a thin plastic bottle with diameter of 4.5 cm, 6.0 cm and 7.5 cm for X-ray energies ranging from 70 to 200 kVp. In order to verify the reliability of the constructed calibration data, the system was tested with a few types of unknown liquids. The developed system could be conveniently employed for security screening in order to discriminate between a threat and an innocuous liquid.



Department: Nuclear Engineering

Field of Study: Nuclear Technology

Academic Year: 2015

Student's Signature

Advisor's Signature

ACKNOWLEDGEMENTS

First I would like to thank my thesis advisor, Associate Professor Somyot Srisatit for his continuous consultation and advice academically, along with his support and motivation on fulfilling my thesis research.

I would also like to thank my thesis committee members; Associate Professor Nares Chankow, Dr. Phannee Saengkaew, Assistant Professor Attaporn Pattarasumunt and Dr. Ilham Mukriz for their constructive criticisms and suggestions that really helped me to polish this work. Not forgetting Dr. Khairul Anuar Mohd Salleh, my co-advisor in Malaysia and those who have given assistance and contributed directly or indirectly to my work.

Thanks also to the European Union and all of the professors in the Nuclear Engineering Department of Chulalongkorn University for the support and allowing us to perform this study, without which the present study could not have been completed. It is my utmost gratitude that I thank you all.



CONTENTS

	Page
THAI ABSTRACT	iv
ENGLISH ABSTRACT.....	v
ACKNOWLEDGEMENTS.....	vi
CONTENTS.....	vii
LIST OF TABLES	ix
LIST OF FIGURES	xi
CHAPTER 1	1
1. Introduction	1
1.1.Objective.....	1
1.2.Scope of Study.....	2
1.3.General Procedure	2
1.4.Research Background.....	3
CHAPTER 2	4
2. Literature Review	4
2.1.Security Perspectives.....	4
2.2.Rules and Regulations in the Civil Aviation Sector.....	8
2.3.Liquid Explosives and Flammable Liquids	10
2.3.1. Threat Posed by Liquid Explosives and Flammable Liquids Based on Their Properties	10
2.4.Methods of Detection	14
2.4.1. Vapour and Trace Detection.....	15
2.4.2. Microwave Radars	16
2.4.3. Raman Spectroscopy	16
2.4.4. Neutron Technologies	17
2.4.5. X-ray Method	17
2.5.Theory and Principles.....	18
2.5.1. Generation of X-rays	18
2.5.2. Fundamental Properties of X-rays.....	19

	Page
2.5.3. Basic Principles of X-ray Radiography	20
2.5.4. Fluoroscopy	21
2.5.5. X-ray Methods for Inspection	22
CHAPTER 3	24
3. Research Methodology	24
3.1. Materials and Equipment	24
3.1.1. X-ray Machine	24
3.1.2. Types of Liquid	26
3.1.3. Imaging System	27
3.2. Experimental Approach	29
3.2.1. Sample Preparation	30
3.2.2. Radiographic Exposure	31
3.2.3. Image Acquisition	32
3.2.4. Data Analysis	33
3.3. Methodology for Inspection	34
3.3.1. Calibration	34
3.3.2. Testing the System: Estimation of Percentage of Error	35
3.3.3. In-Situ Inspection	36
3.4. Research Methodology Flowchart	38
CHAPTER 4	39
4. Results	39
4.1. Calibration of the System	39
4.2. Testing the System: Estimation of Percentage Error	58
4.3. In-Situ Inspection	64
4.4. Comparison between LScan2015 and LScanInsitu	65
4.5. Discussions	66
CHAPTER 5	69
5. Conclusion	69
5.1. Discussion	69

	Page
5.2.Recommendations for Future Research.....	72
REFERENCES	73
APPENDICES	80
VITA.....	105



LIST OF TABLES

Table	Caption	Page
2.1	Historical timeline of incidents in the aviation sector	4
2.2	Different types of flammable liquid and their characteristics	12
3.1	Specifications of the Rigaku Radioflex RF200EGM2 X-ray Machine	25
3.2	Densities of different types of liquids for calibration	26
3.3	Specifications of the Kyokko PI-200 Fluorescent Screen	27
3.4	Technical specifications of the Canon EOS 1100D digital camera	28
3.5	Densities of different types of liquids used for testing the system	35
4.1	Greyscale values after correction with water at X-ray energy = 70 kVp	42
4.2	Greyscale values after correction with water at X-ray energy = 80 kVp	43
4.3	Greyscale values after correction with water at X-ray energy = 90 kVp	44
4.4	Greyscale values after correction with water at X-ray energy = 100 kVp	45
4.5	Greyscale values after correction with water at X-ray energy = 110 kVp	46
4.6	Greyscale values after correction with water at X-ray energy = 120 kVp	47
4.7	Greyscale values after correction with water at X-ray energy = 130 kVp	48
4.8	Greyscale values after correction with water at X-ray energy = 140 kVp	49

4.9	Greyscale values after correction with water at X-ray energy = 150 kVp	50
4.10	Greyscale values after correction with water at X-ray energy = 160 kVp	51
4.11	Greyscale values after correction with water at X-ray energy = 170 kVp	52
4.12	Greyscale values after correction with water at X-ray energy = 180 kVp	53
4.13	Greyscale values after correction with water at X-ray energy = 190 kVp	54
4.14	Greyscale values after correction with water at X-ray energy = 200 kVp	55
4.15	Percentage error between the actual density and the density read out for gasohol 95 at thickness 6.0 cm (Given that actual density of gasohol 95 = 0.7479 g/ml)	58
4.16	Percentage error between the actual density and the density read out for ethanol 85 at thickness 6.0 cm (Given that actual density of ethanol 85 = 0.7834 g/ml)	59
4.17	Percentage error between the actual density and the density read out for diesel at thickness 6.0 cm (Given that actual density of diesel = 0.8220 g/ml)	60
4.18	Percentage error between the actual density and the density read out for unknown A at thickness 6.0 cm (Given that actual density of unknown A = 0.7211 g/ml)	61
4.19	Percentage error between the actual density and the density read out for unknown B at thickness 6.0 cm (Given that actual density of unknown B = 0.7409 g/ml)	62
4.20	Percentage error between the actual density and the density read out for unknown C at thickness 6.0 cm (Given that actual density of unknown C = 0.8108 g/ml)	63

4.21	Measurements for several types of liquid at 140 kVp by using LScanInsitu software	64
4.22	Comparison of density read out obtained by “LScan2015” and “LScanInsitu”	66

LIST OF FIGURES

Figure	Caption	Page
2.1	The 3-1-1 Liquids Rule	9
2.2	A simplified X-ray tube with a stationary anode and a heated filament	19
2.3	The electromagnetic spectrum	19
2.4	Schematic diagram showing principles of radiography	21
3.1	X-ray generator of the Rigaku Radioflex RF200EGM2 X-ray Machine	25
3.2	Control panel of the Rigaku Radioflex RF200EGM2 X-ray Machine	25
3.3	Kyokko PI-200 Fluorescent Screen	27
3.4	Canon EOS 1100D digital camera	28
3.5	Principle design of the X-ray imaging system	30
3.6	Example of measuring the density of liquid by using an electronic analytical balance	31
3.7	Position of the sample during radiographic exposure	31
3.8	Radiographic exposure setup	32
3.9	Image acquisition process	33
3.10	Designing software for data analysis	33
3.11	Software designed for data calibration (LScan2015)	34
3.12	Software designed for in-situ inspection (LScanInsitu)	36
3.13	Research methodology flowchart	38

4.1	Example of images acquired for 4.5 cm thickness of water at X-ray energies ranging from 70 kVp to 200 kVp	39
4.2	Example of images acquired for 6.0 cm thickness of water at X-ray energies ranging from 70 kVp to 200 kVp	40
4.3	Example of images acquired for 7.5 cm thickness of water at X-ray energies ranging from 70 kVp to 200 kVp	41
4.4	Graph of greyscales versus density of liquid at X-ray energy = 70 kVp	42
4.5	Graph of greyscales versus density of liquid at X-ray energy = 80 kVp	43
4.6	Graph of greyscales versus density of liquid at X-ray energy = 90 kVp	44
4.7	Graph of greyscales versus density of liquid at X-ray energy = 100 kVp	45
4.8	Graph of greyscales versus density of liquid at X-ray energy = 110 kVp	46
4.9	Graph of greyscales versus density of liquid at X-ray energy = 120 kVp	47
4.10	Graph of greyscales versus density of liquid at X-ray energy = 130 kVp	48
4.11	Graph of greyscales versus density of liquid at X-ray energy = 140 kVp	49
4.12	Graph of greyscales versus density of liquid at X-ray energy = 150 kVp	50
4.13	Graph of greyscales versus density of liquid at X-ray energy = 160 kVp	51
4.14	Graph of greyscales versus density of liquid at X-ray energy = 170 kVp	52

4.15	Graph of greyscales versus density of liquid at X-ray energy = 180 kVp	53
4.16	Graph of greyscales versus density of liquid at X-ray energy = 190 kVp	54
4.17	Graph of greyscales versus density of liquid at X-ray energy = 200 kVp	55
4.18	Graph of greyscale versus X-ray energy for liquid thickness = 4.5 cm	56
4.19	Graph of greyscale versus X-ray energy for liquid thickness = 6.0 cm	56
4.20	Graph of greyscale versus X-ray energy for liquid thickness = 7.5 cm	57



CHAPTER 1

INTRODUCTION

1. Introduction

The 2006 transatlantic aircraft plot in a large extent has dragged attention to the threat of liquid home-made explosive (HME). Since its inception, the civil aviation sector subsequently declared the new regulations on carry-on prohibitions followed by limited amount of liquids in personal carry-on luggage (Wells and Bradley, 2012).

Decisions have been made by the EU to lift this banned in the future, but this had to be accompanied by the development of a mass-screening technology to detect explosives in fluids. This is to ensure that the security can be maintained whilst reducing the restrictive security burdens upon passengers (Wells and Bradley, 2012).

The aim of this study is to develop a simple but reliable system based on X-ray imaging technique for liquid screening at airport in order to discriminate between a threat and an innocuous liquid. In this case, the main characteristics to be evaluated is the densities of liquid.

1.1. Objective

To study and develop the X-ray imaging technique for liquid screening at airport by using digital camera

1.2. Scope of Study

- The use of Canon DSLR Camera EOS 1100D coupled with GOS fluorescent screen for image viewing system
- X-ray energy ranges from 70 kVp to 200 kVp
- Measuring greyscale from X-ray images acquired for different types of liquid and different thickness of liquids in bottles (4 – 8 cm)
- Constructing a calibration curve of greyscale versus types of liquid for various kVp
- Designing a software to measure the average grey level of the image by using Microsoft Visual Basic 6.0
- Verifying the constructed calibration curve by testing with an unknown liquid

1.3. General Procedure

- I) Research outlook and literature review
- II) Understanding of topics, objective, and scope of study
- III) Understanding methodology
- IV) Proposal presentation
- V) Collect information and specifications of the detection systems and samples under study
- VI) Experimental setup / radiographic exposure
- VII) Designing software for data analysis
- VIII) Data analysis and discussions
- IX) Thesis writing

1.4. Research Background

The perception of identifying liquid explosives and flammable liquids are seen by using X-ray technology as it is inexpensive, fast response and have acceptable false/positive alarm rates, as well as it offers safe and continuous security response.

Major challenges for the inspection of liquid is due to the fact that most of them have comparable densities like typical normal organic and benign products. Turecek (2008) inferred that a wide scope of physical characteristics of unarmful liquids brought by passengers on board the plane will necessarily lead to the fact that some physical characteristics of these unarmful liquids will be identical with some explosives and flammable liquids. Moreover, the concealments complicates the detection situation considerably since there are many existing types of bottles for containment.

One of the limitations (Singh and Singh, 2003) of using X-ray method is that the real density of the objects are poorly known in real inspections and the system only generates an estimation of atomic number, i.e. effective atomic number.

The variation in densities often depends sensitively on the manufacturing routes in which terrorists seems to be well aware on how the X-ray screening system works. By far, it is possible that they would probably be seeking to tailor their technology so that their device would become undetectable (Wells and Bradley, 2012).

However, the possible demands that has been given emphasis by De Ruiter and Lemmens (2008), for the time being are would be able to detect liquid explosives or flammable liquids inside the plastic bags which is presented to security separately and to detect the presence of liquids which are not necessarily explosives or flammable liquids in 100 ml and more containers in carry-on luggage.

CHAPTER 2

LITERATURE REVIEW

2. Literature Review

2.1. Security Perspectives

The timeline of historical incidents in the aviation sector as shown in Table 2.1 indicate that security has adapted to threats as they ascend.

Table 2.1 Historical timeline of incidents in the aviation sector

Year	Incident
1930	<p>First recorded hijacking of the Pan Am mail plane by the Peruvian activists (Wells and Bradley, 2012; ECORYS, 2009)</p> <ul style="list-style-type: none"> • Screening passengers and baggage with purposes: <ol style="list-style-type: none"> i) Illegal movement of goods or prohibited items (local legislative requirements) ii) Fraud and revenue avoidance; and in ever-increasing importance iii) Terrorist threat

Table 2.1 Historical timeline of incidents in the aviation sector (continue)

1970s	<p>i) March 1972 (TSA, 2005)</p> <ul style="list-style-type: none"> • The discovery of a bomb on board an aircraft bound for Los Angeles. The explosive was found by a bomb-sniffing dog 12 minutes before it is set to detonate. • The Federal Aviation Administration (FAA) Explosives Detection Canine Team Program was created. <p>ii) December 1972 – 1973 (TSA, 2005)</p> <ul style="list-style-type: none"> • An emergency rule was issued by the FAA, making inspections of carry-on baggage and scanning of all passengers by airlines mandatory.
1980s – early 1990s	<p>Lockerbie Bombing (TSA, 2005; Rumerman, n.d.)</p> <ul style="list-style-type: none"> • A bomb destroys Pan Am Flight 103 over Lockerbie. The bomb was found concealed in a radio cassette player. • Security measures go into effect for the U.S. carriers at European and Middle East airports which requires all checked baggage to be X-ray or searched and matched to the passengers.
December, 1994 – January, 1995	<p>Operation Bojinka (Markey, 2009)</p> <ul style="list-style-type: none"> • Liquid nitroglycerin-based bombs to be smuggled on board the airlines in innocuous appearing components: a contact lens solution bottle, a Casio watch, and a detonator hidden in the heel of a shoe. • Planned to detonate the bomb on a Philippines Airlines to test the validity of the system. However, the plotters encountered failure while mixing a batch of explosives

Table 2.1 Historical timeline of incidents in the aviation sector (continue)

	<p>which exploded at their apartment and drew the attention of the Philippines authorities. Plotters were later apprehended and brought to the United States to stand trial.</p> <ul style="list-style-type: none"> • The sensitivity of security services was heightened to liquid explosives, but eventually decreases as other tactics emerged.
<p>September 11, 2001</p>	<p>The Attacks on the World Trade Center towers in New York City and the Pentagon (TSA, 2005; Singh and Singh, 2003)</p> <ul style="list-style-type: none"> • Two planes were flown into the World Trade Center buildings; one crashed into the side of the Pentagon in Washington, DC; and the fourth plane crashed into a field in Stony Creek Township, Pennsylvania. • The Transportation Security Administration (TSA) was created to oversee security in all modes of travel. Accordingly, the Aviation and Transportation Security Act (ATSA) was signed into law, which allows the federal government direct responsibility for airport screening. Of most concern is detecting explosives in both checked and carry-on baggage.
<p>December 22, 2001</p>	<p>The Shoe Bomber (TSA, 2005)</p> <ul style="list-style-type: none"> • Richard Reid attempts to detonate an explosive using triacetone triperoxide (TATP) as the initiator on a flight from Paris to Miami, but was unsuccessful. • Implementation of the shoe screening policy by the TSA.

Table 2.1 Historical timeline of incidents in the aviation sector (continue)

August, 2006	<p>Transatlantic Aircraft Plot (Schubert & Kuznetsov, 2008; Casale, 2009)</p> <ul style="list-style-type: none"> • More than 20 men were arrested in an attempt to blow up aircrafts flying from the United Kingdom to the United States with the use of homemade liquid explosives (i.e. peroxide-based liquid explosives) hidden in carry-on luggage. The thwarted operation were discovered and foiled by the British officials on a raid after finding suspicious activities. • The “3-1-1 Liquids Rule” was introduced by the TSA. Afterwards on November 6th, 2006, the EU adopted new measures that restrict the size of hand luggage and the amount of liquid that can be taken through security checkpoints.
-------------------------	--------------------------------------------------------------------------------------------------------------------------------------------------------------------------------------------------------------------------------------------------------------------------------------------------------------------------------------------------------------------------------------------------------------------------------------------------------------------------------------------------------------------------------------------------------------------------------------------------------------------------------------------------------------------------------------------------------------------------------------------------------------

The invention of liquid explosives goes back to the middle 19th century, however, explosives made of nitrogen tetroxide and combustible liquids, such as carbon disulphide, nitrobenzene, nitrotoluene, benzene, gasoline, kerosene, halogenated hydrocarbons, were studied for weapon use as early as the 1880s (Oxley, 2008). Some of the early responses were shown above in Table 2.1.

Attempted air terrorist plot in the Great Britain, August 2006 has firmly placed the adverse effects of liquid explosives and flammable liquids centre-stage. However, it is important to note that liquid explosives and flammable liquids are not considered as a new threat, but the new threat are seen in for the attention of terrorists to use these materials (Mostak, 2008).

The potential risks has led to several countermeasures in the civil aviation security which include the carry-on controls in personal hand-held luggage to specific amount of any liquids by passengers into the cabin of civil planes (Wells and Bradley, 2012).

2.2. Rules and Regulations in the Civil Aviation Sector

The purposes of aviation security are based on the principles stated by Singh and Singh (2003) with attention to reasonable effort should be made to deny terrorists access to civil aviation facilities, together with establishing a system of detection devices and procedures that will prevent further penetration into the facilities.

After recently uncovered the terrorist plots, the security activity in the civil aviation sector has now focused on identification of illicitly-transported explosives as the main threat. The security for civil aviation shifted to the importance of identification and detection efficiency of explosives frequently manifest as homemade explosives (HME) in hand or checked luggage which may be easily confused with benign everyday items of luggage (ECORYS, 2009).

Drawing on lessons learnt from the terrorist's action, on September 2006, the USA responded with an intensive civil plane cabin restrictions concerning liquids carried into the cabin luggage of passengers as formulated in the 3-1-1 Liquids Rule by the TSA.

The 3-1-1 Liquids Rule implied that a passenger is allowed to bring liquids, gels, aerosols, creams and pastes of 3.4 ounces (100 ml) or less in a container placed inside a 1 quart-sized, clear, plastic, zip-top bag, such that each passenger is limited to bring only one bag per passenger (TSA, 2014).

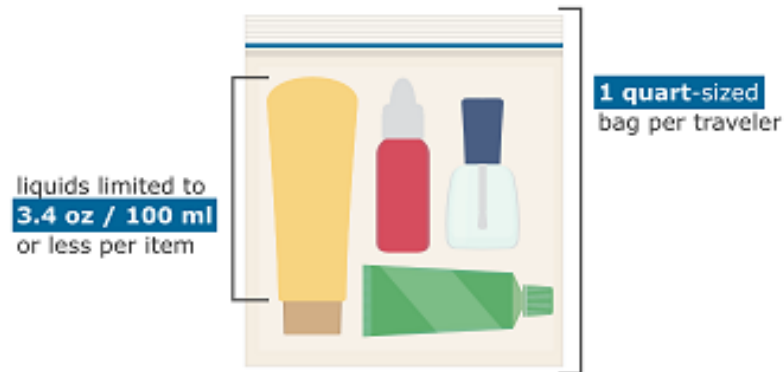


Figure 2.1 The 3-1-1 Liquids Rule (TSA, n.d.)

Two months later, on November 6th, 2006, the European Union introduced the aviation security community with a more stringent regulations on liquids being carried on board in hand luggage. Similar to the 3-1-1 Liquids Rule, the new EU regulation deduced that passengers are permitted to carry liquid, gels and aerosols in individual containers not exceeding 100 ml and all of them are contained in one transparent 1 litre resealable plastic bag. With that in mind, the passenger must present this bag separately at the security checkpoint and only one plastic bag per person is allowed (Condor, n.d.).

Exemptions from the restriction includes for essential liquids such as baby food, medicines and passengers with special dietary requirements for medical needs. Liquids purchased at the airport duty and tax free shops situated behind the passport control are also not restricted to these regulations, being that the liquids are packed in sealed and tamper-free transparent bags (De Ruiter and Lemmens, 2008).

As inferred by Wells and Bradley (2012), the EU hoped to lift this banned in the future, but this had to be accompanied with a mass-screening technology to detect explosives in fluids.

Demands on screening technology are seen in three major approaches which may be applied to avoid liquid explosives or flammable liquids being smuggled into the cabin of an aircraft. One of the approaches is to be able to detect liquid explosives inside a carry-on baggage at operational speed. This is not yet possible with current

technology. However the second best option would be able to detect liquid explosives inside the plastic bag which is presented to security separately, as it is now. Another option would be to detect the presence of liquids (not necessarily explosives) in 100 ml and more containers in the carry-on baggage (De Ruiter and Lemmens, 2008).

2.3. Liquid Explosives and Flammable Liquids

Generally, liquid explosives are non-comparable to solid explosives. Menning and Östmark (2008) defined liquid explosive as an explosive which is in liquid state at ambient temperature (room temperature, surrounding temperature, outdoor temperature etc.).

Liquid explosives can be classified into a broad range depending on their chemical composition and physical state. They can differ in consistency, starting from clear liquids, to suspensions and emulsions and finally, pasty, semi-solid systems. Another logical way to classify these explosives is based on their origin, which are reasonable for the characterisation of these products (Mostak, 2008).

2.3.1. Threat Posed by Liquid Explosives and Flammable Liquids Based on Their Properties

Nevertheless of their classification, such types have large advantages for terrorist action as it can be acquired easily from commercial products and the simplicity of synthesizing different components together for specific application (Schubert, 2008).

Despite for its easy supply, the necessity to transport, store or handle these types of explosives is important and requires proper confinement in relative to their high sensitivity against shock and coarse handling. Shock sensitivity happens when

“hotspots” is created due to possible act of adiabatic compression of an air in the liquid material (Schubert, 2008).

Apart from that, liquid or solid explosive mixture often contains flammable materials, such as fuels or solvents, of which some of these flammable liquids can also be used as components of other hazardous liquids such as peroxides (e.g. acetone) and multi-component liquid explosives (e.g. nitrobenzol) (Kuznetsov and Osetrov, 2008).

A huge number of different flammable liquids are broadly used for daily purposes. Examples are, petrol, diesel, kerosene, alcohols, ethyl acetate, acetone and other ketones, alkanes etc. (Menning and Östmark, 2008). September 11th has shown that flammable liquids reacting in air can caused catastrophic destruction. In military applications, these combinations are called “Fuel-Air-Explosives” (Schubert, 2008).

As a matter of fact, flammable fuels are usually composed of different fractions of carbon hydrates without any functional group (Schubert, 2008). These fuels when brought into a fine distribution in air, either in open atmosphere or in confined spaces, may form a stratified fuel-air mixture. This phenomena can propagate detonation with the presence of an ignition source or may become as a source of fire and environmental hazards itself (Bunama and Karim, 2000).

For a fuel to react with oxygen in the surrounding air, it must have low ignition temperature and a high vapour pressure. It is important to realize that a fire in a cabin of an airplane is very dangerous, because the fire consume oxygen, which is limited and produce heat and poisonous carbonoxyd and carbondioxyd (Schubert, 2008).

Such characteristic is related to the term “flash point” (of volatile material), that is the lowest temperature for vaporization to form an ignitable mixture in air, with the presence of an external ignition source. There are two main types of liquid flash points namely flammable and combustible, that is flash points of less than 60.5°C and above 60.5°C respectively (Ministry of the Solicitor General, 2001). Characteristics of some flammable liquids are listed in Table 2.2.

Table 2.2 Different types of flammable liquid and their characteristics

Item	Chemical formula	Density (g/cm³)	Z_{eff}	Vapour concentration (ppm)	Flash point (°C)
Gasoline	C ₇ H ₁₆	0.76	5.375		< -40
Alcohol	C ₂ H ₅ OH	0.78	6.043	130,000 ppm (40°C)	12.8
Acetone	C ₃ H ₆ O	0.79	6.034	234,000 ppm (35°C)	< -19

SOURCE: Adapted from “Overview of Liquid Explosives’ Detection,” by A. V. Kuznetsov and O.I. Osetrov, 2008.

Some types have low ignition temperature (200-250°C) making them easily inflammable, needless of the traditional detonator or fuse (Kuznetsov and Osetrov, 2008). Ignition temperature differs from flash point since the ignition source is unnecessary. Unlike flash point, ignition point is basically described as the lowest temperature at which volatile material will be vaporized to enkindle flames without the help of any ignition source (PETRO Industry News, 2014). For that, ignition temperature is usually higher than the flash point.

Liquid explosives differs from solid in terms of homogeneity, unless bubbles or other inhomogeneity are somehow introduced. These cavities makes it become easier for it to initiate (Oxley, 2008). Such properties proves that liquid explosives may or may not be initiated by using a detonator or an ignition source.

Therefore it can be concluded that the starting of liquid explosive combustion can be either through spontaneous ignition or forced ignition. Whereby, spontaneous ignition is produced through the self-acceleration of chemical reactions of liquids, meanwhile forced ignition is reached by external heat source at high temperature, in which forced ignition is common in the application of liquid explosives (Liu, 2015).

As mentioned earlier, liquid explosives must be confined properly. This is because they have higher vapour pressure than that of solid explosives, therefore it can only be used in closed containers (Mostak, 2008). Naturally they are closer to the gaseous state, hence they are expected to have a strong vapour signature (Oxley, 2008). They are noncompressible and have fixed density (Liu, 2015).

Knowledge on their chemical and physical properties are essential to increase the probability of detecting explosive compounds. Physical properties are divided into two categories, extensive properties and intensive properties, which can be measured without changing the identity of the sample. Extensive properties are dependent on the size of the sample which include mass, volume, and heat. On the other hand, intensive properties are dependent on the material and not the size of the sample that is density, boiling point and solubility which can be used to identify an unknown volatile liquid (Thomas M. Moffett Jr., 2009).

Basically, density is the ratio of two extensive properties, expressed as the ratio of an object's mass to its volume as stated in Equation 2.1 below (Thomas M. Moffett Jr., 2009):

$$d = \frac{\text{mass, } m}{\text{volume, } v} \quad (\text{Equation 2.1})$$

Density properties can be utilized to differentiate between solid and liquid compounds which makes X-ray based detection methods possible. Density is also crucial in determining other properties of explosive, such as performance, detonability, ignitability etc. (Menning and Östmark, 2008).

According to Kuznetsov and Osetrov (2008), the characteristics of liquid explosives are generally:

- Many liquid explosives have low density (about 1 g/cm³).
- High volatility and high level of evaporation.
- High viscosity (similar to that of oil).
- Some have low stability, and cannot be kept for a long period of time.
- Some can be made at a home lab out of available materials,
- Some can easily be set on fire with a lighter, their burning may turn into detonation.
- Have $Z_{\text{eff}} = 6.5 - 7.5$, same as common organic materials.

Oxley (2008) inferred that it is also important to investigate; what concentration is hazardous and what amount is at security risk. In order to address the problem correctly, it is utmost importance to understand the basic physical and chemical properties of the species to be detected itself i.e. liquid explosives and flammable liquids. Of course, this would give a vital input for research and development for setting the specifications of the screening systems so that the detection probability of explosives in fluids can be increased.

2.4. Methods of Detection

Development of new ways for perpetrators to use liquid explosives and flammable liquids is widening apart of challenges in detecting these materials before posing as a threat to civilians or other personnel. This often depends on availability and terrorist know-how to tailor their method prior to detection (i.e. undetectable) in which they might be well aware on how the system works. Additionally, methods to disguise such material becomes challenging as the technology become smarter at detecting these materials (Singh and Singh, 2003).

In principle, all detection methods can be used since liquid explosives are non-comparable to solid explosives. Unlike solid explosives, liquid-based explosives may not have the traditional fuse and detonator to initiate, which must be in general produced by specialists. Thus, this makes their detection more complicated (Kuznetsov and Osetrov, 2008).

Consequently, a comprehensive method is required to minimize the danger of misusing these liquids for terrorists' attacks. The different detection methods are for instance by vapour and trace detection, microwave radars, Raman spectroscopy, neutron methods, and X-ray screening technology.

2.4.1. Vapour and Trace Detection

Vapour and trace detection methods is based on chemical analysis of small amounts of their vapour in an atmosphere to detect vapour and traces of target samples, since most of the liquid explosives have high vapour pressure. These methods can be implemented by biosensors, ion mobility spectroscopy, gas chromatography, mass-spectrometry etc. (Singh and Singh, 2003).

One of the advantages of vapour and trace detection method is it can detect a wide range of commercially-produced explosives. It is well-known for its high selectivity to highly volatile liquid explosives (Kuznetsov and Osetrov, 2008). Moreover, this method is capable of detecting very small amount of explosives, even for less than a microgram (Singh and Singh, 2003).

However, limitation concerns of this method is that it is incapable to localize the source and determine the mass of explosives. In addition, this method have a high false alarm rate since vapours from common materials can also trigger alarm (Kuznetsov and Osetrov, 2008).

Also, liquid explosives and flammable liquids can only be filled in tight containers. For this reason, the efficiency of using vapour detection is low and often not very effective (Mostak, 2008), thus this method can only be used for detection on partially enclosed explosives (or a fully enclosed, encapsulated in a gas permeable casing) (Menning and Ostmark, 2008).

2.4.2. Microwave Radars

The second detection method to be discussed is microwave radars as offered by *UNI Dai-Ichi Shoji Co. Ltd.* This type of detection method is based on microwave bombardment of an unknown liquid material (contained in a plastic bottle) and the evaluation of specific changes in the wavelengths of reflected microwaves, caused by dielectric constant or electric conductivity of the liquid tested. This detector allows safe, water-based drinking liquids (e.g. mineral water, coffee etc.) to be distinguished from dangerous, flammable or explosive liquids even if only a small amount is present. However, this method is not applicable to detect liquids in other types of containers, specifically metal types as microwaves cannot penetrate through it (Stancl and Kynel, 2008).

2.4.3. Raman Spectroscopy

The next possible method used for detection of liquid explosives as suggested by Bunte et al. (2008) is Raman spectroscopy. Raman spectroscopy is widely used to analyse organic reactions in water since water does not interact with Raman light. The energy scattered displays frequency changes corresponding with the frequency of vibration of atoms in the samples. Frequency shifts probes by Raman spectroscopy indicates chemical composition, which is compared with a reference database of threat and innocuous substances (Johansson et al., 2008).

One major drawback of this technique is that laser beam are unable to penetrate opaque materials, i.e. if the fluid is contained in e.g. ceramic or metallic containers (Stancl and Kynel, 2008), therefore luminescence of bottles and liquids may interfere with the measurements. Apart from that, the need of intensive external laser source used also can endanger human sight (Bunte et al., 2008).

2.4.4. Neutron Technologies

Another type of detection method is by utilizing the potentialities of neutron technologies. In recent times, Associated Particles Techniques (APT)/Nanosecond Neutron Analysis (NNA) is the most advanced among all neutron-based methods. It operates with a tagged neutron flux at energy 14 MeV irradiated to an object under inspection. Secondary radiation is detected when neutrons interact with the nuclei of the object's material. This method allows the recognition of carbon, oxygen, nitrogen, aluminium, sulphur and many other elements, thus reconstructing the chemical formula of material of the object. APT/NNA have the ability to detect partial densities related to carbon, oxygen or nitrogen in different nitrogen-containing materials. Such necessity however is unable to distinguish between neutron from explosives or neutron background from innocent material (Kuznetsov and Osetrov, 2008).

2.4.5. X-ray Method

One of the detection methods to consider having the greatest potential is the use of X-ray which is widely used for detection of explosives. With X-ray method, images of the inspected object is obtained, thus providing information on its density and effective charge. Since X-ray is deployed as an image-based screening device, continuous security responses is accomplished, such that matching ratio can be achieved between the screened items and images of the threat item (Feng and Sahin, 2009).

Very often the liquid explosives and flammable liquids are accompanied with an ignition system that can be as simple as a candle or may be a system hidden in any type of electronic items assembled with an electronic wire (or a detonation tube etc.). In this case, it is significant to use imaging technologies for detection since it can be a marker for the screening operators (Turecek, 2008).

2.5. Theory and Principles

2.5.1. Generation of X-rays

X-rays are usually produced by heating a metal filament (cathode) which then emits electrons that are accelerated towards the target (anode) by a large applied electrical potential between the filament and the target. This rapid deceleration of electrons causes a variety of events including the emission of X-ray radiation, photoelectrons, Auger electrons, and a large amount of heat (Jezeirski, n.d.). In very low voltage tubes, 0.1% of the energy of the electron beam is converted into X-rays. At 100 kV, the X-ray generation efficiency increases to about 1% (IAEA, 1992).

X-rays emitted have different wavelengths and different penetrating powers according to the accelerating voltage. Basically, the following conditions must be met to produce X-rays (Halmshaw, 1982):

- i) A stream of electrons produced and sustained, i.e. a good vacuum, with a source of electrons, which in modern X-ray tubes is a heated filament.
- ii) A means of accelerating the electrons to a high velocity, i.e. a means of producing and applying a high potential difference.
- iii) A 'target' for the electrons to strike; this must also be in the vacuum, aligned with the electron beam, and is therefore an intrinsic part of the X-ray tube.

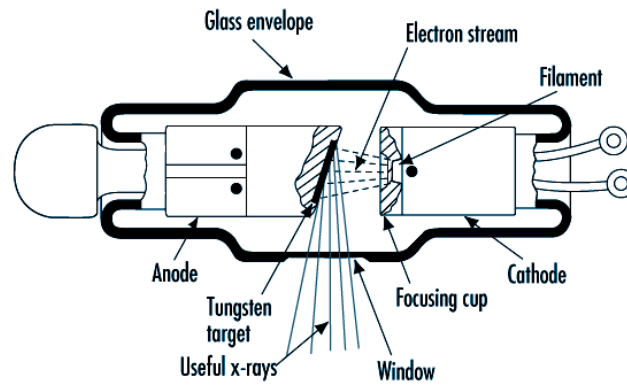


Figure 2.2 A simplified X-ray tube with a stationary anode and a heated filament
(Robert N. Cherry, n.d.)

2.5.2. Fundamental Properties of X-rays

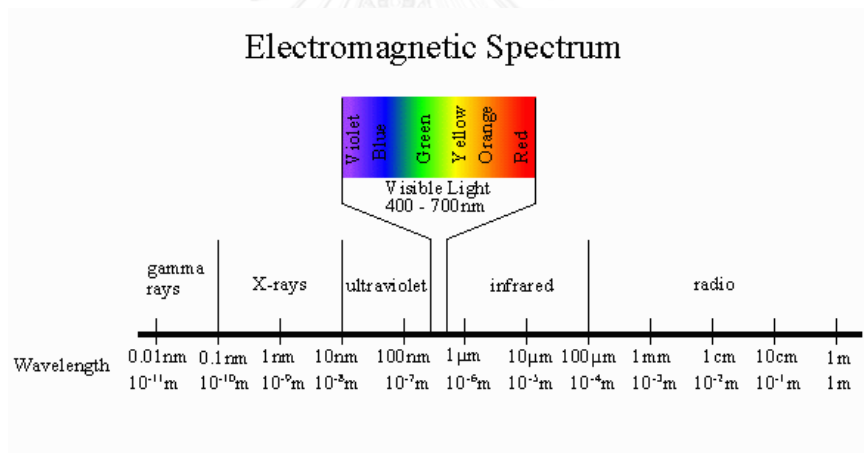


Figure 2.3 The electromagnetic spectrum (NOAA, n.d.)

X-rays are classified as electromagnetic radiation with wavelengths ranging from $10 - 10^{-3}$ nm. The essential difference between X-rays and ultra-violet, light, infrared, radio waves, and gamma rays are seen in terms of wavelength and energy (Waseda et al., 2011).

X-rays travel at the speed of light, c ($\approx 2.998 \times 10^8$ m/s), in straight lines, and are invisible. Being that they are electromagnetic waves, X-rays can also be reflected, refracted, and diffracted (IAEA, 1992).

According to the quantum theory, as proposed by Planck, the electromagnetic wave can be treated as small “packets” called photons or light quanta. Each photon has an energy, E , given by:

$$E = h\nu = \frac{hc}{\lambda} \quad (\text{Equation 2.2})$$

where, h is Planck’s constant (6.6260×10^{-34} J.s) and ν is the frequency of the radiation (Halmshaw, 1982).

X-rays can penetrate matter which is opaque to light and they have a photographic action very similar to light. They pass through material of low density more readily than through high density material, and this property depends on their wavelength (Halmshaw, 1982).

2.5.3. Basic Principles of X-ray Radiography

Radiography is a non-destructive testing method which uses penetrating radiation (X-ray, gamma, or neutron) passing through a specimen to produce a photographic record. In radiography, the object is placed in between the penetrating radiation source and a recording medium (e.g. film). In passing through the specimen, a proportion of the radiation is absorbed as a function of thickness (Halmshaw, 1982).

The density of the recorded radiation intensity varies with the amount of radiation reaching the film. Thicker and denser materials will absorb more radiation, so that more radiation will be penetrated for thinner and less dense area (Halmshaw, 1982).

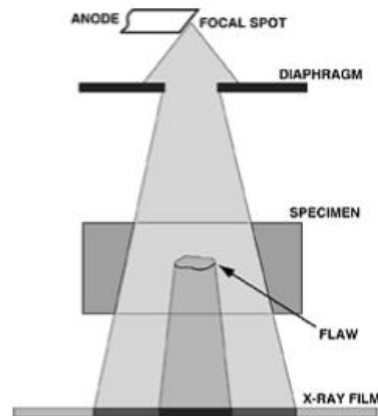


Figure 2.4 Schematic diagram showing principles of radiography (KODAK, 1980)

Instead of recording the variations of intensity of the transmitted radiation on films, another way of recording or displaying this is by letting the rays fall on to a fluorescent screen of a material which converts X-rays into visible light, this is called fluoroscopy (Halmshaw, 1982).

2.5.4. Fluoroscopy

Fluoroscopy is a real-time imaging radiography in which an image is produced electronically rather than the conventional film technique. In fluoroscopy, X-ray transmitted through the specimen falls on to a screen which fluoresces or that emits light within the visible part of the spectrum (Simona Babeti (Pretorian) et al., 2011).

Screens have been made of materials such as gadolinium oxysulfide doped with terbium, $Gd_2O_2S:Tb$ or so called "GOS". With the availability of rare earth materials in high states of purity and at reasonable costs, one can now design new phosphors with improved X-ray absorptions, greater density and higher X-ray to light conversion efficiencies (Link et al., 1989).

After radiation is converted to visible light, the light image is changed to a video signal so that an image can be produced for viewing on a monitor. The imaged form is a “positive image” since brighter areas on the image indicate where higher levels of transmitted radiation reached the screen that is the opposite for film radiography which produced a negative image (Prosch and Larson, 2000).

The X-ray generator is the common source of radiation in this system, being that the image intensifiers are relatively inefficient at converting radiation to light, thus more flux is required than an isotope can offer (Prosch and Larson, 2000).

2.5.5. X-ray Methods for Inspection

In spite of the abundance development of technology available nowadays, X-ray imaging technique offers several advantages over other techniques. The most eminent property of X-rays is their penetrability, which means radiation that penetrate the material undergoes an attenuation. The attenuation at any location in the transmission image is the total X-ray interactive cross-section; the sum of the photoelectric and scattering cross-section (Singh and Singh, 2003). While X-rays pass through some material, they loss some intensity. This phenomenon is called absorption of X-rays in matter (IAEA, 1992).

X-ray technology for inspection of bulky items is proclaimed by its penetrating behaviour and the capability of discriminating materials by energetic X-rays. It is related to the fact that X (and gamma rays) interact weakly with matter via the electromagnetic force, the linear energy transfer (LET) which is associated limited energy loss per unit path length, expressed in $\text{keV } \mu\text{m}^{-1}$. The four principal mechanisms reduces the X-ray flux of a confined beam of photons that traverse through a given medium forming the conventional transmission image (Wells and Bradley, 2012).

The amount of radiation lost depends on the quality of radiation, material/density of the material and the thickness traversed (IAEA, 1992). X-rays which enters a matter are scattered by electrons around the nucleus of atoms in the matter. As the beam passes through a homogenous thickness of matter, the intensity of X-rays or gamma rays is reduced, a proportion of the radiation energy beam is absorbed exponentially, i.e. as the thickness increased, the transmitted intensity decreases (Halmshaw, 1982). A monoenergetic incident beam of X-rays obeys the Beer Lambert law,

$$I = I_o \exp(-\mu t) \quad (\text{Equation 2.3})$$

where,

I = intensity transmitted through a medium, I_o = incident photon intensity, μ = linear attenuation coefficient of medium, and t = medium thickness.

Meanwhile, in terms of mass attenuation coefficient, μ_m gives:

$$I = I_o \exp(-\mu_m \rho t) \quad (\text{Equation 2.4})$$

where,

$$\mu_m = \frac{\mu}{\rho} \quad (\text{Equation 2.5})$$

such that, ρ is the physical density of such material (Wells and Bradley, 2012).

Principles of X-ray transmission (De Ruiter and Lemmens, 2008) to an extent can be applied to detect liquids in hand-held luggage as they are well known for explosives detection in hold-baggage. In this case, the main characteristics to be evaluated are density (and possibly Z_{eff} value) calculated from absorption spectra.

CHAPTER 3

RESEARCH METHODOLOGY

3. Research Methodology

3.1. Materials and Equipment

The materials and equipment consisted the following parts:

- Rigaku Radioflex RF-200EGM2 X-ray Machine
 - Type: 200 kV Microcomputerized Directional Industrial X-ray System
- 35 × 35 × 60 cm light-tight box
- 30 × 30 cm Kyokko FS PI-200 Fluorescent Screen
- Reflective mirror
- Canon EOS 1100D DSLR camera
- Lead block
- 3 mm thick lead sheets
- Various types of liquid of different densities
- Thin plastic bottles of thickness ranging from 4.0 – 8.0 cm

3.1.1. X-ray Machine

In this study, the Rigaku Radioflex RF-200EGM2 X-ray Machine as shown in Figure 3.1 and Figure 3.2 acts as a generator to produce radiation source for exposure of test samples. The details and specifications of the X-ray machine is summarized in Table 3.1.

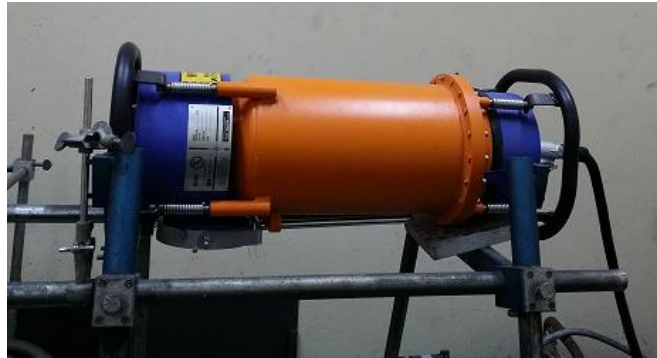


Figure 3.1 X-ray generator of the Rigaku Radioflex RF200EGM2 X-ray Machine



Figure 3.2 Control panel of the Rigaku Radioflex RF200EGM2 X-ray Machine

Table 3.1 Specifications of the Rigaku Radioflex RF200EGM2 X-ray Machine

Characteristics	Description
Tube voltage	70 kV ~ 200 kV in steps of 2 kV
Tube current	STD mode 5 mA (at 90 kV or more) LOW mode ~ 4 mA (at 90 kV or more)
Duty cycle	Intermittent continuous (1.1 Max. 6 min at 25°C)
X-ray tube	Ceramic; Focal spot size (nominal) 2.0 × 2.0 mm

Table 3.1 Specifications of the Rigaku Radioflex RF200EGM2 X-ray Machine
(continue)

Inherent filter	Aluminium 2 mm + Beryllium 1 mm
Dimensions	Generator: 262 (W) × 262 (D) × 617 (H) mm Controller: 360 (W) × 340 (D) × 208 (H) mm
Weight (kg)	Generator: 21.0 Controller: 16.5
Power supply	Single phase AC 190 V – 240V (50/60 Hz)
Power consumption (kVA)	STD mode: 3.1 Low mode: 2.4
Generator insulator	SF ₆ insulation gas
Generator cooling	Anode earth, forced air cooling by radiator

SOURCE: (Rigaku Corporation, 2014: online)

3.1.2. Types of Liquid

Different types of liquid of different densities as shown in Table 3.2 were used to construct the calibration data of the system.

Table 3.2 Densities of different types of liquids for calibration

Type of Liquid	Density (g/ml)
Gasohol 91	0.7422
Ethanol 20	0.7502
Ethanol	0.7828
Cooking Oil	0.8989
Water	1.0000
Shampoo	1.0205
Concentrated Syrup	1.3171
Pure Honey	1.4238

3.1.3. Imaging System

The imaging system mainly consists of a Kyokko PI-200 fluorescent screen and a Canon EOS 1100D digital camera. The fluorescent screen is made of Tb-activated gadolinium oxysulfide (GOS:Tb or GOST) which has been known useful as an X-ray excited phosphor (GTE Products Corporation, 1980). With the availability of rare earth materials in high states of purity and at reasonable costs, one can now design new phosphors with improved X-ray absorptions, greater density and higher X-ray to light conversion efficiencies (Link et al., 1989).

After penetrating the sample, the radiation emitted by X-ray source impinges on the fluorescent screen. The energy of the incident radiation is partially converted into visible light. This light produces a visible radiographic image on the entrance screen (Link et al, 1989). Figure 3.3 shows the fluorescent screen used in this study with its details tabulated in Table 3.3.



Figure 3.3 Kyokko PI-200 Fluorescent Screen

Table 3.3 Specifications of the Kyokko PI-200 fluorescent screen

Model	Type	Size (cm)	Manufacturer
Kyokko PI-200 Fluorescent Screen	Gd ₂ O ₂ S:Tb	30 × 30	Mitsubishi Chemical Corporation

The image formed on the fluorescent screen is reflected to the digital camera with the help of a mirror. The camera used in this study is the Canon EOS 1100D digital camera as shown in Figure 3.4 and Table 3.4 summarizes the technical specifications of the camera. The digital camera is equipped with a software that allows the remote control settings, as well as to display and store the image via a USB cable connected to a laptop.



Figure 3.4 Canon EOS 1100D digital camera (Shakib, 2011)

Table 3.4 Technical specifications of the Canon EOS 1100D digital camera

Characteristics	Description
General	
Camera type	Digital SLR
LCD monitor	2.7" TFT Colour Liquid Crystal (Approx. 230k dots)
Dimensions (W × H × D) mm	129.9 × 99.7 × 77.9 mm
Weight (body only) g	500 g
Battery	Lithium Ion LP-E10
External interface	Hi-Speed USB/HDMI mini/Remote control terminal

Table 3.4 Technical specifications of the Canon EOS 1100D digital camera
(continue)

Features	
Imaging sensor/Effective pixels	CMOS / 12.2 Megapixels
Effective sensor size	22.0 × 14.7 mm
Max. output resolution	4272×2848
Other resolutions	(M) 3088×2056, (S1) 2256×1504, (S2) 1920×1280, (S3) 720×480
Image formats	JPEG, Raw (.CR2)
Auto focus	TTL-CT-SIR, 9-point (1 cross-type)
Manual focus	Yes
Optical zoom	3.1×
ISO speed range	100 - 6400
Shutter speed	1/4000 – 30 sec
Shooting speed	3 fps

SOURCE: (Canon Inc., n.d.: online)

3.2. Experimental Approach

The principle of Digital Fluoroscopy System is applied to the system. Such system is built from a 35 × 35 × 60 cm light tight box lined with 3 mm thick lead sheets in the inner walls except for the front side where a 30 × 30 cm Kyokko DRZ fluorescent screen made up of gadolinium oxysulfide(terbium) ($Gd_2O_2S:Tb$ or so called “GOS”) was fitted. Lead lining is important in order to prevent scattered X-rays within the box, meanwhile GOS was used to convert transmitted X-ray intensity to light. The image viewing system was constructed for real time imaging by making use of the fluorescent screen, the Canon 1100D digital camera and a mirror as shown in Figure 3.5. The camera is equipped with a software capable for remote control setting via a USB cable connected to a laptop which allows the images to be acquired. Additionally, a lead block

was placed beside the camera since the image sensitive “complementary metal-oxide-semiconductor (CMOS)” chip camera is also sensitive to X-rays causing noisy signals.

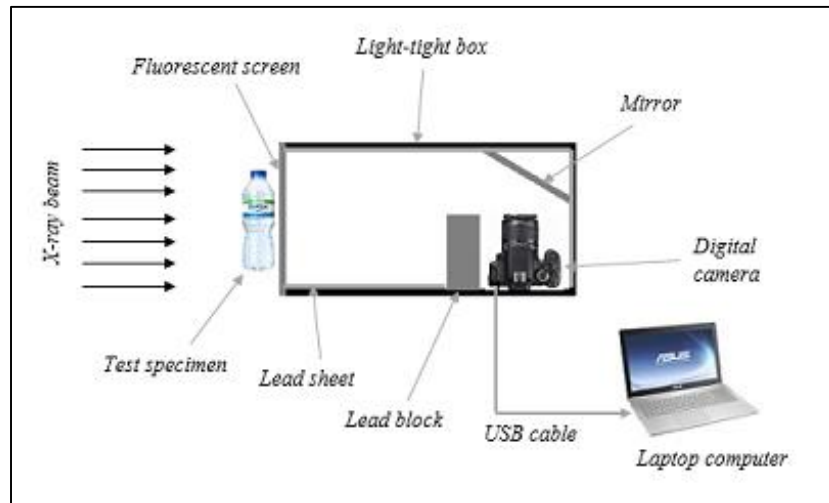


Figure 3.5 Principle design of the X-ray imaging system

3.2.1. Sample Preparation

Liquids of different densities were prepared together with plastic bottles containers of thickness 4.5, 6.0 and 7.5 cm. The density of the liquid samples was measured at room temperature by using an electronic analytical balance as shown in Figure 3.6.

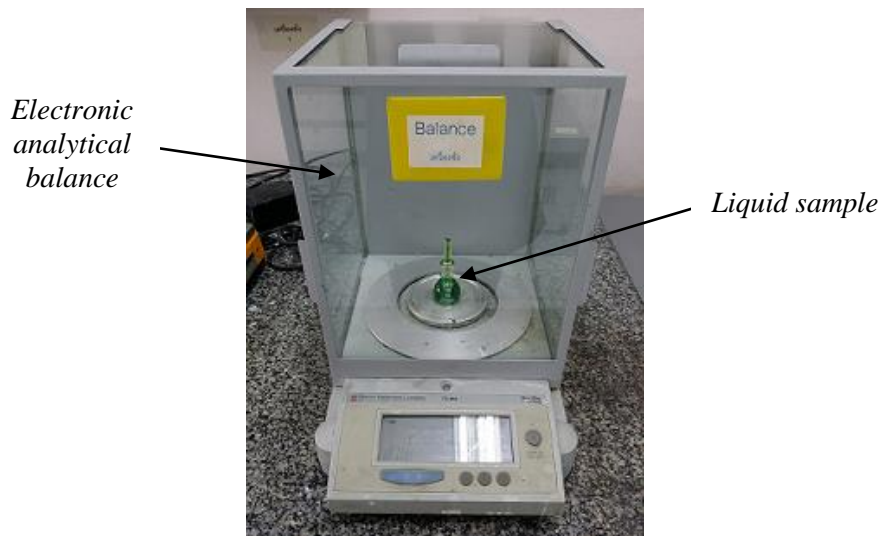


Figure 3.6 Example of measuring the density of liquid by using an electronic analytical balance

3.2.2. Radiographic Exposure

The X-ray tube, the sample and the fluorescent screen were encased in a shielding room, whereas the sample is placed between the X-ray tube and the fluorescent screen, as illustrated in Figure 3.7.

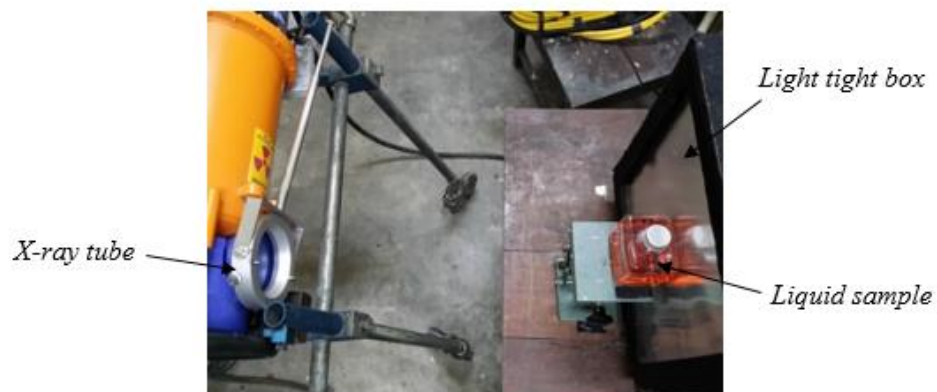


Figure 3.7 Position of the sample during radiographic exposure

Each samples was exposed with X-rays for various energies ranging from 70 kVp to 200 kVp with 10 kVp interval so that a total of 14 raw images were obtained for the construction of the calibration data. Each raw images was exposed for 10 seconds exposure time with the tube current, mA set to “STD” exposure as a normal setting.

Before taking radiographs in changing any variables (e.g. thickness of liquid), the system was tested with exposure with water to ensure that the system remained constant. Figure 3.8 shows the setup for radiographic exposure.

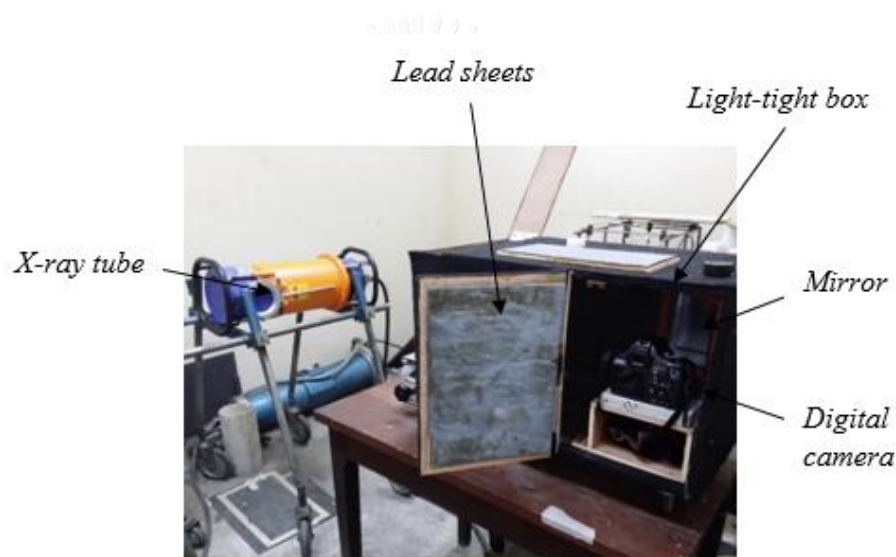


Figure 3.8 Radiographic exposure setup

3.2.3. Image Acquisition

The digital camera was equipped with a software for remote control of the camera which was connected to a laptop via the USB cable. This feature as depicted in Figure 3.9 allows user to display, capture and store the images acquired from the radiographic exposure for data analysis. The camera settings were set to be the same for all exposure i.e. with aperture f14, shutter speed 2”5 and ISO 400.

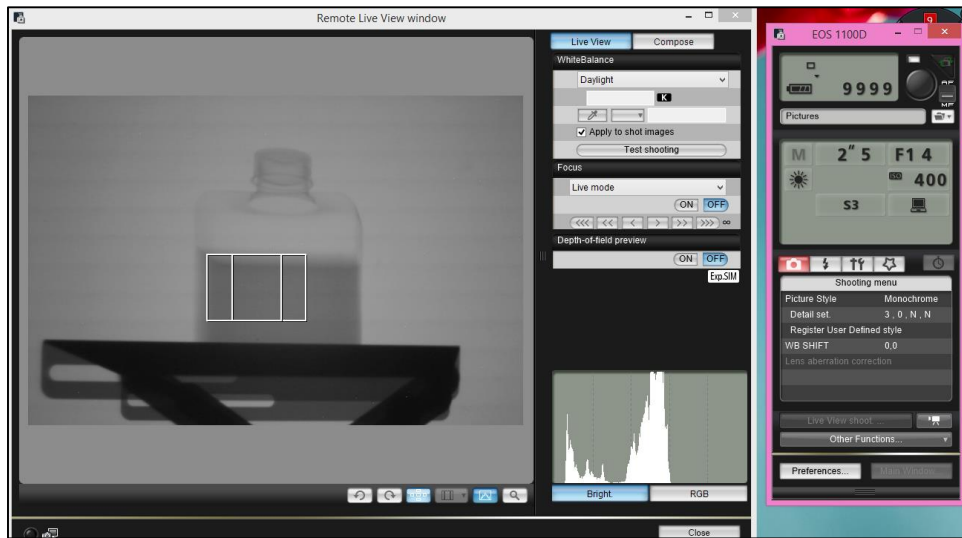


Figure 3.9 Image acquisition process

3.2.4. Data Analysis

The data was analysed by reading the greyscale of the images acquired which was designed by using Microsoft Visual Basic 6.0 as seen in Figure 3.10.

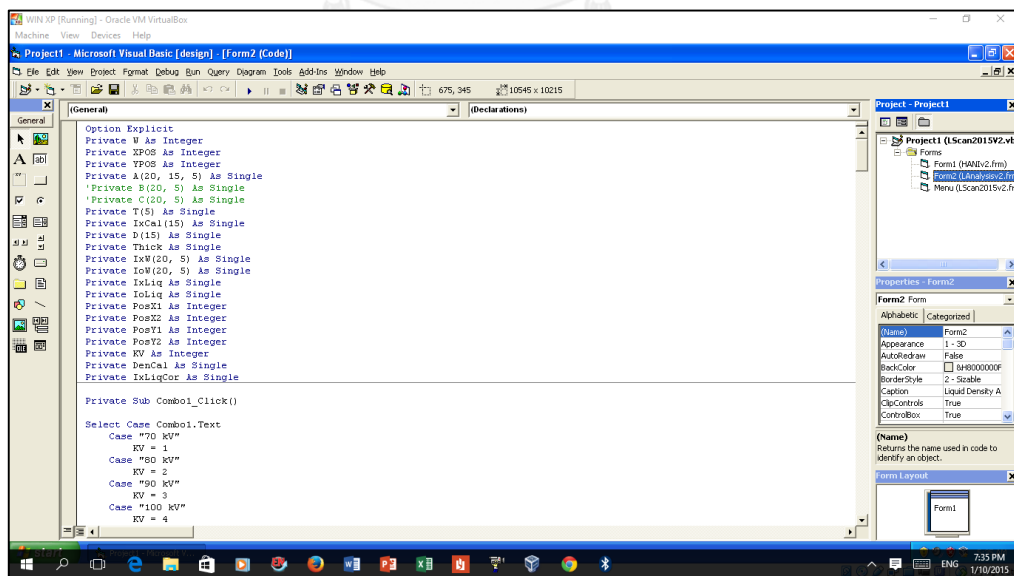


Figure 3.10 Designing software for data analysis

3.3. Methodology for Inspection

3.3.1. Calibration

The calibration data was constructed from eight different types of liquid of different densities as listed in Table 3.2. This was done by reading the greyscale values of each images acquired by using the software designed for data calibration as shown in Figure 3.11. The full program code form for calibration is shown in Appendix A.

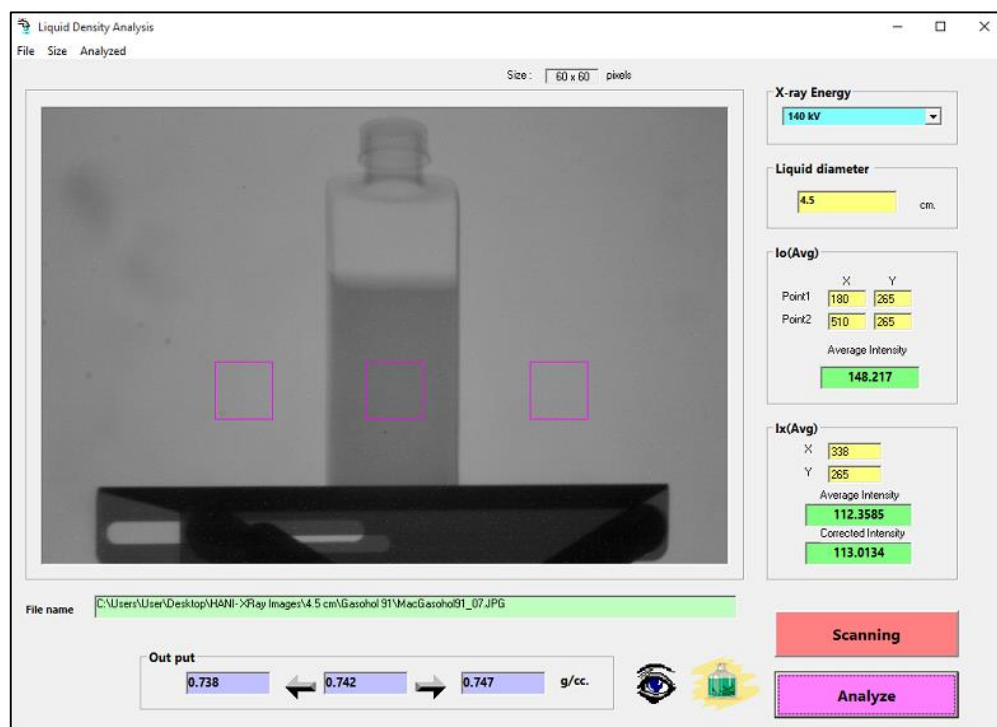


Figure 3.11 Software designed for data calibration (LScan2015)

All of the greyscale values obtained were corrected with water by making use of the following Equation 3.1. The raw data input for calibration were summarized in Appendix B. (Note that: Intensity is also refer as greyscale.)

$$I_{corrected} = \frac{I_{o(water)}}{I_{o(liquid)}} \cdot I_{x(liquid)} \quad (\text{Equation 3.1})$$

where,

$I_{corrected}$ = Corrected intensity of liquid

$I_{o(water)}$ = Incident photon intensity of water

$I_{o(liquid)}$ = Incident photon intensity of liquid

$I_{x(liquid)}$ = Intensity transmitted through liquid

3.3.2. Testing the System: Estimation of Percentage of Error

In addition, the system was tested with several types of liquid as shown in Table 3.5 at thickness 6.0 cm which is the standard thickness of liquids in bottles.

Table 3.5 Densities of different types of liquids used for testing the system

Type of Liquid	Density (g/ml)
Gasohol 95	0.7479
Ethanol 85	0.7834
Diesel	0.8220
Unknown A	0.7211
Unknown B	0.7409
Unknown C	0.8108

(Note: Unknown A is Base 2, Unknown B is Base 1, and Unknown C is a type of diesel.)

Consequently, the estimation of percentage error between the actual density and the density read out by the system was calculated from Equation 3.2 below:

$$\text{Percentage error (\%)} = \frac{|Actual\ Density - Density\ Read\ Out|}{Actual\ Density} \times 100 \quad (\text{Equation 3.2})$$

where, the *Actual Density* is the actual density of liquid and the *Density Read Out* is the density read out by the system from the software designed.

3.3.3. In-Situ Inspection

There are some cases when the calibration data set constructed cannot be applied for the liquid density analysis. This is seen when the geometry settings of the system is not fixed. Therefore, the suitable method for this is by applying the in-situ technique. After setting the geometry of the system, the calibration must be done by exposing the liquids in Table 3.2 with the appropriate X-ray energy for calibration.

Correspondingly, the different types of liquids listed in Table 3.5 was also tested by this method by using the software as shown in Figure 3.12 below which is more preferable for routine inspection. The full program code form for in-situ measurement software is shown in Appendix C.

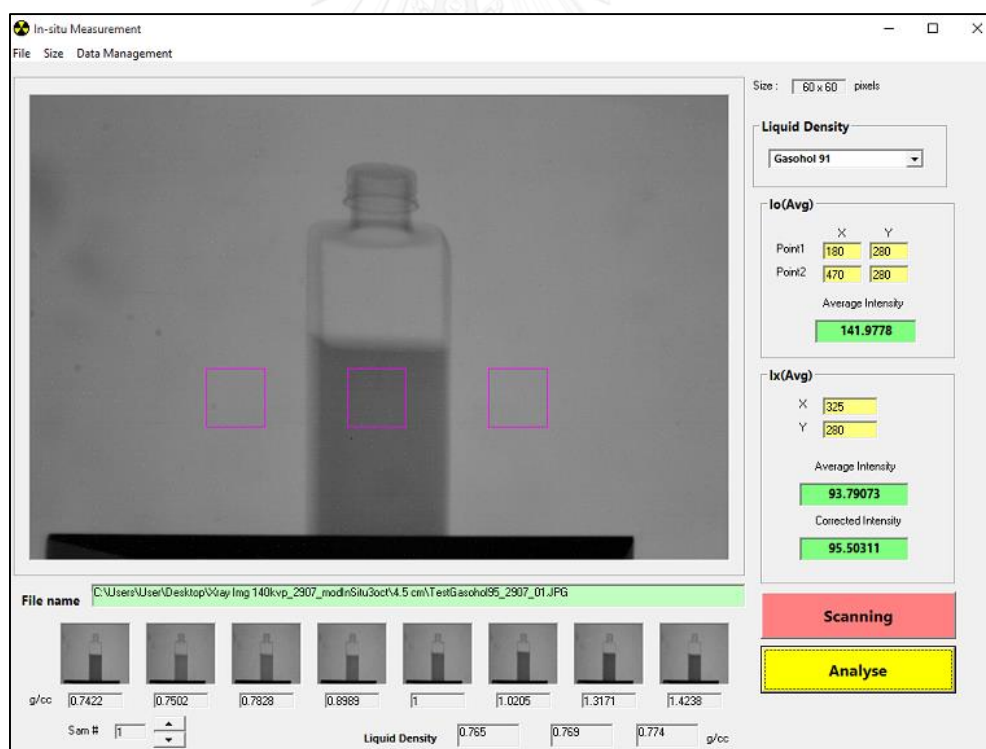


Figure 3.12 Software designed for in-situ inspection (LScanInsitu)

Basically, the following steps are necessary during/for in-situ inspection:

- I. The liquids used for calibration were radiographed randomly at any certain appropriate X-ray energy, followed by the unknown liquids or the liquids to be inspected. In this study, they were radiographed at 140 kVp since this is the approximate minimum of percentage error obtained in accordance to Section 3.3.2.
- II. The greyscale values of all the liquids were obtained and correction was made with reference to water.
- III. Analysis of the unknown liquid is done based on the corrected calibration data at that certain X-ray energy. Appendix D shows the example of raw data input obtained for in-situ measurement done at 140 kVp. A step-by-step tutorial on how to use the software is further shown in Appendix E.

3.4. Research Methodology Flowchart

The research methodology is based on the experimental approach summarized as the following in Figure 3.13:

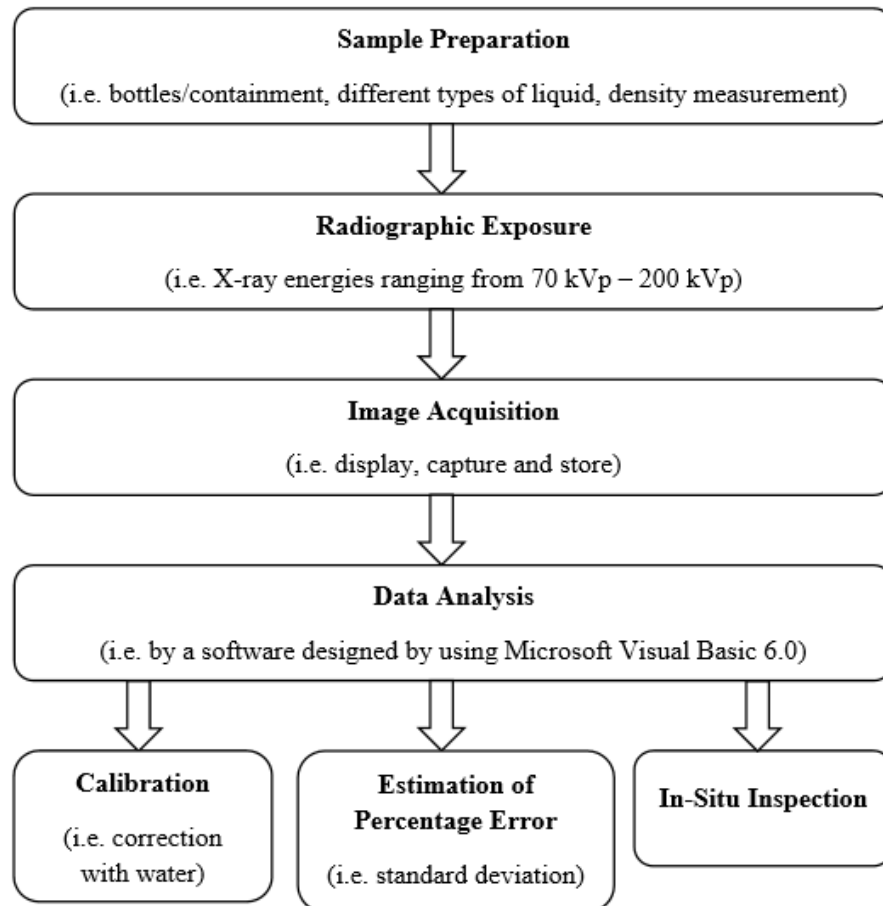


Figure 3.13 Research methodology flowchart

CHAPTER 4

RESULTS AND DISCUSSIONS

4. Results

In this study, the attenuated X-ray intensities that penetrated the samples are measured in greyscales. When X-ray photons interact with the fluorescent screen and deposit its energy, a certain fraction of this energy is converted to visible light. More energy is absorbed as density increases, hence, darker images will be formed. This is true for real time imaging technique or specifically known as digital fluoroscopic system.

4.1. Calibration of the System

Figure 4.1, Figure 4.2 and Figure 4.3 show some examples of the images obtained during radiographic exposure for water at three different thicknesses i.e. 4.5, 6.0 and 7.5 cm respectively.

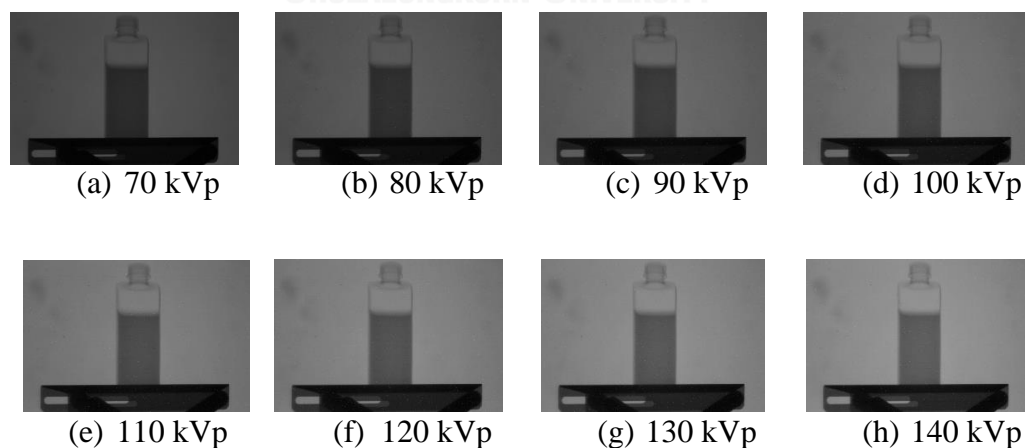


Figure 4.1 Examples of images acquired for 4.5 cm thickness of water at X-ray energies ranging from 70 kVp to 200 kVp

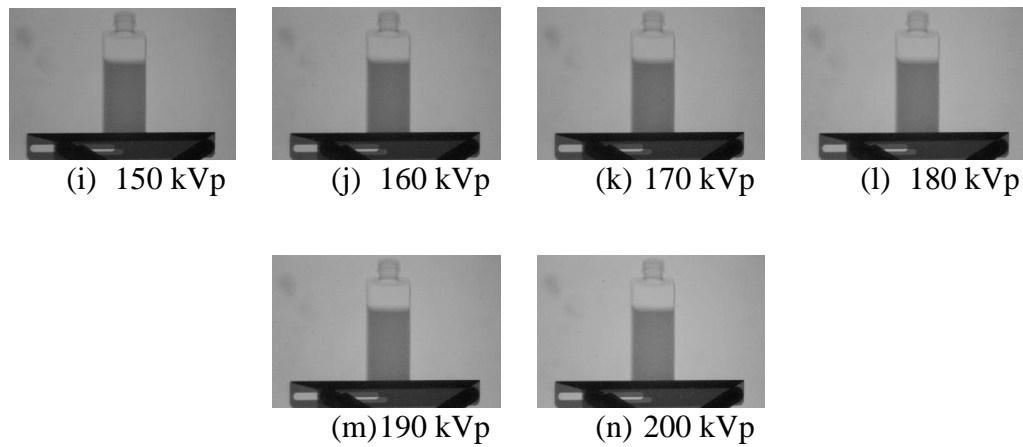


Figure 4.1 Examples of images acquired for 4.5 cm thickness of water at X-ray energies ranging from 70 kVp to 200 kVp (continue)

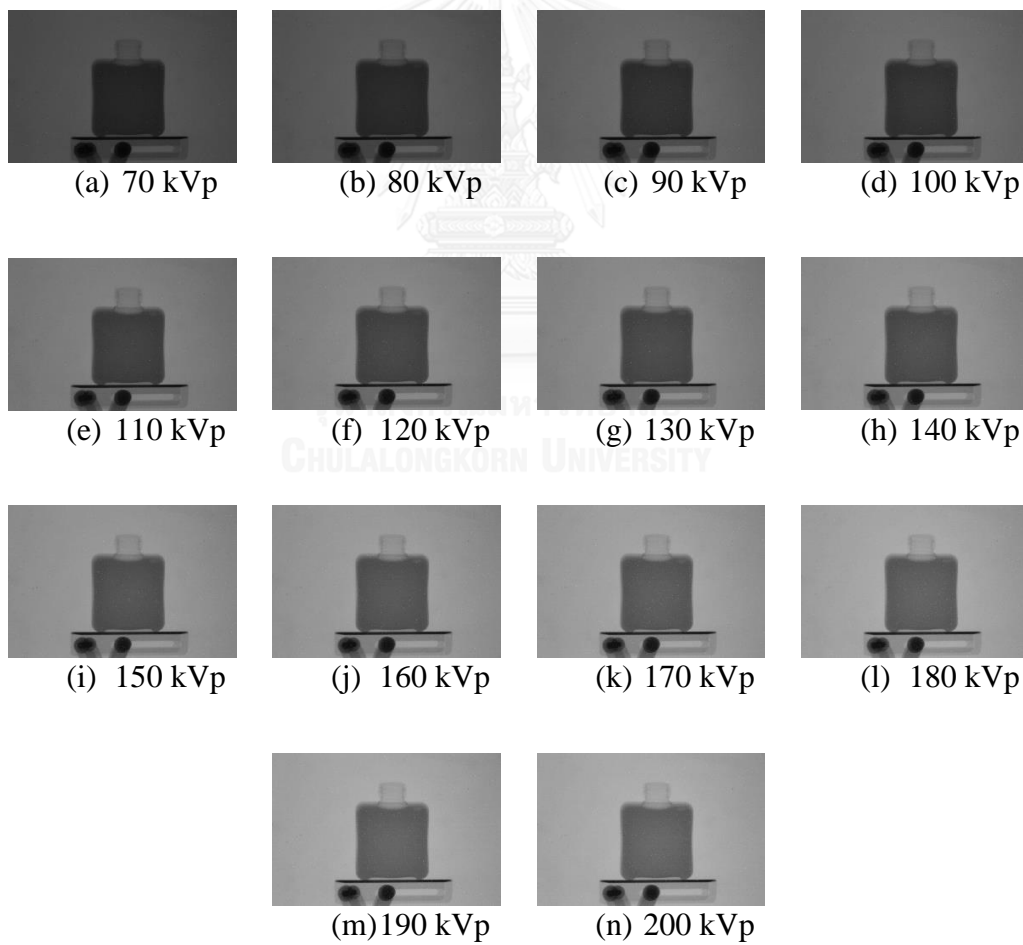


Figure 4.2 Examples of images acquired for 6.0 cm thickness of water at X-ray energies ranging from 70 kVp to 200 kVp

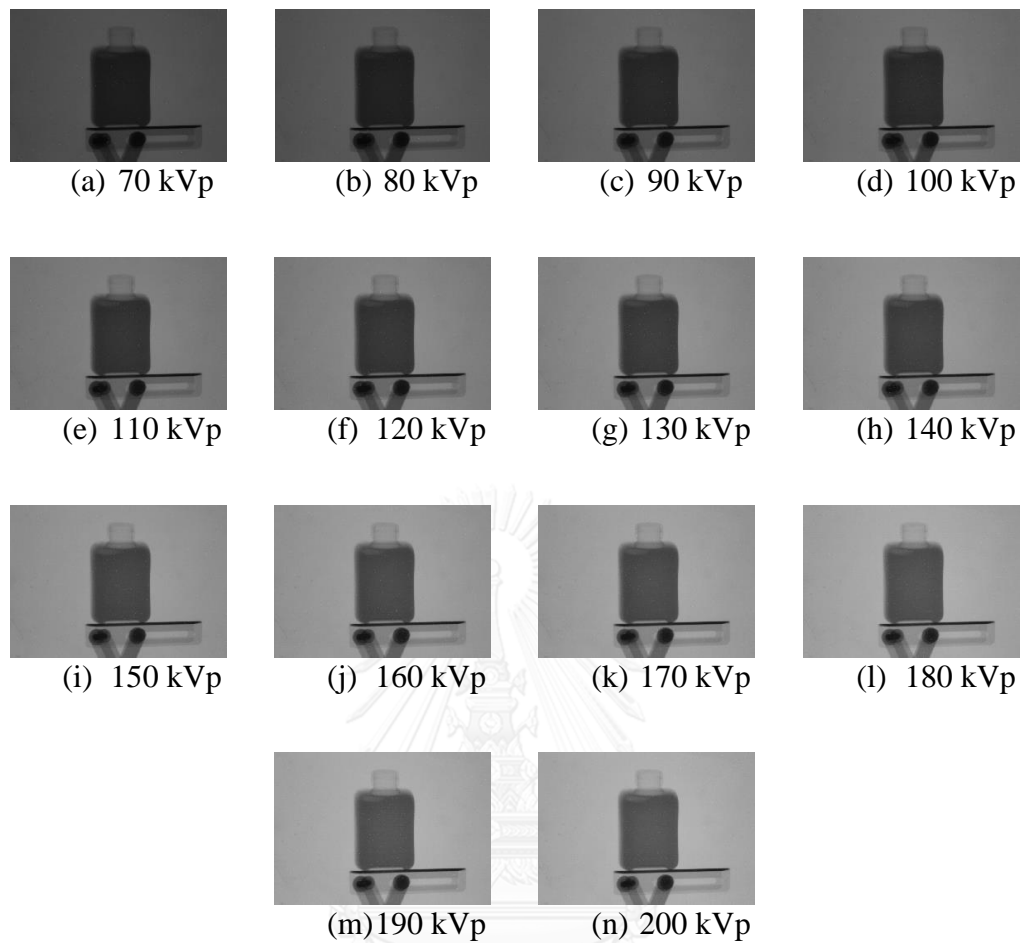


Figure 4.3 Examples of images acquired for 7.5 cm thickness of water at X-ray energies ranging from 70 kVp to 200 kVp

The calibration data of greyscale values after normalization with water were obtained by using the developed software called “LScan2015” software. The results are tabulated in Table 4.1 to Table 4.14 for X-ray energies ranging from 70 kVp to 200 kVp accordingly, followed by the graph of greyscale versus density of liquid for each X-ray energy depicted in Figure 4.4 to Figure 4.17.

i) 70 kVp

Table 4.1 Greyscale values after correction with water at X-ray energy = 70 kVp

Type of Liquid	Density of Liquid (g/ml)	Thickness (cm)		
		4.5	6.0	7.5
Gasohol 91	0.7422	56.1132	51.9712	42.0946
Ethanol 20	0.7502	56.0281	50.7071	40.9998
Ethanol	0.7828	54.3584	49.2009	39.9310
Cooking Oil	0.8989	51.4739	47.4420	36.3507
Water	1.0000	45.8734	39.4857	30.0702
Shampoo	1.0205	42.8240	37.8147	26.6028
Concentrated Syrup	1.3171	38.9509	32.8898	22.4638
Pure Honey	1.4238	37.7475	30.8388	21.1967

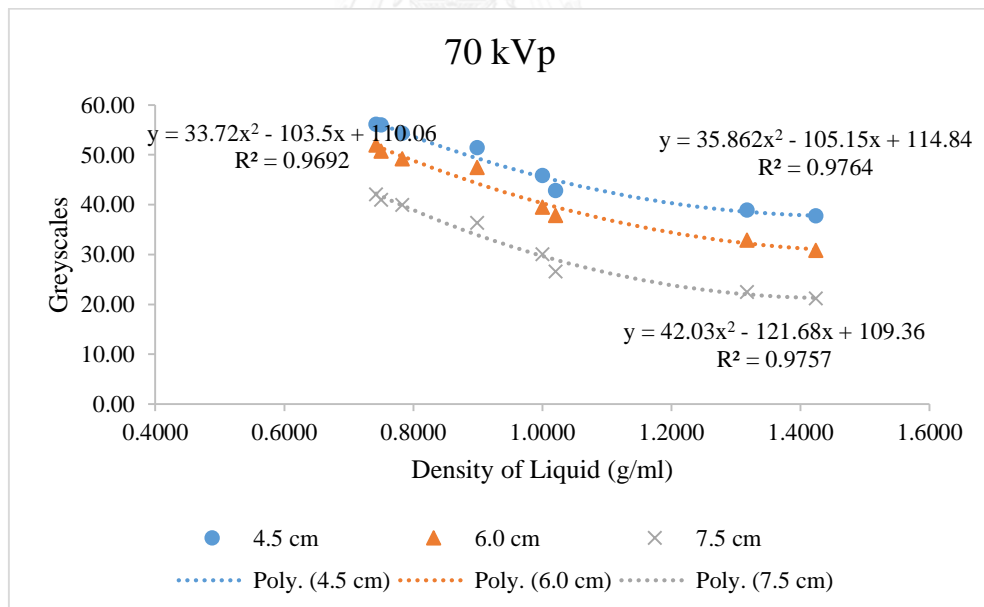


Figure 4.4 Graph of greyscale values versus density of liquid at X-ray energy = 70 kVp

ii) 80 kVp

Table 4.2 Greyscale values after correction with water at X-ray energy = 80 kVp

Type of Liquid	Density of Liquid (g/ml)	Thickness (cm)		
		4.5	6.0	7.5
Gasohol 91	0.7422	62.0254	58.3288	47.1900
Ethanol 20	0.7502	61.7397	57.1454	45.8049
Ethanol	0.7828	59.9423	55.2513	44.4872
Cooking Oil	0.8989	57.0060	53.9407	40.8443
Water	1.0000	50.4938	44.9394	34.3972
Shampoo	1.0205	48.0798	42.9049	31.1209
Concentrated Syrup	1.3171	43.5320	37.7210	26.4426
Pure Honey	1.4238	42.6681	35.9350	25.0876

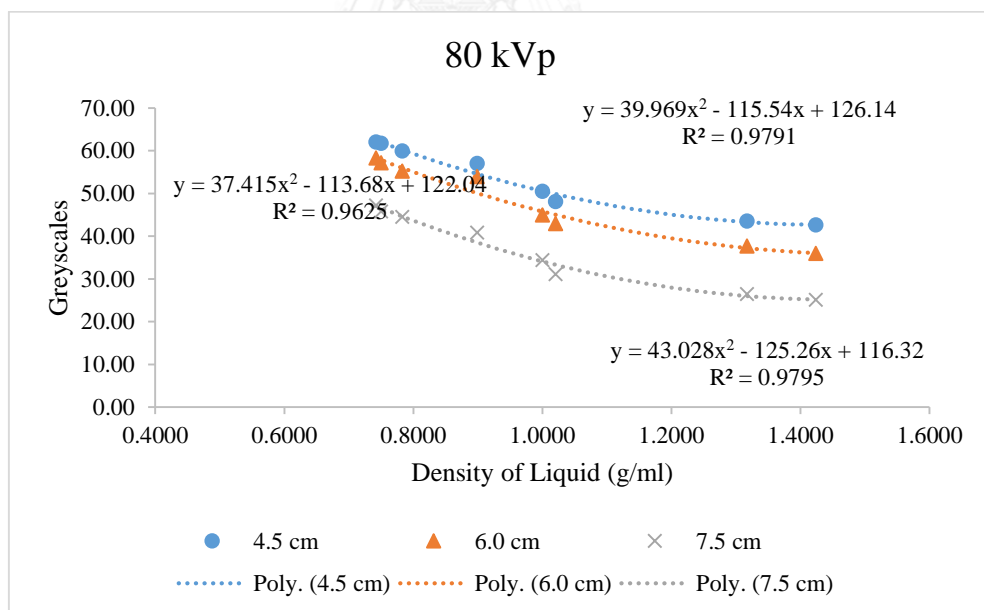


Figure 4.5 Graph of greyscales versus density of liquid at X-ray energy = 80 kVp

iii) 90 kVp

Table 4.3 Greyscale values after correction with water at X-ray energy = 90 kVp

Type of Liquid	Density of Liquid (g/ml)	Thickness (cm)		
		4.5	6.0	7.5
Gasohol 91	0.7422	74.4601	68.0216	55.9351
Ethanol 20	0.7502	73.9772	66.7583	55.0079
Ethanol	0.7828	72.2464	64.6245	53.4573
Cooking Oil	0.8989	68.8587	63.4493	48.9882
Water	1.0000	62.0464	52.4153	41.7601
Shampoo	1.0205	58.5397	51.7437	38.0096
Concentrated Syrup	1.3171	53.2290	45.5964	31.6622
Pure Honey	1.4238	51.7915	43.3712	30.2761

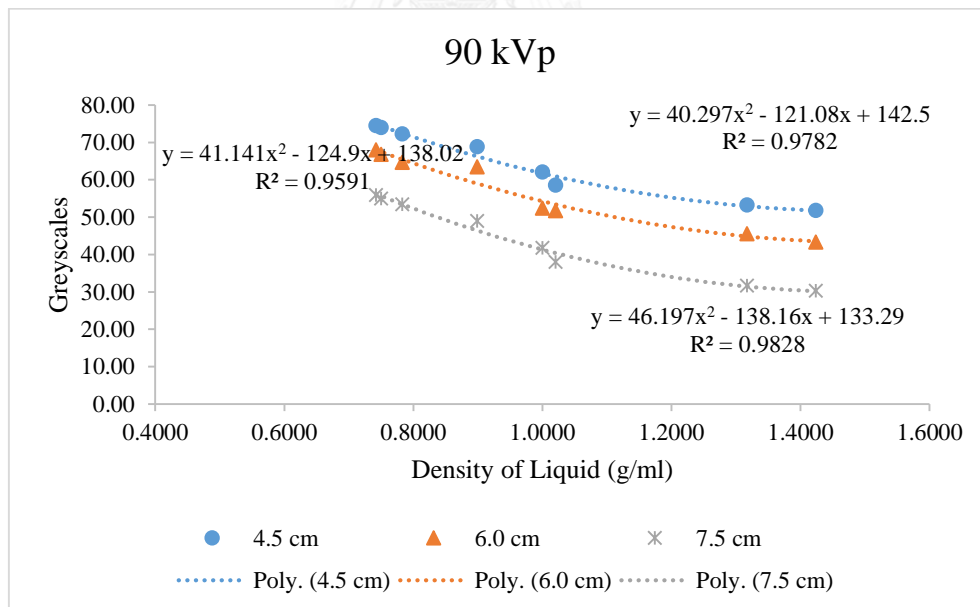


Figure 4.6 Graph of greyscales versus density of liquid at X-ray energy = 90 kVp

iv) 100 kVp

Table 4.4 Greyscale values after correction with water at X-ray energy = 100 kVp

Type of Liquid	Density of Liquid (g/ml)	Thickness (cm)		
		4.5	6.0	7.5
Gasohol 91	0.7422	85.1018	73.7568	62.0728
Ethanol 20	0.7502	84.5164	73.0322	60.7457
Ethanol	0.7828	82.0501	70.1397	59.1562
Cooking Oil	0.8989	78.5764	68.0934	54.0227
Water	1.0000	71.4724	56.8885	46.1320
Shampoo	1.0205	67.4150	55.4714	42.4196
Concentrated Syrup	1.3171	62.0201	48.3313	35.5396
Pure Honey	1.4238	60.2839	44.9406	33.7117

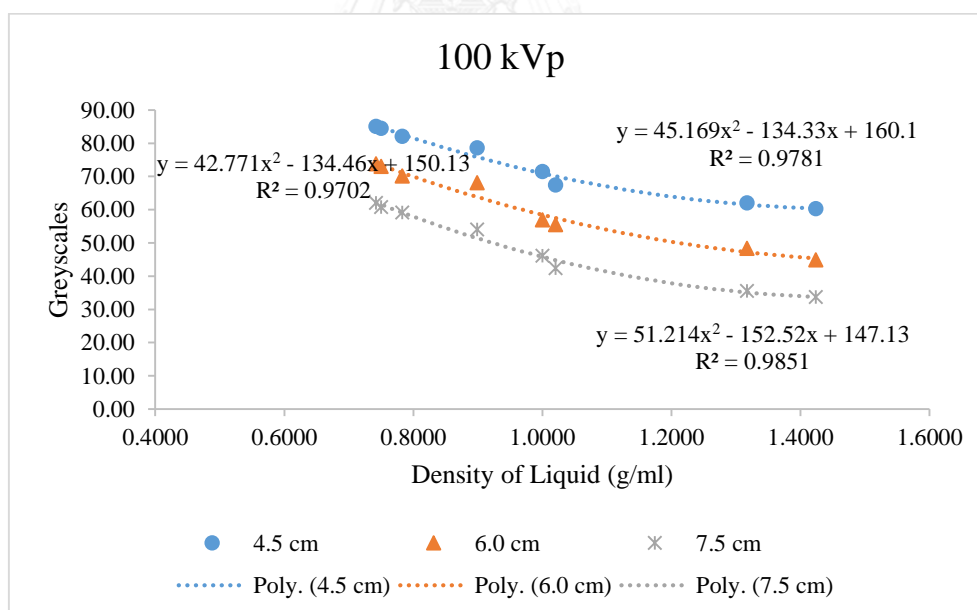


Figure 4.7 Graph of greyscales versus density of liquid at X-ray energy = 100 kVp

v) 110 kVp

Table 4.5 Greyscale values after correction with water at X-ray energy = 110 kVp

Type of Liquid	Density of Liquid (g/ml)	Thickness (cm)		
		4.5	6.0	7.5
Gasohol 91	0.7422	94.7167	86.5773	70.7119
Ethanol 20	0.7502	94.1843	84.4572	69.1277
Ethanol	0.7828	92.2338	81.7582	67.0519
Cooking Oil	0.8989	88.3045	79.2610	61.4384
Water	1.0000	80.0586	68.5080	53.4349
Shampoo	1.0205	76.5914	65.4353	48.5726
Concentrated Syrup	1.3171	70.5136	57.0911	41.0118
Pure Honey	1.4238	69.1071	53.2579	39.1152

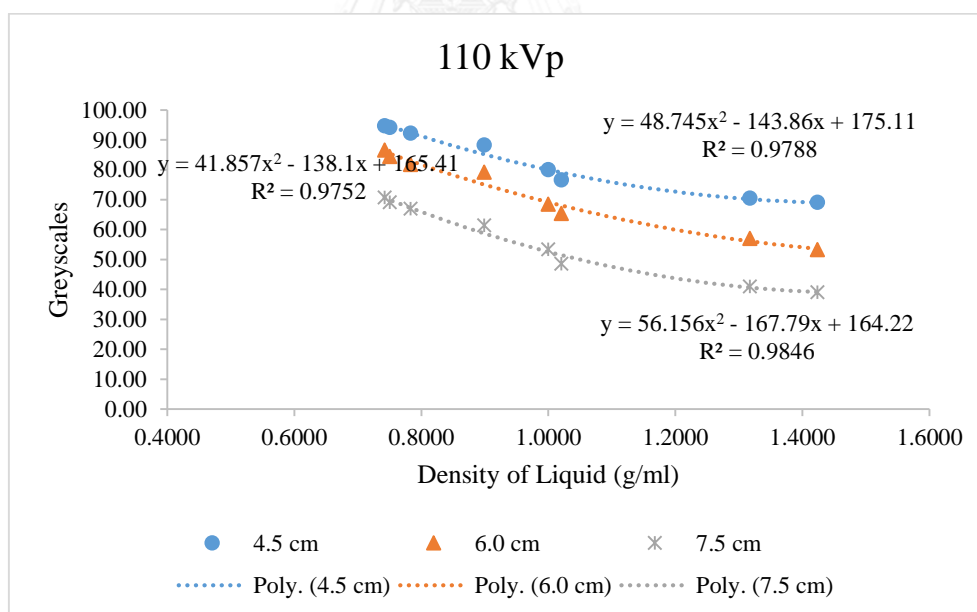


Figure 4.8 Graph of greyscales versus density of liquid at X-ray energy = 110 kVp

vi) 120 kVp

Table 4.6 Greyscale values after correction with water at X-ray energy = 120 kVp

Type of Liquid	Density of Liquid (g/ml)	Thickness (cm)		
		4.5	6.0	7.5
Gasohol 91	0.7422	99.4373	93.2920	75.9486
Ethanol 20	0.7502	98.9019	91.4293	74.2380
Ethanol	0.7828	98.1976	88.9784	71.9214
Cooking Oil	0.8989	94.3697	85.5006	65.5425
Water	1.0000	86.7872	74.8740	56.8151
Shampoo	1.0205	82.4691	70.8278	51.9756
Concentrated Syrup	1.3171	75.7664	62.0302	43.6965
Pure Honey	1.4238	73.9069	57.7180	41.2022

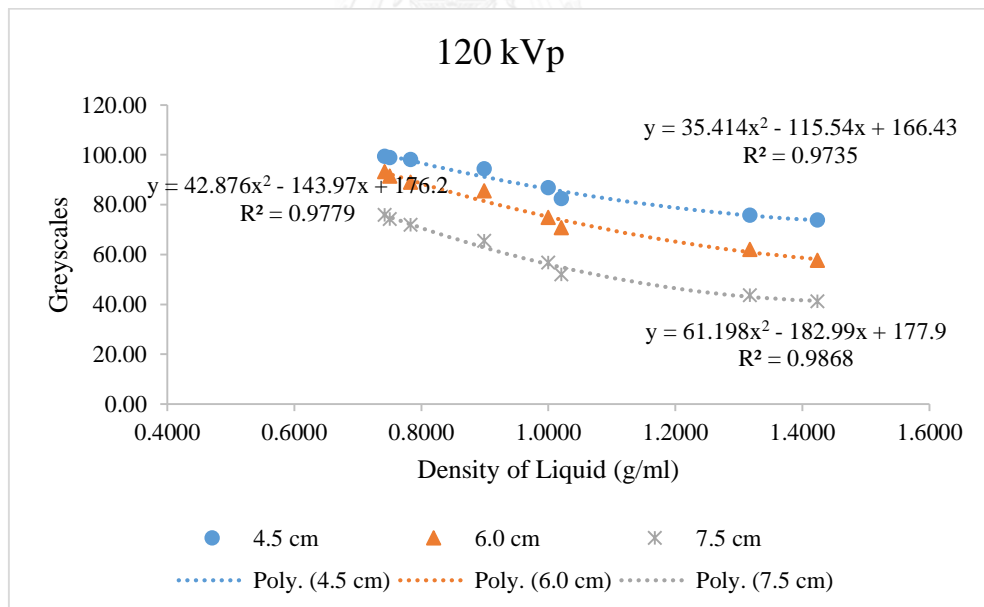


Figure 4.9 Graph of greyscales versus density of liquid at X-ray energy = 120 kVp

vii) 130 kVp

Table 4.7 Greyscale values after correction with water at X-ray energy = 130 kVp

Type of Liquid	Density of Liquid (g/ml)	Thickness (cm)		
		4.5	6.0	7.5
Gasohol 91	0.7422	105.7119	98.3019	81.9482
Ethanol 20	0.7502	104.6723	95.6839	80.3285
Ethanol	0.7828	103.8321	93.5681	77.8528
Cooking Oil	0.8989	100.0324	90.8308	72.3220
Water	1.0000	91.8389	79.1195	62.5476
Shampoo	1.0205	88.0075	74.1455	56.9519
Concentrated Syrup	1.3171	81.2487	67.3362	48.4157
Pure Honey	1.4238	79.8875	63.3159	45.7471

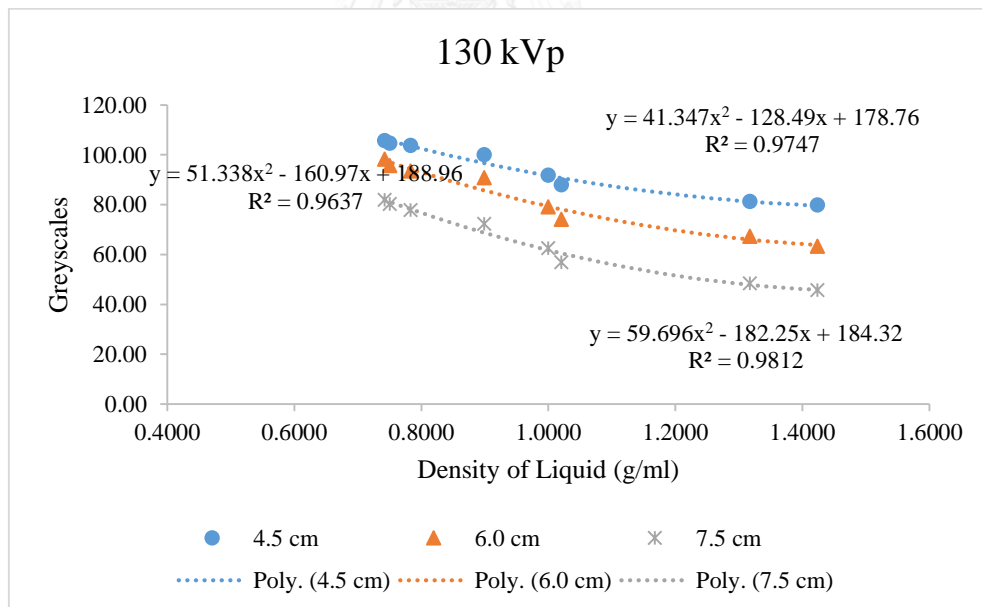


Figure 4.10 Graph of greyscales versus density of liquid at X-ray energy = 130 kVp

viii) 140 kVp

Table 4.8 Greyscale values after correction with water at X-ray energy = 140 kVp

Type of Liquid	Density of Liquid (g/ml)	Thickness (cm)		
		4.5	6.0	7.5
Gasohol 91	0.7422	113.0134	103.5710	87.1897
Ethanol 20	0.7502	112.6243	101.8920	85.2967
Ethanol	0.7828	110.2359	97.7569	83.3552
Cooking Oil	0.8989	106.2220	96.6541	77.2106
Water	1.0000	98.0271	84.8044	67.7450
Shampoo	1.0205	93.6152	80.7930	63.0545
Concentrated Syrup	1.3171	86.6317	72.9029	52.8207
Pure Honey	1.4238	84.5143	67.5928	50.2049

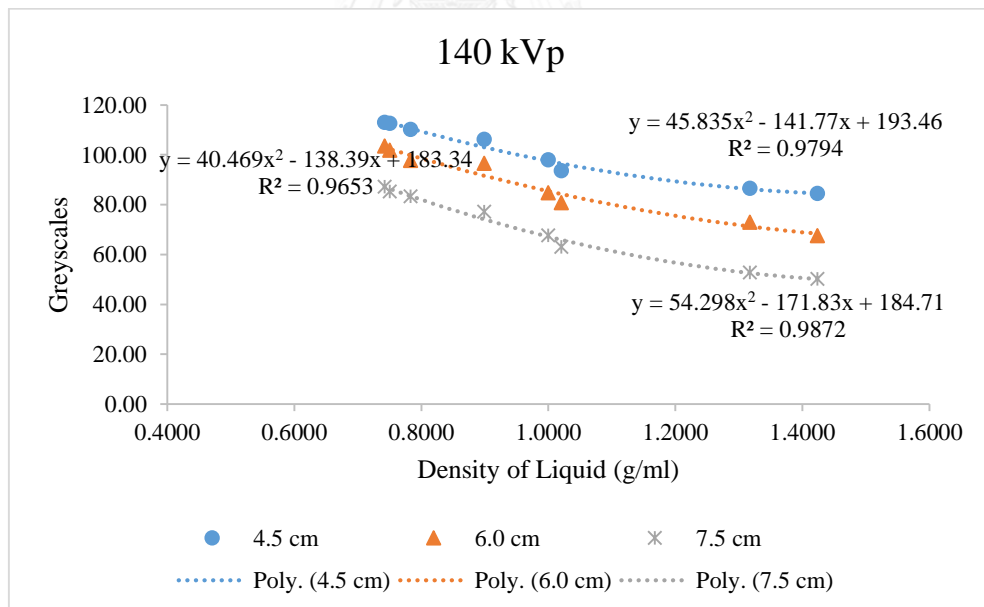


Figure 4.11 Graph of greyscale values versus density of liquid at X-ray energy = 140 kVp

ix) 150 kVp

Table 4.9 Greyscale values after correction with water at X-ray energy = 150 kVp

Type of Liquid	Density of Liquid (g/ml)	Thickness (cm)		
		4.5	6.0	7.5
Gasohol 91	0.7422	118.6862	108.6456	91.7818
Ethanol 20	0.7502	118.0404	106.6492	90.2233
Ethanol	0.7828	115.4417	103.5743	87.6266
Cooking Oil	0.8989	111.3190	101.5667	81.8865
Water	1.0000	103.0904	88.8294	72.2863
Shampoo	1.0205	98.4366	85.0384	67.6479
Concentrated Syrup	1.3171	91.4121	75.0447	56.9598
Pure Honey	1.4238	89.4016	71.5135	53.6950

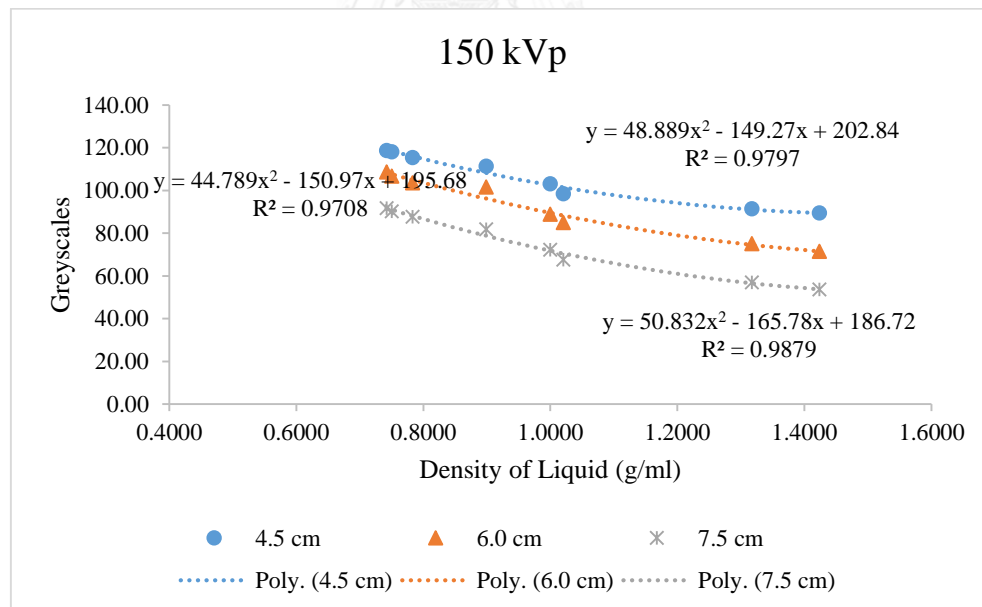


Figure 4.12 Graph of greyscales versus density of liquid at X-ray energy = 150 kVp

x) 160 kVp

Table 4.10 Greyscale values after correction with water at X-ray energy = 160 kVp

Type of Liquid	Density of Liquid (g/ml)	Thickness (cm)		
		4.5	6.0	7.5
Gasohol 91	0.7422	124.0151	112.6457	97.1109
Ethanol 20	0.7502	122.8270	110.6394	95.4040
Ethanol	0.7828	121.2401	107.9585	92.7931
Cooking Oil	0.8989	116.6598	105.6531	87.0132
Water	1.0000	108.3537	92.2423	76.4147
Shampoo	1.0205	103.7347	90.4777	70.8845
Concentrated Syrup	1.3171	96.5146	80.3311	60.7106
Pure Honey	1.4238	94.0905	75.6534	57.3221

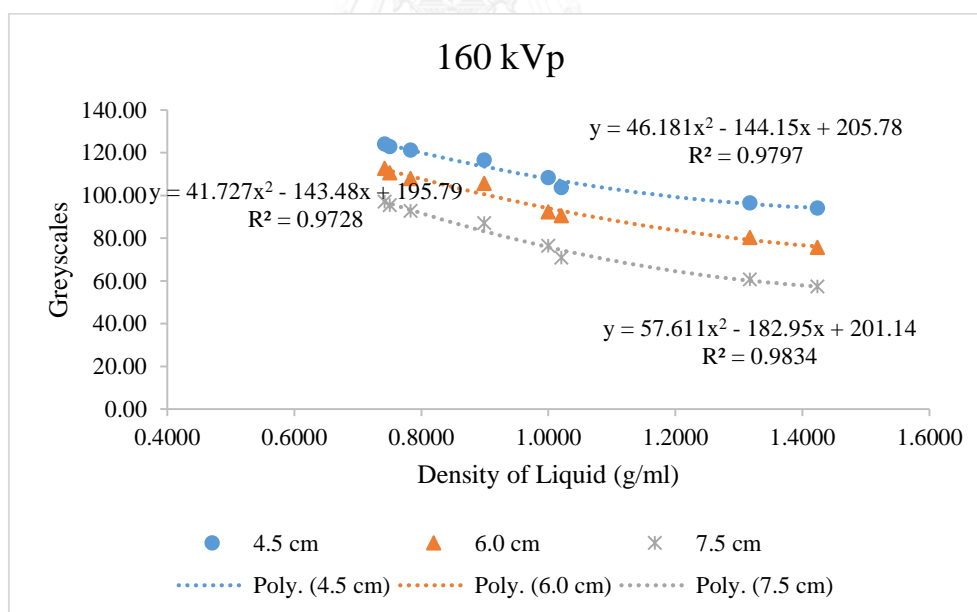


Figure 4.13 Graph of greyscales versus density of liquid at X-ray energy = 160 kVp

xi) 170 kVp

Table 4.11 Greyscale values after correction with water at X-ray energy = 170 kVp

Type of Liquid	Density of Liquid (g/ml)	Thickness (cm)		
		4.5	6.0	7.5
Gasohol 91	0.7422	129.5031	118.5767	101.1479
Ethanol 20	0.7502	128.9320	116.5479	98.4296
Ethanol	0.7828	126.2914	113.1404	96.6424
Cooking Oil	0.8989	122.0802	110.9155	90.0923
Water	1.0000	113.6888	97.9611	79.0181
Shampoo	1.0205	109.4583	94.7990	75.0020
Concentrated Syrup	1.3171	100.5544	83.7641	63.7342
Pure Honey	1.4238	99.0806	80.6100	60.5772

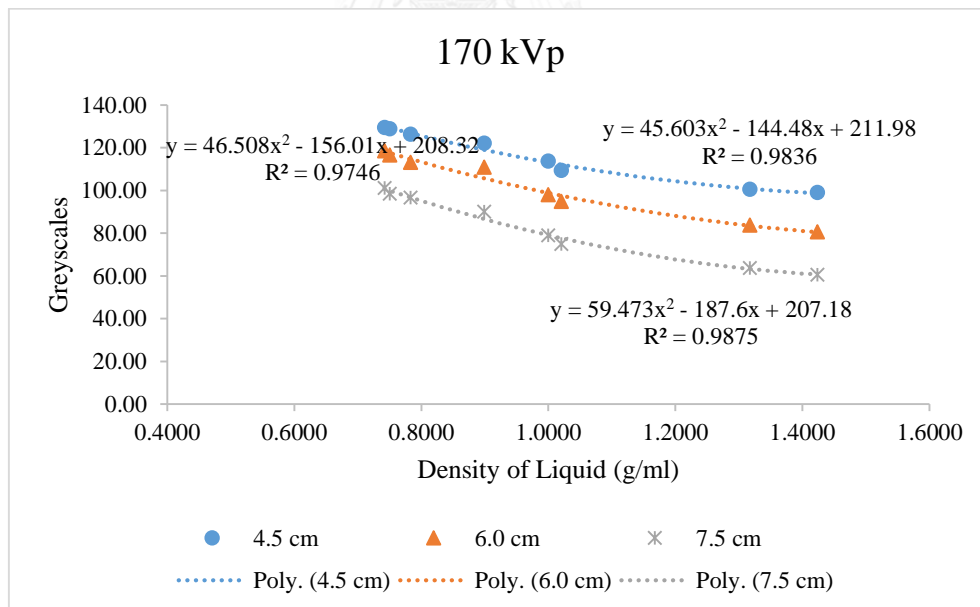


Figure 4.14 Graph of greyscales versus density of liquid at X-ray energy = 170 kVp

xii) 180 kVp

Table 4.12 Greyscale values after correction with water at X-ray energy = 180 kVp

Type of Liquid	Density of Liquid (g/ml)	Thickness (cm)		
		4.5	6.0	7.5
Gasohol 91	0.7422	135.6170	124.0732	106.4800
Ethanol 20	0.7502	134.8187	121.8458	106.3264
Ethanol	0.7828	132.0174	118.6081	102.8749
Cooking Oil	0.8989	128.4357	115.8651	96.2821
Water	1.0000	119.5440	102.8639	85.8053
Shampoo	1.0205	114.6266	99.6981	80.2556
Concentrated Syrup	1.3171	106.7600	88.2262	68.6324
Pure Honey	1.4238	104.2633	84.3725	65.3584

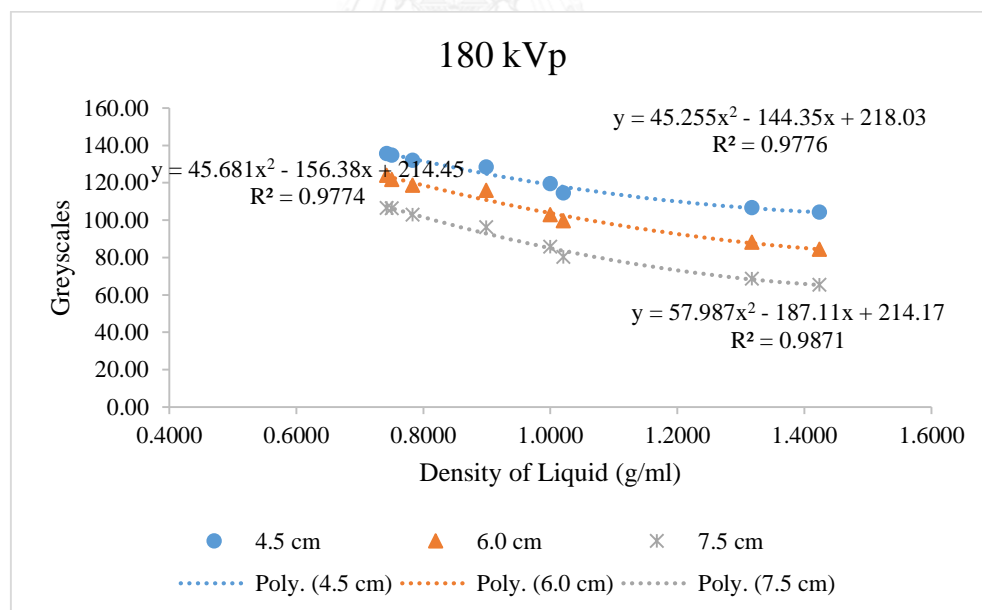


Figure 4.15 Graph of greyscales versus density of liquid at X-ray energy = 180 kVp

xiii) 190 kVp

Table 4.13 Greyscale values after correction with water at X-ray energy = 190 kVp

Type of Liquid	Density of Liquid (g/ml)	Thickness (cm)		
		4.5	6.0	7.5
Gasohol 91	0.7422	139.2144	126.6422	110.2825
Ethanol 20	0.7502	138.7633	124.7674	108.4139
Ethanol	0.7828	135.7054	120.8725	105.1857
Cooking Oil	0.8989	131.2523	118.5798	99.5483
Water	1.0000	122.7334	104.9385	86.7803
Shampoo	1.0205	117.4250	102.2453	82.0036
Concentrated Syrup	1.3171	109.0654	91.1443	69.9639
Pure Honey	1.4238	107.1914	87.0041	66.5746

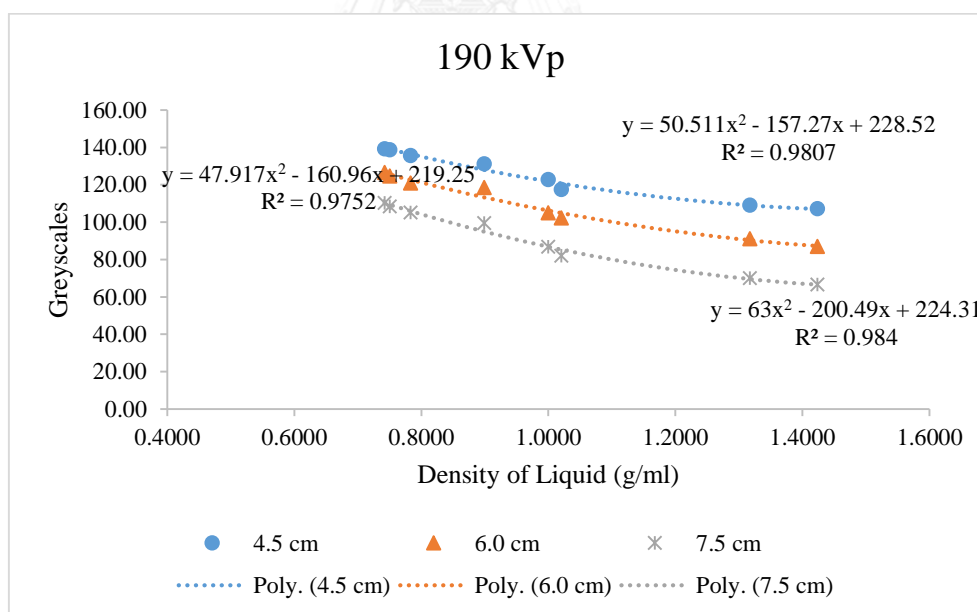


Figure 4.16 Graph of greyscales versus density of liquid at X-ray energy = 190 kVp

xiv) 200 kVp

Table 4.14 Greyscale values after correction with water at X-ray energy = 200 kVp

Type of Liquid	Density of Liquid (g/ml)	Thickness (cm)		
		4.5	6.0	7.5
Gasohol 91	0.7422	144.2335	130.7125	113.8804
Ethanol 20	0.7502	143.7526	129.1742	112.0391
Ethanol	0.7828	141.3603	123.5301	109.4480
Cooking Oil	0.8989	136.8436	121.2999	102.6933
Water	1.0000	127.8404	108.3790	89.6302
Shampoo	1.0205	122.8953	105.5383	85.0659
Concentrated Syrup	1.3171	114.4079	93.3882	73.3248
Pure Honey	1.4238	112.4352	89.4922	69.0720

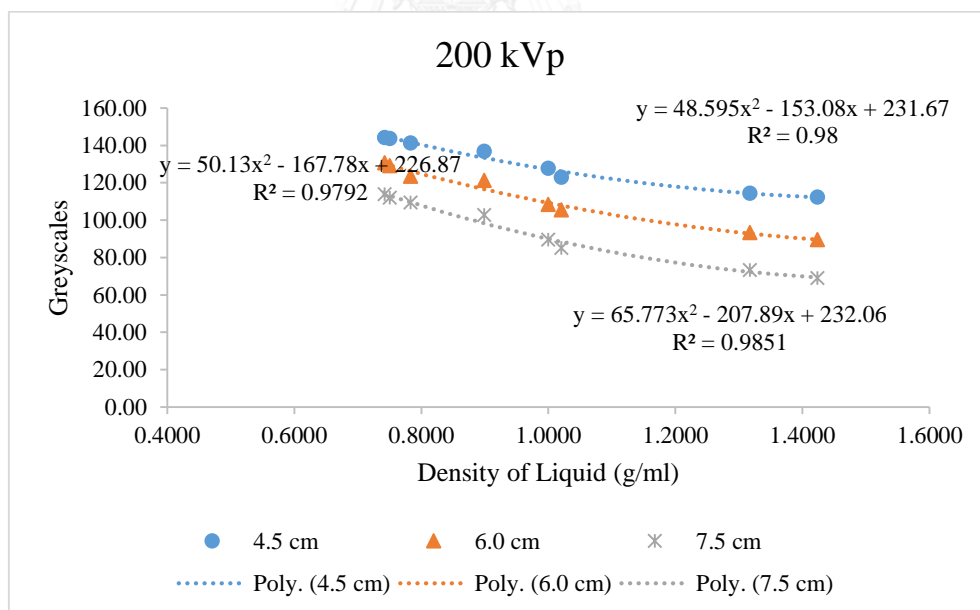


Figure 4.17 Graph of greyscales versus density of liquid at X-ray energy = 200 kVp

Meanwhile Figure 4.18, Figure 4.19 and Figure 4.20 shows the graphs of greyscale versus X-ray energy summarized from the data obtained after correction (Appendix F) for three different liquid thickness 4.5, 6.0 and 7.5 cm respectively.

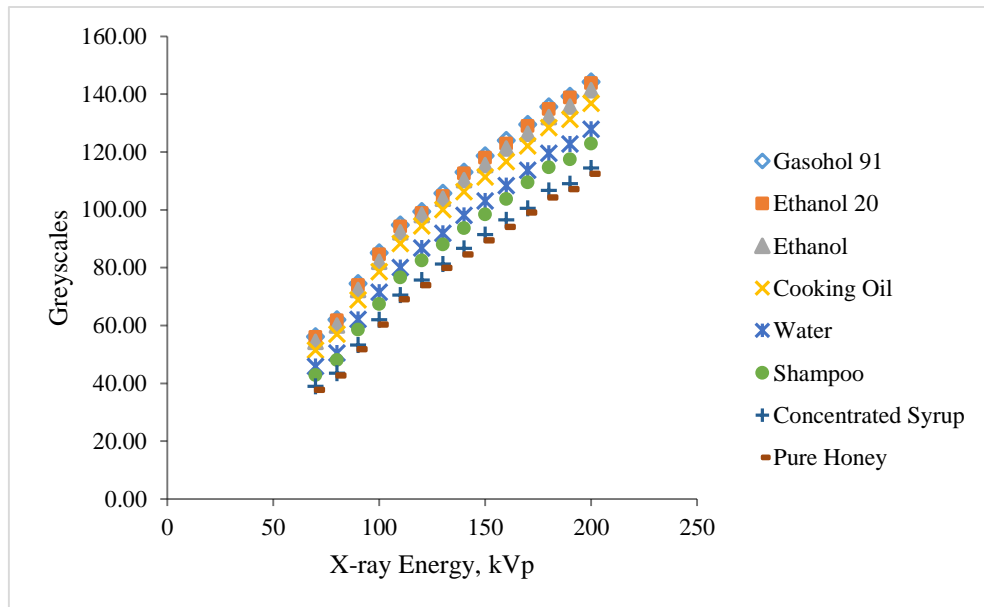


Figure 4.18 Graph of greyscale versus X-ray energy for liquid thickness = 4.5 cm

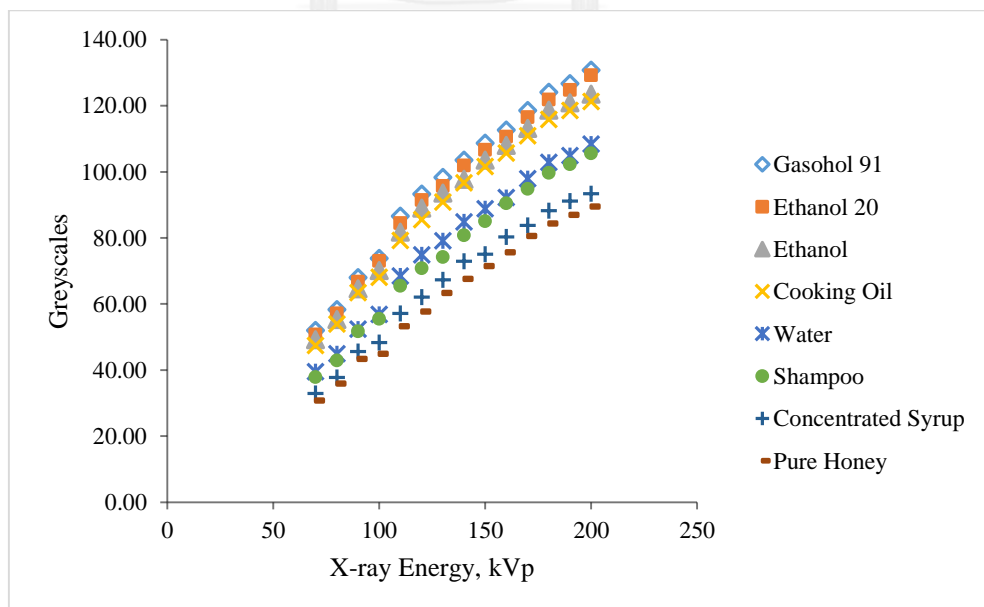


Figure 4.19 Graph of greyscale versus X-ray energy for liquid thickness = 6.0 cm

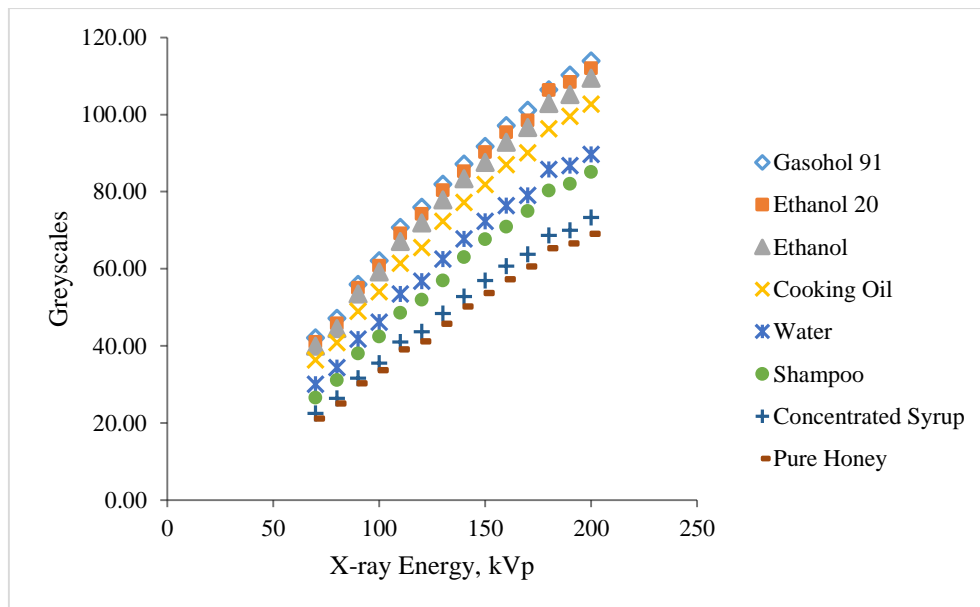


Figure 4.20 Graph of greyscale versus X-ray energy for liquid thickness = 7.5 cm

Based on the analysed data shown in Figure 4.18, Figure 4.19 and Figure 4.20, when X-ray energy increases, the greyscale values also increases. This is because more energetic photons were generated, thus the images appears lighter which in tend gives higher greyscale values.

One can see that the flammable liquids can be separated from innocuous liquids, regardless of the liquid thickness variations. The greyscale values of flammable liquids i.e. gasohol 91, ethanol 20, ethanol, cooking oil are greater than that of water, proving that they have low density, which is one of the important properties in determining explosives. As mentioned by Kalinin et al. (2008), flammable liquids contains less or almost no oxygen compared to innocuous liquids which consists of mostly water solutions.

4.2. Testing the System: Estimation of Percentage Error

The estimation of percentage error between the actual density and the density read out by the system are summarized in Table 4.15 to Table 4.20 for the liquids mentioned in Table 3.5.

Table 4.15 Percentage error between the actual density and the density read out for gasohol 95 at thickness 6.0 cm (Given that actual density of gasohol 95 = 0.7479 g/ml)

X-ray Energy, kVp	Density Read Out (g/ml)	Percentage Error (%)
70	0.7478	0.0176
80	0.7505	0.3501
90	0.7529	0.6630
100	0.7436	0.5773
110	0.7509	0.3971
120	0.7518	0.5275
130	0.7469	0.1353
140	0.7471	0.1084
150	0.7457	0.2893
160	0.7468	0.1527
170	0.7466	0.1758
180	0.7523	0.5860
190	0.7466	0.1715
200	0.7430	0.6545

The liquid tested in Table 4.16 above is gasohol 95. Gasohol 95 is composed of 95% octane gasoline and 5% ethanol. The percentage error obtained is small since the composition of gasohol 95 is most likely similar to the composition of the liquid used for calibration, thus the X-rays interaction is similar.

Table 4.16 Percentage error between the actual density and the density read out for ethanol 85 at thickness 6.0 cm (Given that actual density of ethanol 85 = 0.7834 g/ml)

X-ray Energy, kVp	Density Read Out (g/ml)	Percentage Error (%)
70	0.8188	4.5157
80	0.8245	5.2435
90	0.8085	3.2003
100	0.8592	9.6801
110	0.8051	2.7715
120	0.7932	1.2533
130	0.7960	1.6050
140	0.7807	0.3495
150	0.8136	3.8590
160	0.8237	5.1415
170	0.7926	1.1746
180	0.7961	1.6217
190	0.7823	0.1412
200	0.7772	0.7874

From Table 4.16, the percentage error obtained for ethanol 85 is a little higher. This is because ethanol 85 is composed of mixture between base oil and ethanol which makes it different from the liquids used for calibration. However, it can still be recognized as a flammable liquid since the density read out is still less than 1.0 g/ml i.e. the density of water.

Table 4.17 Percentage error between the actual density and the density read out for diesel at thickness 6.0 cm (Given that actual density of diesel = 0.8220 g/ml)

X-ray Energy, kVp	Density Read Out (g/ml)	Percentage Error (%)
70	0.7594	7.6194
80	0.7591	7.6543
90	0.7624	7.2532
100	0.7596	7.5951
110	0.7546	8.2050
120	0.7588	7.6931
130	0.7640	7.0572
140	0.7617	7.3418
150	0.7679	6.5835
160	0.7570	7.9092
170	0.7505	8.7042
180	0.7567	7.9443
190	0.7604	7.4884
200	0.7643	7.0219

Table 4.17 shows that the percentage error of diesel is high but consistent. Diesel is composed of higher HC composition than in normal fuel used for calibration, thus showing that the X-ray interaction is also different. However, diesel can be distinguished from innocuous liquid as the density read out is less than 1.0 g/ml i.e. the density of water.

Table 4.18 Percentage error between the actual density and the density read out for unknown A at thickness 6.0 cm (Given that actual density of unknown A = 0.7211 g/ml)

X-ray Energy, kVp	Density Read Out (g/ml)	Percentage Error (%)
70	0.7660	6.2240
80	0.7470	3.5908
90	0.7450	3.3183
100	0.7481	3.7494
110	0.7428	3.0119
120	0.7427	3.0012
130	0.7427	2.9943
140	0.7444	3.2380
150	0.7498	3.9733
160	0.7461	3.4644
170	0.7486	3.8071
180	0.7470	3.5980
190	0.7518	4.2601
200	0.7557	4.8027

From Table 4.18, the density read out by the system for unknown A is greater than the given actual density i.e. 0.7211 g/ml. In fact, the composition of liquid unknown A comprises of low atomic number since it is composed of pure base fuel. The percentage error is consistent for all kVp except at 70 kVp, in which the X-ray energy might be too low for penetration compared to at high kVp. Hence, the error is from the calibration data set as the composition of unknown A does not matches the group of liquid used for calibration.

Table 4.19 Percentage error between the actual density and the density read out for unknown B at thickness 6.0 cm (Given that actual density of unknown B = 0.7409 g/ml)

X-ray Energy, kVp	Density Read Out (g/ml)	Percentage Error (%)
70	0.8162	10.1641
80	0.7618	2.8262
90	0.7529	1.6134
100	0.7634	3.0403
110	0.7462	0.7208
120	0.7440	0.4168
130	0.7479	0.9429
140	0.7501	1.2394
150	0.7625	2.9177
160	0.7540	1.7656
170	0.7552	1.9309
180	0.7562	2.0598
190	0.7573	2.2102
200	0.7613	2.7550

จุฬาลงกรณ์มหาวิทยาลัย
CHULALONGKORN UNIVERSITY

The percentage error for unknown B summarized in Table 4.19 is the smallest among other liquids. Notably, the composition of unknown B is most likely similar to the liquids in the calibration data set. However, the percentage error for unknown B is the highest at 70 kVp, in which this may be due to the statistical error originates from the X-ray energy, kVp for being too low and does not penetrate well compared to at higher kVp.

Table 4.20 Percentage error between the actual density and the density read out for unknown C at thickness 6.0 cm (Given that actual density of unknown C = 0.8108 g/ml)

X-ray Energy, kVp	Density Read Out (g/ml)	Percentage Error (%)
70	0.8747	7.8761
80	0.7797	3.8418
90	0.7637	5.8075
100	0.7738	4.5620
110	0.7527	7.1613
120	0.7547	6.9200
130	0.7516	7.3001
140	0.7563	6.7264
150	0.7701	5.0234
160	0.7727	4.7038
170	0.7667	5.4365
180	0.7713	4.8720
190	0.7687	5.1880
200	0.7678	5.3090

จุฬาลงกรณ์มหาวิทยาลัย
CHULALONGKORN UNIVERSITY

Unknown C is known as a type of diesel obtained from CALTEX, which is basically a flammable liquid. However, the density read out by the system as shown in Table 4.20 is slightly different compared to its actual density, which is approximately 0.8108 g/ml. Similar to diesel, unknown C is composed of higher HC composition compared to other types of fuel used for calibration. Even so, it is still separable from the innocuous types of liquid as the density read out is still less than water i.e. 1.0 g/ml.

4.3. In-Situ Inspection

The corrected raw data obtained for in-situ calibration at 140 kVp is summarized in Appendix D. Meanwhile, Table 4.21 shows the summarized data for in-situ measurement of liquids in Table 3.5 which was done randomly at 140 kVp i.e. the approximate minimum percentage error obtained in accordance to the estimation of percentage error in section 4.2.

Table 4.21 Measurements for several types of liquid at 140 kVp by using LScanInsitu software

Thickness (cm)	Type of Liquid	Actual Density (g/ml)	Density Read Out (g/ml)	Percentage Error (%)
4.5	Gasohol 95	0.7479	0.766	2.4201
	Ethanol 85	0.7834	0.799	1.9913
	Diesel	0.8220	0.778	5.3528
	Fish Sauce	1.2177	> 1.420	Out of Range
6.0	Unknown A	0.7211	< 0.740	Out of Range
	Unknown B	0.7409	< 0.740	Out of Range
	Unknown C	0.8108	< 0.740	Out of Range
	Fish Sauce	1.2177	> 1.420	Out of Range
7.5	Unknown A	0.7211	0.747	3.5917
	Unknown B	0.7409	0.747	0.8233
	Unknown C	0.8108	0.749	7.6221
	Fish Sauce	1.2177	> 1.420	Out of Range

(Note: Out of Range simply means the percentage error is not in the range of the calibration data set, as the greyscale values are either above or below the maximum and minimum range of the calibrated data set.)

As seen in Table 4.21, the density read out for the tested samples at 4.5, 6.0, and 7.5 cm thickness satisfies with the actual densities except for fish sauce. Fish sauce is basically a type of liquid solution, compared to the other types of liquid which is a type

of liquid compound. Fish sauce is mainly composed of sodium, Na and iodine, I. The probability of X-rays interaction occurring are dependent on the photon energies and the atomic number of the material. This is explained by the photoelectric interaction as it increases with atomic number Z , where the binding energy moves closer to the photon energy. Iodine, I have the k-electron binding energy of approximately 33 keV. When the k-electron binding energy is higher than 33 keV, they interact with the k-shells electron. More electrons in the material are available for interactions which caused the sudden increase in the attenuation coefficient at the k-shell energy. Hence, the attenuation coefficient below the k-edge i.e. 5.6 jumps up to 36 keV (Sprawls, n.d.).

Generally, the probability of photoelectric interactions (attenuation coefficient values) is proportional to Z^3 . To put it another way, the conditions that increase the probability of photoelectric interactions are low photon energies and high atomic number materials (Sprawls, n.d.).

On the contrary, liquids of unknown A, B and C at 6.0 cm have the density output closer to the lower limit of the liquid density range i.e. 0.740 g/ml. This is because, the greyscale read out is higher than the maximum range of the calibrated data set i.e. in between greyscale values of 62.1979 to 97.86608 (see Appendix D). The maximum greyscale value 97.86608 is shown for brighter images proving that the calculated density is less than the minimum density of 0.740 g/ml.

4.4. Comparison between LScan2015 and LScanInsitu

The calibrated data after correction for three different thickness 4.5, 6.0 and 7.5 cm at 140 kVp for LScan2015 and LScanInsitu is summarized in Appendix H, and Table 4.22 summarizes the comparison of the density read out by the software.

Table 4.22 Comparison of density read out obtained by LScan2015 and LScanInsitu

Thickness (cm)	Type of Liquid	Actual Density (g/ml)	Density Read Out by LScan2015 (g/ml)	Density Read Out by LScanInsitu (g/ml)
4.5	Gasohol 95	0.7479	0.991	0.766
	Ethanol 85	0.7834	1.005	0.799
	Diesel	0.822	1.001	0.778
	Fish Sauce	1.2177	> 1.420	> 1.420
6.0	Unknown A	0.7211	0.757	< 0.740
	Unknown B	0.7409	0.757	< 0.740
	Unknown C	0.8108	0.771	< 0.740
	Fish Sauce	1.2177	> 1.420	> 1.420
7.5	Unknown A	0.7211	0.770	0.747
	Unknown B	0.7409	0.744	0.747
	Unknown C	0.8108	0.790	0.749
	Fish Sauce	1.2177	> 1.420	> 1.420

The percentage error obtained from the LScan2015 software is higher than that in LScanInsitu, this is because of the difference in the calibration data. In LScan2015, the calibration was done by referring to the corrected raw data done on separate days in which the settings might have been slightly changed. Meanwhile for LScanInsitu, the calibration was done on the same day with the inspection of liquids which reduces the probability of changes in the geometry settings of the system.

4.5. Discussions

According to the data obtained, the actual density and the density read out by the system is not constant, provided that the X-ray beam output during radiographic exposure is not constant. Increase in kV results in the generation of more energetic (more

penetrating) X-rays (IAEA, 1992). Voltage differ and the maximum X-ray output occurs when voltage peaks. This is true for conventional X-ray tube as used in this study, therefore output tends to vary with time (Prosch and Larson, 2000).

Likewise, the intensity of X-rays produced also depends on the number of electrons hitting the target i.e. the tube current (mA). Tube current can be controlled by controlling the number of electrons emitted by the filament i.e. by controlling the heating current. Increasing the milliamperage increases the number of electrons that are available to strike the target. This in turn increases the quantity or the intensity of X-rays (IAEA, 1992). However, the mA applied in this study cannot be adjusted since the Rigaku Radioflex RF200EGM2 X-ray Machine used does not have this feature.

Comparatively, the spectrum of photon energies within an X-ray beam is most directly affected and controlled by the kV, therefore the sensitivity is inconsistent but changes with the kV selected. Significant exposure errors can occur if technical parameters such as kV and mAs are not adjusted to compensate for the variation in sensitivity (Sprawls, n.d.).

Besides, the geometry of the system might have been slightly changed causing the centre of the X-ray beam to deviate from the original position. In either case, both were believed to have caused the fluctuations in the attenuation thus creating the inconsistent reading of the greyscale level. In order to overcome this problem, the geometry settings of the system should be kept constant at all time as this may interfere with the screening process as well as causing imbalance to the fluoroscopic system.

Apart from that, since the densities of liquids were measured by using an electronic analytical balance, all measurements may be associated with some uncertainty. Many influences affect accuracy and precision of the weighing results. Such influences originate from the balance and the weighing of samples (e.g. repeatability, eccentric load of the sample, operator etc.) especially with small sample masses (Salahinejad, 2007). It is important to minimise the uncertainty for a more accurate and precise measurement. A few recommendations are by checking the

measurements by repeating them or by refining the measurement method or technique using a more sensitive balance which has less value of readability (i.e. rounding off the measurement values correctly) (Salahinejad, 2007; Bell, 1999).



CHAPTER 5

CONCLUSION

5. Conclusion

5.1. Discussion

The main objective of this research is to study and develop the X-ray imaging technique for liquid screening at airport by using digital camera for data acquisition. This method was selected since the principle of real-time imaging radiography provides tremendous cost savings and fast inspection. In lieu of this, the use of Canon EOS 1100D DSLR camera coupled with a GOS fluorescent screen for image viewing system is the primary scope of this research. The camera settings were set constant for all exposure i.e. with aperture values f14, shutter speed 2”5, and ISO 400.

X-rays of energies ranging from 70 kVp to 200 kVp were used as the radiation source. As a matter of fact, X-ray physics are well known and easy to understand and the X-ray machine is easy to operate. Furthermore, X-rays is capable of inspecting fluids in closed/unopened containers with safe and continuous security surveillance.

Besides, systems with fluorescent screens are suitable for the inspection of light materials (Link et al., 1989), in this case, for different types of liquid (i.e. densities ranging from 0.7 to 1.4 g/ml) of different thickness in bottles.

This study uses gasoline obtained from the gasoline pumps station. There are many types of gasoline available commercially, such as gasohol 91 (green in colour), gasohol 95 (orange in colour) and diesel, and each types differs from each companies. These flammable liquids were filled into thin plastic bottles of 4.5, 6.0 and 7.5 cm dimension. Other liquids that were used were ethanol, ethanol 20, cooking oil, water,

shampoo, concentrated syrup and pure honey, whereby water, shampoo, concentrated syrup and pure honey represents the innocuous types of liquid.

After exposing to each X-ray energy, the greyscales of the X-ray images were normalized with water since water contents are capable of distinguishing flammable and innocuous liquids. The calibration data was constructed by measuring the greyscale values of these liquids with the software designed by using Microsoft Visual Basic 6.0. The calibrated data set is shown in Appendix B, in which they were used as the data input of the developed software called LScan2015.

To satisfy the objective of this research, the system was tested with several types of unknown liquids to verify the constructed calibration data set. The different types of liquid used for testing were gasohol 95, ethanol 85, diesel, unknown A, unknown B and unknown C. They were exposed with the same condition as it was done for constructing the calibration data set. The images obtained were analysed by the LScan2015 software. In order to identify the type of liquid present being either innocuous or threat, interpolation technique was applied to the calibration data set which gives the estimation of the exact value of the liquid density.

From the analysis, liquids of which have similar compositions to the liquid in the calibration data set will have higher accuracy. Meanwhile, liquids such as diesel and unknown C shows lower accuracy as their composition is slightly different from that of the calibration data sets.

All things considered, the measurement with such system were influenced by several factors. First, the X-ray intensity output which is inconsistent. Second, the geometry settings of the system is considered to have the greatest influence since a slightest change in geometry settings can cause fluctuations in the measurement. Another reason which influenced the measurement is the fluorescent screen as it is also dependant on the X-ray energies. Low X-ray energy gives low intensities on the fluorescence screen, and conversely high X-ray energy will give higher intensities.

In case of a system of an unstable geometry settings, the in-situ technique should be put into consideration. The results obtained by this method shows higher accuracy, since the calibration data constructed was done at the same geometry settings. Appendix D summarizes the calibration data obtained by in-situ technique i.e. from LScanInsitu software.

In short, the system developed in this study has the potential to discriminate between a threat and an innocuous liquid, thus minimizing the threat of misusing these hazardous liquids for terrorist attack. Such system typically takes about 2-3 minutes of inspection time to interpret the results and to deduce the type of liquid present i.e. either innocuous or threat. This shows that the system offers short exposure/inspection time with acceptable false/positive alarm rates.

Under those circumstances, the following are important considerations for deploying the X-ray screening technology at airports (Singh and Singh, 2003):

- i) The ability to detect various types and quantities of explosives since they can be hidden and modified in variety of ways.
- ii) False alarms must be resolved either by human intervention or technical means, given that there are millions of passengers travelling every day.
- iii) Resolving alarms depend on human operators either to inspect the images acquired or by other means of detection. Hence, operator training is required.
- iv) Laboratory test performance often works much better rather than in real life operational performance.

5.2. Recommendations for Future Research

The following recommendations are seen for enhancing the efficiency of the system:

- i) Expansion on the range of densities of different types of liquid used for calibration since there are many existing products available in the market.
- ii) It is also preferable to use a camera which has an adapter installed for recharging the battery instead of changing the battery itself like what was done in this study as this process may disrupt the geometry settings, thus causing imbalance to the system.
- iii) To use a computer with higher greyscale colour depth (other than 8-bit greyscale as used in this study) which increases the ability to distinct each pixel in a single sample.
- iv) To test with different types of container (e.g. glass bottles) in order to check the consistency of the data. This can be done by identifying and comparing the greyscales of the different types of empty containers.
- v) Exposing water simultaneously with the liquids used for calibration instead of at different times.
- vi) Measuring greyscales of the images with smaller region of interest (i.e. smaller than 60×60 pixels) as this is favourable for other types of thin plastic bottles of different diameters (i.e. round plastic bottles) instead of a typical square/rectangular shape of thin plastic bottles as used in this study.

REFERENCES

Akaranate, A., and et al. Fast and low cost x-ray stereoradiography displayed on a 3D monitor. **Open Journal of Applied Sciences** 3 (2013): 308-311.

Bell, S. **A Beginner's Guide to Uncertainty of Measurement**. Measurement Good Practice Guide No. 11 (Issue 2). United Kingdom: Crown Copyright, 1999.

Bunama, R. M., and Karim, G. A. Modeling the formation of flammable atmospheres within cylindrical containers containing some liquid fuel. **Proceedings of the Combustion Institute** Vol. 28 (2000): 2867-2874.

Canon Inc. EOS 1100D Digital SLR Camera. [Online.] (n.d.). Available from: https://www.canon.com.au/~media/Product%20Brochures/Camera/Digital%20SLR%20Cameras/EOS/EOS%201100D%20Tech%20Sheet_FINAL.ashx [20 September 2015].

Casale, D. EU measures on transportation security against terrorism. In Tahmisoğlu, M., and Özen, C., **Transportation Security against Terrorism**, 99-107. Ankara, Turkey: IOS Press BV, 2009.

De Ruiter, C.J., and Lemmens, O. M. E. J. Liquid explosives – The threat to civil aviation and the European response. In Kuznetsov, A. V., and Schubert, H., **Detection of Liquid Explosives and Flammable Agents in Connection with Terrorism**, 205-213. Saint-Petersburg, Russia: Springer Science + Business Media B. V., 2008.

ECORYS. Study on the competitiveness of the EU security industry within the framework contract for sectoral competitiveness studies – ENTR/06/054 [Online]. 2009. Available from: http://ec.europa.eu/enterprise/policies/security/files/study_on_the_competitiveness_of_the_eu_security_industry_en.pdf [4 November 2014].

Feng, Q., Sahin, H., and Kapur, Kailash C. Designing airport checked-baggage-screening strategies considering system capability and reliability. **Reliability Engineering and System Safety** 94 (2009): 618-627.

Gaft, M., and Nagli, L. Liquid explosives detection in transparent containers. In Harmon, R. S., Holloway, J. H., and Broach, J. T., **Proc. SPIE 7664 Detection and Sensing of Mines, Explosives Objects, and Obscured Targets**, 2010.

Garrett, W.R., Splettstosser, H. R., Titus, D. E., and et al. **Radiography in Modern Industry**. Fourth Edition. New York: Eastman Kodak Company, 1980.

GTE Products Corporation. Terbium-activated gadolinium oxysulfide X-ray phosphor. [Online.] 1980. Available from: <http://patents.justia.com/patent/4507560> [8 September 2015].

Halmshaw, R. **Industrial Radiology: Theory and Practice**. England: Applied Science LTD, 1982.

IAEA. **Industrial Radiography**. Training Course Series No. 3. Vienna: International Atomic Energy Agency, 1992.

Jezeirski, G., X-ray Generation. [Online.] (n.d.). Available from: <http://xrayweb.chem.ou.edu/notes/xray.html> [2 September 2015].

Kalinin, V. A., et al. Detector of hazardous substances based on nanosecond neutron analysis. In Kuznetsov, A. V., and Schubert, H., **Detection of Liquid Explosives and Flammable Agents in Connection with Terrorism**, 71-78. Saint-Petersburg, Russia: Springer Science + Business Media B. V., 2008.

Krausa, M. Vapor detection of explosives for counterterrorism. In Krausa, M., and Reznev, A. A., **Vapour and Trace Detection of Explosives for Anti-Terrorism Purposes**, 1-9. Pfinztal, Germany: Kluwer Academic Publishers, 2004.

Kuznetsov, A. V., and Osetrov, O.I. Overview of Liquid Explosives' Detection. In Kuznetsov, A. V., and Schubert, H., **Detection of Liquid Explosives and Flammable Agents in Connection with Terrorism**, 7-13. Saint-Petersburg, Russia: Springer Science + Business Media B. V., 2008.

Link, R., and et al. Weld inspection using real-time radiography. In McGonnagle, W. J., **International Advances in Nondestructive Testing: Volume 14**, 143-173. Switzerland: Gordon and Breach Science, 1989.

Liu, J. **Liquid Explosives**. Vol. 11. 1st ed. Verlag Berlin Heidelberg: Springer, 2015.

Markey, J. Terrorism risk for public transportation systems. In Tahmisoğlu, M., and Özen, C., **Transportation Security against Terrorism**, 116-150. Ankara, Turkey: IOS Press BV, 2009.

Menning, D., and Östmark, H. Detection of Liquid and Homemade Explosives: What Do We Need to Know About Their Properties? In Kuznetsov, A. V., and Schubert, H., **Detection of Liquid Explosives and Flammable Agents in Connection with Terrorism**, 55-70. Saint-Petersburg, Russia: Springer Science + Business Media B. V., 2008.

Ministry of the Solicitor General. Commentary on Part 4 of the Ontario Fire Code O. Reg. 388/97. [Online.] 2001. Available from: <http://www.mcscs.jus.gov.on.ca/stellent/groups/public/@mcscs/@www/@ofm/documents/webasset/ecofm000350.pdf> [9 September 2015].

Mostak, P. Chemistry and Properties in Liquid Explosives. In Kuznetsov, A. V., and Schubert, H., **Detection of Liquid Explosives and Flammable Agents in Connection with Terrorism**, 15-25. Saint-Petersburg, Russia: Springer Science + Business Media B. V., 2008.

Mueller, J. Case 1: The Shoe Bomber. [Online.] 2011. Available from: <http://politicalscience.osu.edu/faculty/jmueller/01SHOE7.pdf> [3 September 2015].

NAOO. Solar Calculator Glossary – Electromagnetic Spectrum. [Online.] (n.d.). Available from: <http://www.esrl.noaa.gov/gmd/grad/solcalc/glossary.html> [2 September 2015].

PETRO Industry News. Analytical Instrumentation: What is the difference between flash point and ignition temperature? [Online.] 2014. Available from: http://www.petro-online.com/news/analytical-instrumentation/11/breaking_news/what_is_the_difference_between_flash_point_and_ignition_temperature/30656/ [16 June 2015].

Prosch, A., and Larson, B. **Real-time Radiography: An Introductory Course Module for NDT Students**. Iowa State: NSF-ATE, 2000.

Robert N. Cherry, Jr. Chapter 48 – Radiation: Ionizing. [Online.] (n.d.). Available from: <http://www.ilocis.org/documents/chpt48e.htm> [2 September 2015].

Rumerman, J. Aviation Security. [Online.] (n.d.). Available from: http://www.centennialofflight.net/essay/Government_Role/security/POL18.htm [4 September 2015].

Salahinejad, M. and Aflaki, F. Uncertainty measurement of weighing results from an electronic analytical balance. **Measurement Science Review** 7 (2007): 67-75.

Schubert, H. The Terrorist Pallet of Liquid Explosives and Flammable Fuels. In Kuznetsov, A. V., and Schubert, H., **Detection of Liquid Explosives and Flammable Agents in Connection with Terrorism**, 1-5. Saint-Petersburg, Russia: Springer Science + Business Media B. V., 2008.

Sameer Singh and Maneesha Singh. Explosives detection systems (EDS) for aviation security. **Signal Processing** 83 (January 2003): 31-55.

Simona Babeti (Pretorian) et al. Testing a low cost digital fluoroscopic system. **Romanian Journal Physics** Vol. 57 (January 2012): 1293-1307.

Sprawls, P. The physical principles of medical imaging. [Online.] (n.d.). Available from: <http://www.sprawls.org/ppmi2/> [3 October 2015].

Sudac, D., and Valkovic, V. Discrimination of the explosives from other materials by using the tagged neutron beam. In Kuznetsov, A. V., and Schubert, H., **Detection of Liquid Explosives and Flammable Agents in Connection with Terrorism**, 167-178. Saint-Petersburg, Russia: Springer Science + Business Media B. V., 2008.

Thomas M. Moffett Jr. Identifying a liquid using physical properties. [Online.] 2009. [http://faculty.plattsburgh.edu/craig.hoag/Chem111/ExperimentalWriteups/Identifying %20a%20Liquid.pdf](http://faculty.plattsburgh.edu/craig.hoag/Chem111/ExperimentalWriteups/Identifying%20a%20Liquid.pdf) [9 September 2015].

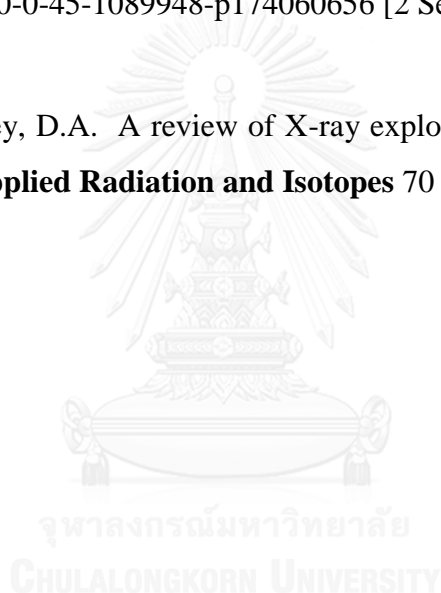
TSA. Intro: The evolution timeline of airline security measures. [Online.] 2005. Available from: http://www.tsa.gov/video/evolution/TSA_evolution_timeline.pdf [13 June 2015].

TSA. Traveller Information: 3-1-1 Liquids Rule. [Online.] (n.d.). Available from: <http://www.tsa.gov/traveler-information/3-1-1-liquids-rule> [27 June 2015].

Turecek, J. Possibilities of Liquid Explosives Countermeasures at Airports. In Kuznetsov, A. V., and Schubert, H., **Detection of Liquid Explosives and Flammable Agents in Connection with Terrorism**, 133-141. Saint-Petersburg, Russia: Springer Science + Business Media B. V., 2008.

Waseda, Y., Matsubara, E., and Shinoda, K. X-ray Diffraction Crystallography – Introduction, Examples and Solved Problems. [Online.] 2011. Available from: http://www.springer.com/cda/content/document/cda_downloaddocument/9783642166341-c1.pdf?SGWID=0-0-45-1089948-p174060656 [2 September 2015].

Wells, K., and Bradley, D.A. A review of X-ray explosives detection techniques for checked baggage. **Applied Radiation and Isotopes** 70 (January 2012): 1729-1746.



APPENDICES

APPENDIX A

Full Program Code of Liquid Scan Analysis for Calibration (LScan2015)

```

Option Explicit
Private W As Integer
Private XPOS As Integer
Private YPOS As Integer
Private A(20, 15, 5) As Single
Private B(20, 5) As Single
Private C(20, 5) As Single
Private T(5) As Single
Private IxCal(15) As Single
Private D(15) As Single
Private Thick As Single
Private IxW(20, 5) As Single
Private IoW(20, 5) As Single
Private IxLiq As Single
Private IoLiq As Single
Private PosX1 As Integer
Private PosX2 As Integer
Private PosY1 As Integer
Private PosY2 As Integer
Private KV As Integer
Private DenCal As Single
Private IxLiqCor As Single

Case "100 kV"
KV = 4
Case "110 kV"
KV = 5
Case "120 kV"
KV = 6
Case "130 kV"
KV = 7
Case "140 kV"
KV = 8
Case "150 kV"
KV = 9
Case "160 kV"
KV = 10
Case "170 kV"
KV = 11
Case "180 kV"
KV = 12
Case "190 kV"
KV = 13
Case "200 kV"
KV = 14
End Select

Private Sub Combo1_Click()

End Sub

Select Case Combo1.Text
Case "70 kV"
KV = 1
Case "80 kV"
KV = 2
Case "90 kV"
KV = 3
Private Sub Command1_Click()
Dim i As Integer
Dim j As Integer
Dim Sum1 As Single
Dim Sum2 As Single
Dim Sum3 As Single

```

```

Dim DenIo1 As Single
Dim DenIo2 As Single
Dim STD As Single
Dim SNR As Single

Picture1.Cls

Picture1.Line (XPOS, YPOS)-(XPOS + W, YPOS
+ W), QBColor(13), B
Sum1 = 0
For i = XPOS + 1 To XPOS + W - 1
    For j = YPOS + 1 To YPOS + W - 1
        Sum1 = Sum1 + Picture1.Point(i, j) Mod 256
    Next j
Next i
IxLiq = Sum1 / ((W - 2) * (W - 2))
Label10.Caption = IxLiq ' Ix(avg)

Picture1.Line (PosX1, PosY1)-(PosX1 + W,
PosY1 + W), QBColor(13), B
Sum2 = 0
For i = PosX1 + 1 To PosX1 + W - 1
    For j = PosY1 + 1 To PosY1 + W - 1
        Sum2 = Sum2 + Picture1.Point(i, j) Mod 256
    Next j
Next i
DenIo1 = Sum2 / ((W - 2) * (W - 2))

Picture1.Line (PosX2, PosY2)-(PosX2 + W,
PosY2 + W), QBColor(13), B
Sum3 = 0
For i = PosX2 + 1 To PosX2 + W - 1
    For j = PosY2 + 1 To PosY2 + W - 1
        Sum3 = Sum3 + Picture1.Point(i, j) Mod 256
    Next j
Next i
DenIo2 = Sum3 / ((W - 2) * (W - 2))

IoLiq = (DenIo1 + DenIo2) / 2
Label6.Caption = IoLiq
Label21.Caption = ""
Label17.Caption = ""

Label19.Caption = ""
Label20.Caption = ""

End Sub

Private Sub Command2_Click()
Dim Response As Variant
Dim i As Integer
Dim j As Integer
Dim ThickPos As Integer
Dim DiffThick As Single
Dim RangeThick As Single
Dim RangeIx As Single
Dim IxPos As Integer
Dim DiffIx As Single
Dim RangeIxCal As Single
Dim RangeDen As Single
Dim RangeIow As Single
Dim IoWint As Single

'Select kV of X-ray
If KV = 0 Then
    Response = MsgBox("Please select kV of x-ray",
vbOKOnly, "Liquid Scan")
    Combo1.SetFocus
    GoTo EndLoop
End If

Thickness Indication
If Thick < 4.5 Or Thick > 7.5 Then
    Response = MsgBox("Please input Liquid
thickness between 4.5 - 7.5 cm.", vbOKOnly, "Liquid
Scan")
    Text7.SetFocus
    GoTo EndLoop
End If

For i = 1 To 3
    If Thick = T(i) Then
        ThickPos = i
        GoTo CalIx
    End If

```

```

If Thick < T(i) Then
    ThickPos = i - 1
    GoTo CalIx
End If
Next i

'Interpolation of Liquid Intensity vs Liquid Density
at given thickness
CallX:
    DiffThick = Thick - T(ThickPos) 'Thicknes Index
    RangeThick = T(ThickPos + 1) - T(ThickPos)
    For j = 1 To 8
        RangeIx = A(KV, j, ThickPos + 1) - A(KV, j,
ThickPos)
        IxCal(j) = A(KV, j, ThickPos) + (RangeIx /
RangeThick * DiffThick)
    Next j

'Calculation of Liquid Density
RangeLow = IoW(KV, ThickPos + 1) - IoW(KV,
ThickPos)
IoWint = IoW(KV, ThickPos) + RangeLow *
DiffThick / RangeThick
IxLiqCor = IoW(KV, ThickPos) / IoLiq * IxLiq
IxLiqCor = IoWint / IoLiq * IxLiq
Label21.Caption = IxLiqCor

If IxLiqCor > IxCal(1) Then
    Response = MsgBox("Input intensity is higher than
maximun limit !!!", vbOKOnly, "Liquid Scan")
    Call CheckData
    GoTo EndLoop
End If

If IxLiqCor < IxCal(8) Then
    Response = MsgBox("Input intensity is lower than
minimum limit !!!", vbOKOnly, "Liquid Scan")
    Call CheckData
    GoTo EndLoop
End If

Intensity Indication
For i = 1 To 8
    If IxLiqCor = IxCal(i) Then
        IxPos = i
        GoTo CalDen
    End If
    If IxLiqCor > IxCal(i) Then
        IxPos = i - 1
        GoTo CalDen
    End If
Next i

CalDen:
    DiffIx = IxCal(IxPos) - IxLiqCor 'Diff.
Intensity Index
    RangeIxCal = IxCal(IxPos) - IxCal(IxPos + 1)
    RangeDen = D(IxPos + 1) - D(IxPos)
    DenCal = D(IxPos) + (RangeDen / RangeIxCal) *
DiffIx
    Label17.Caption = Round(DenCal, 3)
    Label19.Caption = Round((DenCal - DenCal *
0.006), 3)
    Label20.Caption = Round((DenCal + DenCal *
0.006), 3)
EndLoop:
If DenCal < 1 Then
    Image1.Visible = True
    Image2.Visible = False
Else
    Image2.Visible = True
    Image1.Visible = False
End If

End Sub
Sub CheckData()
Dim Response As Variant

If IxLiqCor > IxCal(1) And IxLiqCor < (IxCal(1) +
IxCal(1) * 0.006) Then

```

```

Label17.Caption = " 0.74"
Label19.Caption = " 0.7326"
Label20.Caption = " 0.7474"
GoTo EndLoop
End If

If IxLiqCor > (IxCal(1) + IxCal(1) * 0.006) Then
    Response = MsgBox("Liquid density is lower than
0.74 g/cc", vbOKOnly, "Liquid Scan")
    Label17.Caption = " < 0.74"
    Label19.Caption = ""
    Label20.Caption = ""
    GoTo EndLoop
End If

If IxLiqCor < IxCal(8) And IxLiqCor > (IxCal(8) -
IxCal(8) * 0.006) Then
    Label17.Caption = " 1.42"
    Label19.Caption = " 1.4058"
    Label20.Caption = " 1.4342"
    GoTo EndLoop
End If

If IxLiqCor < (IxCal(8) - IxCal(8) * 0.006) Then
    Response = MsgBox("Liquid density is higher
than 1.42 g/cc", vbOKOnly, "Liquid Scan")
    Label17.Caption = " > 1.42"
    Label19.Caption = ""
    Label20.Caption = ""
    GoTo EndLoop
End If

EndLoop:
End Sub

Private Sub Form_Load()
Combo1.AddItem "70 kV"
Combo1.AddItem "80 kV"
Combo1.AddItem "90 kV"
Combo1.AddItem "100 kV"
Combo1.AddItem "110 kV"
Combo1.AddItem "120 kV"

Combo1.AddItem "130 kV"
Combo1.AddItem "140 kV"
Combo1.AddItem "150 kV"
Combo1.AddItem "160 kV"
Combo1.AddItem "170 kV"
Combo1.AddItem "180 kV"
Combo1.AddItem "190 kV"
Combo1.AddItem "200 kV"

W = 60
KV = 1
PosX1 = 120
PosY1 = 230
PosX2 = 500
PosY2 = 230
Text1.Text = PosX1
Text2.Text = PosY1
Text3.Text = PosX2
Text4.Text = PosY2
XPOS = 315 Picture1.ScaleWidth \ 2
YPOS = 230 Picture1.ScaleHeight \ 2
Text5.Text = XPOS
Text6.Text = YPOS
Label15.Caption = "60 x 60"
Command2.Enabled = False
Image1.Visible = False
Image2.Visible = False

End Sub

Private Sub mnu20x20pixels_Click()
W = 20
Label15.Caption = "20 x 20"
End Sub

Private Sub mnu40x40pixels_Click()
W = 40
Label15.Caption = "40 x 40"
End Sub

Private Sub mnu60x60pixels_Click()

```

```

W = 60
Label15.Caption = "60 x 60"
End Sub

Private Sub mnuCalibrateData_Click()
Dim SourceName As String
Dim i As Integer
Dim j As Integer
Dim k As Integer
Dim fd As String
Dim aa As Single
Dim TT As Single
Dim dd As Single

On Error GoTo Err
CommonDialog1.ShowOpen
SourceName = CommonDialog1.FileName
Open SourceName For Input As #1
For i = 1 To 14
Input #1, fd
Input #1, fd
For j = 1 To 8
Input #1, dd
D(j) = Val(dd)
For k = 1 To 3
Input #1, aa
A(i, j, k) = Val(aa)
Next k
Next j
Next i

Input #1, fd

For i = 1 To 14
Input #1, fd
For j = 1 To 3
Input #1, TT
T(j) = Val(TT)
Input #1, aa
IoW(i, j) = Val(aa)
Next j
Next i

Close #1
MsgBox ("Input data completed !!")
Command2.Enabled = True
Err:
End Sub

Private Sub mnuExit_Click()
Form2.Hide
Menu.Show
End Sub

Private Sub mnuOpenImage_Click()
Dim SourceName As String

On Error GoTo Err
CommonDialog1.ShowOpen
SourceName = CommonDialog1.FileName
Picture1.Picture = LoadPicture(SourceName)
Label14.Caption = SourceName
Combo1.Text = "Select kV"
KV = 0
Label17.Caption = ""
Label19.Caption = ""
Label20.Caption = ""
Err:
End Sub

Private Sub Text1_Change()
PosX1 = Val(Text1.Text)
End Sub

Private Sub Text2_Change()
PosY1 = Val(Text2.Text)
End Sub

Private Sub Text3_Change()
PosX2 = Val(Text3.Text)
End Sub

Private Sub Text4_Change()
PosY2 = Val(Text4.Text)

```

End Sub

Private Sub Text5_Change()

XPOS = Val(Text5.Text)

End Sub

Private Sub Text6_Change()

YPOS = Val(Text6.Text)

End Sub

Private Sub Text7_Change()

Thick = Val(Text7.Text)

End Sub



APPENDIX B

Summary Raw Data of Liquid Scan Analysis for Calibration (LScan2015)

	4.5 cm	6.0 cm	7.5 cm
Density	70 kVp	70 kVp	70 kVp
0.7422	56.11320486	51.97120054	42.09457599
0.7502	56.02814623	50.70713753	40.99980667
0.7828	54.35836477	49.20094972	39.93103424
0.8989	51.47386112	47.44201595	36.35069712
1	45.87336	39.48573	30.07015
1.0205	42.82395604	37.81466672	26.602849
1.3171	38.95085441	32.88977554	22.46383687
1.4238	37.74752854	30.83879791	21.19665440
	4.5 cm	6.0 cm	7.5 cm
Density	80 kVp	80 kVp	80 kVp
0.7422	62.02536267	58.32880621	47.19001770
0.7502	61.73974475	57.14540675	45.80493821
0.7828	59.94229605	55.25129003	44.48721034
0.8989	57.00604499	53.94065675	40.84430273
1	50.49376	44.93936	34.39715
1.0205	48.07981959	42.90491033	31.12092616
1.3171	43.53203526	37.72098603	26.44263339
1.4238	42.66814352	35.93497147	25.08755669
	4.5 cm	6.0 cm	7.5 cm
Density	90 kVp	90 kVp	90 kVp
0.7422	74.46013033	68.02157854	55.93511812
0.7502	73.97724212	66.75825492	55.00787998
0.7828	72.24642349	64.62452881	53.45728871
0.8989	68.85865709	63.44928683	48.98822678
1	62.04637	52.41528	41.76011
1.0205	58.53974423	51.74366246	38.00960016
1.3171	53.22901482	45.59644959	31.66222561
1.4238	51.79151088	43.37124602	30.27609109
	4.5 cm	6.0 cm	7.5 cm
Density	100 kVp	100 kVp	100 kVp
0.7422	85.10179838	73.75681847	62.07280705
0.7502	84.51642045	73.03217523	60.74571249
0.7828	82.05010789	70.13966709	59.15623386
0.8989	78.57643607	68.09344332	54.0227287

1	71.47235	56.88853	46.13198
1.0205	67.4150273	55.47143511	42.41955923
1.3171	62.02013063	48.33127192	35.53962913
1.4238	60.28391729	44.94058717	33.71168612
	4.5 cm	6.0 cm	7.5 cm
Density	110 kVp	110 kVp	110 kVp
0.7422	94.7167151	86.57729001	70.71192274
0.7502	94.18427119	84.45716897	69.12767114
0.7828	92.2338075	81.75824584	67.05186847
0.8989	88.30454442	79.26102456	61.43839547
1	80.05856	68.50803	53.4349
1.0205	76.59140051	65.43526293	48.57258023
1.3171	70.51364331	57.09106554	41.01183937
1.4238	69.10713997	53.2578938	39.11522361
	4.5 cm	6.0 cm	7.5 cm
Density	120 kVp	120 kVp	120 kVp
0.7422	99.43725226	93.29195856	75.948582
0.7502	98.901938	91.42925677	74.2380326
0.7828	98.19759104	88.97837192	71.92142369
0.8989	94.36966994	85.50055295	65.54249619
1	86.78716	74.87396	56.8151
1.0205	82.46907623	70.82775329	51.97555074
1.3171	75.76640041	62.03018033	43.69651642
1.4238	73.90686607	57.71801584	41.20221072
	4.5 cm	6.0 cm	7.5 cm
Density	130 kVp	130 kVp	130 kVp
0.7422	105.7119852	98.30186441	81.94824399
0.7502	104.672321	95.68385576	80.32849404
0.7828	103.8320983	93.56814697	77.85281353
0.8989	100.0324493	90.83079134	72.32199777
1	91.83888	79.1195	62.54756
1.0205	88.00752986	74.14548911	56.95186928
1.3171	81.24870660	67.33624926	48.4157212
1.4238	79.88749562	63.31589376	45.74710022
	4.5 cm	6.0 cm	7.5 cm
Density	140 kVp	140 kVp	140 kVp
0.7422	113.0133946	103.5709748	87.18970235
0.7502	112.6243357	101.8919584	85.29670747
0.7828	110.2359063	97.75693785	83.35515838
0.8989	106.2220413	96.65409064	77.21058484
1	98.02705	84.8044	67.74495
1.0205	93.61519691	80.79303972	63.05445501

1.3171	86.63167166	72.90285657	52.82065372
1.4238	84.51433718	67.59276164	50.20485601
	4.5 cm	6.0 cm	7.5 cm
Density	150 kVp	150 kVp	150 kVp
0.7422	118.6862483	108.645569	91.78179131
0.7502	118.0403997	106.6491945	90.22334546
0.7828	115.44172	103.5742948	87.62660616
0.8989	111.3189597	101.566663	81.88653771
1	103.09040	88.82937	72.28627
1.0205	98.43662884	85.0384356	67.64787567
1.3171	91.4121132	75.04469185	56.95981932
1.4238	89.40158014	71.51349667	53.69497968
	4.5 cm	6.0 cm	7.5 cm
Density	160 kVp	160 kVp	160 kVp
0.7422	124.0151022	112.6456776	97.11093459
0.7502	122.826983	110.6394193	95.40403968
0.7828	121.2400710	107.958483	92.79310783
0.8989	116.6598408	105.6531351	87.01320196
1	108.35370	92.24227	76.41469
1.0205	103.7346846	90.47773784	70.8845113
1.3171	96.51456984	80.33109079	60.71057393
1.4238	94.09046522	75.65339351	57.32211402
	4.5 cm	6.0 cm	7.5 cm
Density	170 kVp	170 kVp	170 kVp
0.7422	129.5030665	118.5767081	101.1478948
0.7502	128.9320478	116.5479125	98.42960017
0.7828	126.2913632	113.140448	96.64236198
0.8989	122.0801818	110.9155103	90.09230848
1	113.68880	97.96106	79.01814
1.0205	109.4583011	94.79902947	75.00202845
1.3171	100.5544465	83.76405282	63.73421201
1.4238	99.08055578	80.60997825	60.57716375
	4.5 cm	6.0 cm	7.5 cm
Density	180 kVp	180 kVp	180 kVp
0.7422	135.6169513	124.0732248	106.4800246
0.7502	134.8186514	121.8457827	106.3263721
0.7828	132.0173948	118.6080706	102.8749055
0.8989	128.4356945	115.8650639	96.28206983
1	119.54400	102.86390	85.80529
1.0205	114.6266234	99.6981424	80.25555618
1.3171	106.7600145	88.22619291	68.63241002
1.4238	104.2633378	84.37252474	65.35835355

	4.5 cm	6.0 cm	7.5 cm
Density	190 kVp	190 kVp	190 kVp
0.7422	139.2144292	126.6422101	110.2824981
0.7502	138.7633268	124.7673522	108.4139201
0.7828	135.7053567	120.8725060	105.1856630
0.8989	131.2523376	118.5797945	99.54833806
1	122.73340	104.93850	86.78032
1.0205	117.4249711	102.2452861	82.00360395
1.3171	109.0654216	91.14432288	69.96387665
1.4238	107.1913707	87.00407447	66.57457106
	4.5 cm	6.0 cm	7.5 cm
Density	200 kVp	200 kVp	200 kVp
0.7422	144.2335328	130.7125059	113.8804220
0.7502	143.7525644	129.1741537	112.0390631
0.7828	141.3603318	123.5301364	109.4479813
0.8989	136.8435832	121.2999443	102.6933321
1	127.84040	108.37900	89.63020
1.0205	122.8953228	105.5383199	85.06586403
1.3171	114.4079394	93.3881661	73.32479115
1.4238	112.4352078	89.49216807	69.07203019
	Io(water)		
70	4.5	81.8949	
	6.0	83.4236	
	7.5	83.9197	
80	4.5	89.4507	
	6.0	93.8744	
	7.5	92.4128	
90	4.5	103.2606	
	6.0	107.0617	
	7.5	106.0100	
100	4.5	116.1131	
	6.0	112.8858	
	7.5	115.8924	
110	4.5	126.5647	
	6.0	129.5276	
	7.5	129.1151	
120			

	4.5	134.5223
	6.0	138.2552
	7.5	137.2539
130		
	4.5	141.1599
	6.0	143.2857
	7.5	145.4559
140		
	4.5	149.0809
	6.0	150.1950
	7.5	150.8710
150		
	4.5	154.7872
	6.0	154.5340
	7.5	155.5363
160		
	4.5	160.4007
	6.0	159.6733
	7.5	161.5480
170		
	4.5	165.9724
	6.0	166.3477
	7.5	166.9551
180		
	4.5	172.0441
	6.0	172.3780
	7.5	174.7478
190		
	4.5	175.1986
	6.0	174.1473
	7.5	177.1240
200		
	4.5	180.4630
	6.0	177.4278
	7.5	180.9177



APPENDIX C

Full Program Code for Liquid Scan Analysis (LScanInsitu)

```

Option Explicit                                Case "110 kV"
Private W As Integer                          KV = 110
Private XPOS As Integer                       Case "120 kV"
Private YPOS As Integer                       KV = 120
Private T(5) As Single                        Case "130 kV"
Private IxCal(15) As Single                   KV = 130
Private D(15) As Single                       Case "140 kV"
Private Thick As Single                       KV = 140
Private IxW(20, 5) As Single                  Case "150 kV"
Private IoW(20, 5) As Single                  KV = 150
Private IxL(20) As Single                     Case "160 kV"
Private IoL(20) As Single                     KV = 160
Private IxLCor(20) As Single                  Case "170 kV"
Private IxLiq As Single                       KV = 170
Private IoLiq As Single                       Case "180 kV"
Private PosX1 As Integer                      KV = 180
Private PosX2 As Integer                      Case "190 kV"
Private PosY1 As Integer                      KV = 190
Private PosY2 As Integer                      Case "200 kV"
Private KV As Integer                         KV = 200
Private DenCal As Single                      End Select
Private IxLiqCor As Single                    End Sub
Private SamName(15) As String
Private ThickNess(20) As String
Private ThickNum As Integer

Private Sub Combo1_Click()
Select Case Combo1.Text
Case "70 kV"
KV = 70
Case "80 kV"
KV = 80
Case "90 kV"
KV = 90
Case "100 kV"
KV = 100

```

```

Select Case Combo3.Text

```

```

Case "Gasohol 91"

```

```

D(1) = 0.7422

```

```

CommonDialog1.ShowOpen

```

```

SamName(1) = CommonDialog1.FileName

```

```

Image1.Picture = LoadPicture(SamName(1))

```

```

Label14.Caption = D(1)

```

```

Case "Ethanol 20"

```

```

D(2) = 0.7502

```

```

CommonDialog1.ShowOpen

```

```

SamName(2) = CommonDialog1.FileName

```

```

Private Sub Combo3_Click()

```

```

Image2.Picture = LoadPicture(SamName(2))
Label19.Caption = D(2)
Case "Ethanol"
D(3) = 0.7828
CommonDialog1.ShowOpen
SamName(3) = CommonDialog1.FileName
Image3.Picture = LoadPicture(SamName(3))
Label20.Caption = D(3)
Case "Cooking oil"
D(4) = 0.8989
CommonDialog1.ShowOpen
SamName(4) = CommonDialog1.FileName
Image4.Picture = LoadPicture(SamName(4))
Label21.Caption = D(4)
Case "Water"
D(5) = 1#
CommonDialog1.ShowOpen
SamName(5) = CommonDialog1.FileName
Image5.Picture = LoadPicture(SamName(5))
Label22.Caption = D(5)
Case "Shampoo"
D(6) = 1.0205
CommonDialog1.ShowOpen
SamName(6) = CommonDialog1.FileName
Image6.Picture = LoadPicture(SamName(6))
Label23.Caption = D(6)
Case "Conc. soda"
D(7) = 1.3171
CommonDialog1.ShowOpen
SamName(7) = CommonDialog1.FileName
Image7.Picture = LoadPicture(SamName(7))
Label24.Caption = D(7)
Case "Pure honey"
D(8) = 1.4238
CommonDialog1.ShowOpen
SamName(8) = CommonDialog1.FileName
Image8.Picture = LoadPicture(SamName(8))
Label25.Caption = D(8)
End Select

End Sub

Private Sub Command1_Click()
Dim i As Integer
Dim j As Integer
Dim Sum1 As Single
Dim Sum2 As Single
Dim Sum3 As Single
Dim DenIo1 As Single
Dim DenIo2 As Single
Dim STD As Single
Dim SNR As Single

Picture1.Cls

Picture1.Line (XPOS, YPOS)-(XPOS + W, YPOS
+ W), QBColor(13), B
Sum1 = 0
For i = XPOS + 1 To XPOS + W - 1
For j = YPOS + 1 To YPOS + W - 1
Sum1 = Sum1 + Picture1.Point(i, j) Mod 256
Next j
Next i
IxLiq = Sum1 / ((W - 1) * (W - 1))
Label10.Caption = IxLiq ' Ix(avg)

Picture1.Line (PosX1, PosY1)-(PosX1 + W,
PosY1 + W), QBColor(13), B
Sum2 = 0
For i = PosX1 + 1 To PosX1 + W - 1
For j = PosY1 + 1 To PosY1 + W - 1
Sum2 = Sum2 + Picture1.Point(i, j) Mod 256
Next j
Next i
DenIo1 = Sum2 / ((W - 1) * (W - 1))

Picture1.Line (PosX2, PosY2)-(PosX2 + W,
PosY2 + W), QBColor(13), B
Sum3 = 0
For i = PosX2 + 1 To PosX2 + W - 1
For j = PosY2 + 1 To PosY2 + W - 1
Sum3 = Sum3 + Picture1.Point(i, j) Mod 256
Next j
Next i

```

```

DenIo2 = Sum3 / ((W - 1) * (W - 1))

IoLiq = (DenIo1 + DenIo2) / 2
Label6.Caption = IoLiq

End Sub

Private Sub Command2_Click()
Dim Response As Variant
Dim i As Integer
Dim j As Integer
Dim ThickPos As Integer
Dim DiffThick As Single
Dim RangeThick As Single
Dim RangeIx As Single
Dim IxPos As Integer
Dim DiffIx As Single
Dim RangeIxCal As Single
Dim RangeDen As Single
Dim RangeLow As Single
Dim IoWint As Single

'Select kV of X-ray
If KV = 0 Then
    Response = MsgBox("Please select kV of x-ray",
vbOKOnly, "In situ Liquid Scan")
    Combo1.SetFocus
    GoTo EndLoop
End If

'Thickness Indication
If Thick = 0 Then
    Response = MsgBox("Please select Liquid
thickness", vbOKOnly, "Liquid Scan")
    GoTo EndLoop
End If

IxLiqCor = IoL(5) / IoLiq * IxLiq
Label11.Caption = IxLiqCor
If IxLiqCor > IxLCor(1) Then
    Response = MsgBox("Input intensity is higher than
maximun limit !!!", vbOKOnly, "Liquid Scan")

Call CheckData
GoTo EndLoop
End If

If IxLiqCor < IxLCor(8) Then
    Response = MsgBox("Input intensity is lower than
minimum limit !!!", vbOKOnly, "Liquid Scan")
    Call CheckData
    GoTo EndLoop
End If

'Intensity Indication
For i = 1 To 8
    If IxLiqCor = IxLCor(i) Then
        IxPos = i
        GoTo CalDen
    End If
    If IxLiqCor > IxLCor(i) Then
        IxPos = i - 1
        GoTo CalDen
    End If
Next i

CalDen:
DiffIx = IxLCor(IxPos) - IxLiqCor      'Diff.
Intensity Index
RangeIxCal = IxLCor(IxPos) - IxLCor(IxPos + 1)
RangeDen = D(IxPos + 1) - D(IxPos)
DenCal = D(IxPos) + (RangeDen / RangeIxCal) *
DiffIx

Label37.Caption = Round(DenCal, 3)
Label38.Caption = Round((DenCal - DenCal *
0.006), 3)
Label39.Caption = Round((DenCal + DenCal *
0.006), 3)

EndLoop:

End Sub
Sub CheckData()

```

```

Dim Response As Variant

If IxLiqCor > IxLCor(1) And IxLiqCor < (IxLCor(1)
+ IxLCor(1) * 0.006) Then
    Label37.Caption = " 0.74"
    Label38.Caption = " 0.7326"
    Label39.Caption = " 0.7474"
    GoTo EndLoop
End If

If IxLiqCor > (IxLCor(1) + IxLCor(1) * 0.006) Then
    Response = MsgBox("Liquid density is lower than
0.74 g/cc", vbOKOnly, "Liquid Scan")
    Label37.Caption = " < 0.74"
    Label38.Caption = ""
    Label39.Caption = ""
    GoTo EndLoop
End If

If IxLiqCor < IxLCor(8) And IxLiqCor > (IxLCor(8)
- IxLCor(8) * 0.006) Then
    Label37.Caption = " 1.42"
    Label38.Caption = " 1.4058"
    Label39.Caption = " 1.4342"
    GoTo EndLoop
End If

If IxLiqCor < (IxLCor(8) - IxLCor(8) * 0.006) Then
    Response = MsgBox("Liquid density is higher
than 1.42 g/cc", vbOKOnly, "Liquid Scan")
    Label37.Caption = " > 1.42"
    Label38.Caption = ""
    Label39.Caption = ""
    GoTo EndLoop
End If

EndLoop:
End Sub

Private Sub Form_Load()
    Combo1.AddItem "70 kV"
    Combo1.AddItem "80 kV"
    Combo1.AddItem "90 kV"
    Combo1.AddItem "100 kV"
    Combo1.AddItem "110 kV"
    Combo1.AddItem "120 kV"
    Combo1.AddItem "130 kV"
    Combo1.AddItem "140 kV"
    Combo1.AddItem "150 kV"
    Combo1.AddItem "160 kV"
    Combo1.AddItem "170 kV"
    Combo1.AddItem "180 kV"
    Combo1.AddItem "190 kV"
    Combo1.AddItem "200 kV"
    Combo3.AddItem "Gasohol 91"
    Combo3.AddItem "Ethanol 20"
    Combo3.AddItem "Ethanol"
    Combo3.AddItem "Cooking oil"
    Combo3.AddItem "Water"
    Combo3.AddItem "Shampoo"
    Combo3.AddItem "Conc. soda"
    Combo3.AddItem "Pure honey"
    ThickNum = 0
    W = 60
    PosX1 = 120
    PosY1 = 230
    PosX2 = 500
    PosY2 = 230
    Text1.Text = PosX1
    Text2.Text = PosY1
    Text3.Text = PosX2
    Text4.Text = PosY2
    XPOS = 315 * Picture1.ScaleWidth \ 2
    YPOS = 230 * Picture1.ScaleHeight \ 2
    Text5.Text = XPOS
    Text6.Text = YPOS
    Label15.Caption = "60 x 60"
    Command2.Enabled = False
End Sub

```

```

Private Sub mnu20x20pixels_Click()
    W = 20
    Label15.Caption = "20 x 20"
End Sub

Private Sub mnu40x04pixels_Click()
    W = 40
    Label15.Caption = "40 x 40"
End Sub

Private Sub mnu60x60pixels_Click()
    W = 60
    Label15.Caption = "60 x 60"
End Sub

Private Sub Image1_Click()
    Picture1.Picture = LoadPicture(SamName(1))
    Label18.Caption = SamName(1)
End Sub

Private Sub Image2_Click()
    Picture1.Picture = LoadPicture(SamName(2))
    Label18.Caption = SamName(2)
End Sub

Private Sub Image3_Click()
    Picture1.Picture = LoadPicture(SamName(3))
    Label18.Caption = SamName(3)
End Sub

Private Sub Image4_Click()
    Picture1.Picture = LoadPicture(SamName(4))
    Label18.Caption = SamName(4)
End Sub

Private Sub Image5_Click()
    Picture1.Picture = LoadPicture(SamName(5))
    Label18.Caption = SamName(5)
End Sub

Private Sub Image6_Click()
    Picture1.Picture = LoadPicture(SamName(6))
    Label18.Caption = SamName(6)
End Sub

Private Sub Image7_Click()
    Picture1.Picture = LoadPicture(SamName(7))
    Label18.Caption = SamName(7)
End Sub

Private Sub Image8_Click()
    Picture1.Picture = LoadPicture(SamName(8))
    Label18.Caption = SamName(8)
End Sub

Private Sub mnuCorrectionData_Click()
    Dim i As Integer
    For i = 1 To 8
        IxLCor(i) = IxL(i) * (IoL(5) / IoL(i))
    Next i
    MsgBox ("Correction completed!!!")
End Sub

Private Sub mnuExit_Click()
    Dim Response As Variant
    Response = MsgBox("Are you sure to terminate ?",
vbOKCancel + vbQuestion, "LScanInSitu")
    If Response = vbOK Then
        End
    End If
End Sub

Private Sub mnuInputData_Click()
    Dim i As Integer
    Dim TargetName As String
    Dim a As Single
    CommonDialog1.ShowOpen
    TargetName = CommonDialog1.FileName

```

```

Open TargetName For Input As #1
    Input #1, KV
    For i = 1 To 8
        Input #1, a
        D(i) = Val(a)
        Input #1, a
        IoL(i) = Val(a)
        Input #1, a
        IxLCor(i) = Val(a)
    Next i
Close #1

MsgBox ("Input data completed!!!")
Command2.Enabled = True
Combo1.Text = "Select kV"
KV = 0

End Sub

Private Sub mnuOpenImage_Click()
Dim SourceName As String

On Error GoTo Err
CommonDialog1.ShowOpen
SourceName = CommonDialog1.FileName
Picture1.Picture = LoadPicture(SourceName)
Label18.Caption = SourceName
KV = 0
Label37.Caption = ""
Label38.Caption = ""
Label39.Caption = ""

Err:
End Sub

Private Sub mnuSaveCorrectedData_Click()
Dim i As Integer
Dim TargetName As String

CommonDialog1.ShowSave
TargetName = CommonDialog1.FileName
Open TargetName For Output As #1
    Write #1, KV
    For i = 1 To 8
        Write #1, D(i), Tab(20); IoL(i), Tab(40);
        IxLCor(i)
    Next i
Close #1
MsgBox ("Save corrected data completed!!!")

End Sub

Private Sub mnuSaveRawData_Click()
Dim i As Integer
Dim TargetName As String

CommonDialog1.ShowSave
TargetName = CommonDialog1.FileName
Open TargetName For Output As #1
    Write #1, KV
    For i = 1 To 8
        Write #1, D(i), Tab(20); IoL(i), Tab(40);
        IxL(i)
    Next i
Close #1
MsgBox ("Save raw data completed!!!")

End Sub

Private Sub Text1_Change()
PosX1 = Val(Text1.Text)

End Sub

Private Sub Text2_Change()
PosY1 = Val(Text2.Text)

End Sub

Private Sub Text3_Change()
PosX2 = Val(Text3.Text)

End Sub

Private Sub Text4_Change()
PosY2 = Val(Text4.Text)

End Sub

```

```

Private Sub Text5_Change()
XPOS = Val(Text5.Text)
End Sub

Private Sub Text6_Change()
YPOS = Val(Text6.Text)
End Sub

Private Sub VScroll1_Change()
Dim i As Integer

i = VScroll1.Value

Picture1.Picture = LoadPicture(SamName(i))
Label18.Caption = SamName(i)
Label36.Caption = i
Call ScanImage
IxL(i) = IxLiq
IoL(i) = IoLiq

End Sub
Sub ScanImage()
Dim i As Integer
Dim j As Integer
Dim Sum1 As Single
Dim Sum2 As Single
Dim Sum3 As Single
Dim DenIo1 As Single
Dim DenIo2 As Single
Dim STD As Single
Dim SNR As Single
Dim Response As Variant

Picture1.Cls

Picture1.Line (XPOS, YPOS)-(XPOS + W, YPOS
+ W), QBColor(13), B
Sum1 = 0
For i = XPOS + 1 To XPOS + W - 1
For j = YPOS + 1 To YPOS + W - 1
Sum1 = Sum1 + Picture1.Point(i, j) Mod 256
Next j
Next i
IxLiq = Sum1 / ((W - 1) * (W - 1))
Label10.Caption = IxLiq ' Ix(avg)

Picture1.Line (PosX1, PosY1)-(PosX1 + W,
PosY1 + W), QBColor(13), B
Sum2 = 0
For i =PosX1 + 1 To PosX1 + W - 1
For j = PosY1 + 1 To PosY1 + W - 1
Sum2 = Sum2 + Picture1.Point(i, j) Mod 256
Next j
Next i
DenIo1 = Sum2 / ((W - 1) * (W - 1))

Picture1.Line (PosX2, PosY2)-(PosX2 + W,
PosY2 + W), QBColor(13), B
Sum3 = 0
For i = PosX2 + 1 To PosX2 + W - 1
For j = PosY2 + 1 To PosY2 + W - 1
Sum3 = Sum3 + Picture1.Point(i, j) Mod 256
Next j
Next i
DenIo2 = Sum3 / ((W - 1) * (W - 1))

IoLiq = (DenIo1 + DenIo2) / 2
Label6.Caption = IoLiq

EndLoop:
End Sub

```

APPENDIX D

Summary Raw Data for In-Situ Calibration at 140 kVp (LScanInsitu)

Raw Data: 4.5 cm, 140 kVp

0		
.7422,	141.4674,	95.21314
.7502,	141.6045,	94.85909
.7828,	142.9077,	93.46076
.8989,	144.6411,	90.75149
1,	144.57,	84.94946
1.0205,	143.989,	80.1088
1.3171,	145.8268,	73.98306
1.4238,	147.0987,	73.61058

Corrected Raw Data: 4.5 cm, 140 kVp

0		
.7422,	141.4674,	97.30129
.7502,	141.6045,	96.84566
.7828,	142.9077,	94.5479
.8989,	144.6411,	90.70691
1,	144.57,	84.94946
1.0205,	143.989,	80.43205
1.3171,	145.8268,	73.34542
1.4238,	147.0987,	72.34518

Raw Data: 6.0 cm, 140 kVp

0		
.7422,	147.8469,	97.05827
.7502,	147.3991,	93.88823
.7828,	148.9453,	94.34216
.8989,	148.2775,	91.63169
1,	149.0774,	82.8368
1.0205,	150.2886,	77.01992
1.3171,	148.3249,	68.0116
1.4238,	149.7039,	62.45927

Corrected Raw Data: 6.0 cm, 140 kVp

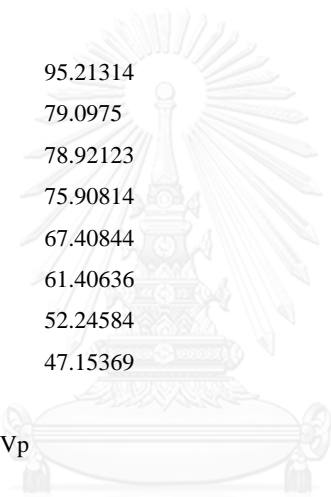
0		
.7422,	147.8469,	97.86608
.7502,	147.3991,	94.95729
.7828,	148.9453,	94.42584
.8989,	148.2775,	92.12604
1,	149.0774,	82.8368
1.0205,	150.2886,	76.39921
1.3171,	148.3249,	68.35665
1.4238,	149.7039,	62.1979

Raw Data: 7.5 cm, 140 kVp

0		
.7422,	147.8469,	95.21314
.7502,	147.6885,	79.0975
.7828,	148.9828,	78.92123
.8989,	149.6474,	75.90814
1,	150.3133,	67.40844
1.0205,	149.9747,	61.40636
1.3171,	147.5507,	52.24584
1.4238,	147.8688,	47.15369

Corrected Raw Data: 7.5 cm, 140 kVp

0		
.7422,	147.8469,	96.80152
.7502,	147.6885,	80.5033
.7828,	148.9828,	79.62608
.8989,	149.6474,	76.2459
1,	150.3133,	67.40844
1.0205,	149.9747,	61.54499
1.3171,	147.5507,	53.22405
1.4238,	147.8688,	47.93323



จุฬาลงกรณ์มหาวิทยาลัย
CHULALONGKORN UNIVERSITY

APPENDIX E

Step-by-Step Tutorial on How to Use the In-Situ Measurement Software

Step 1: Calibration

- i) Select type of liquid at the “Liquid Density” option.
- ii) Select the image file of type of liquid used for calibration (e.g. liquids in Table3.2).
- iii) Repeat (ii) until all of the images used for calibration are selected.

Step 2: Data Management

- i) Select “Data Management”.
- ii) Select “Save raw data” and rename file (e.g. Raw Data).
- iii) Select “Data Correction”.
- iv) Select “Correction Data”.
- v) Select “Save corrected data” and rename the file with a different name (e.g. Corrected Raw Data).
- vi) Select “Input Data” and open the file saved in part (v).

Step 3: Testing/Inspection

- i) Select “File” and open the image of the radiographed liquid to be tested/inspected (e.g. Unknown A).
- ii) Select “Scanning”.
- iii) Select “Analysis”.

APPENDIX F

Corrected greyscale of different liquid at thickness 4.5, 6.0 and 7.5 cm (LScan2015)

Table F1 Greyscale values of different types of liquid at thickness 4.5 cm

Type of Liquid	X-ray Energy, kVp													
	70	80	90	100	110	120	130	140	150	160	170	180	190	200
Gasohol 91	56.1152	62.0254	74.4601	85.1018	94.7167	99.4373	105.7119	113.0134	118.6862	124.0151	129.5031	135.6170	139.2144	144.2355
Ethanol 20	56.0281	61.7397	73.9772	84.5164	94.1843	98.9019	104.6723	112.6243	118.0404	122.8270	128.9320	134.8187	138.7633	143.7526
Ethanol	54.3584	59.9423	72.2464	82.0501	92.2338	98.1976	103.8321	110.2359	115.4417	121.2401	126.2914	132.0174	133.7054	141.3603
Cooking Oil	51.4739	57.0060	68.8587	78.5764	88.3045	94.3697	100.0324	106.2220	111.3190	116.6598	122.0802	128.4357	131.2523	136.8436
Water	45.8734	50.4938	62.0464	71.4724	80.0586	86.7872	91.8389	98.0271	103.0904	108.3537	113.6888	119.5440	122.7334	127.8404
Shampoo	42.8240	48.0798	58.5397	67.4150	76.5914	82.4691	88.0075	93.6152	98.4366	103.7347	109.4583	114.6266	117.4250	122.8953
Concentrated Soda	38.9509	43.5320	53.2290	62.0201	70.5136	75.7664	81.2487	86.6317	91.4121	96.5146	100.5544	106.7600	109.0654	114.4079
Pure Honey	37.7475	42.6681	51.7915	60.2839	69.1071	73.9069	79.8875	84.5143	89.4016	94.0905	99.0806	104.2633	107.1914	112.4352

Table F2 Greyscale values of different types of liquid at thickness 6.0 cm

Type of Liquid	X-ray Energy, kVp													
	70	80	90	100	110	120	130	140	150	160	170	180	190	200
Gasohol 91	51.9712	58.3288	68.0216	73.7568	86.5773	93.2920	98.3019	103.5710	108.6456	112.6457	118.5767	124.0732	126.6422	130.7125
Ethanol 20	50.7071	57.1454	66.7583	73.0322	84.4572	91.4293	95.6839	101.8920	106.6492	110.6394	116.5479	121.8458	124.7674	129.1742
Ethanol	49.2009	55.2513	64.6245	70.1397	81.7582	88.9784	93.5681	97.7569	103.5743	107.9585	113.1404	118.6081	120.8725	123.5301
Cooking Oil	47.4420	53.9407	63.4493	68.0934	79.2610	85.5006	90.8308	96.6541	101.5667	105.6531	110.9155	115.8651	118.5798	121.2999
Water	39.4857	44.9394	52.4153	56.8885	68.5080	74.8740	79.1195	84.8044	88.8294	92.2423	97.9611	102.8639	104.9385	108.3790
Shampoo	37.8147	42.9049	51.7437	55.4714	65.4533	70.8278	74.1455	80.7930	85.0384	90.4777	94.7990	99.6981	102.2453	105.5383
Concentrated Soda	32.8898	37.7210	45.5964	48.3313	57.0911	62.0302	67.3362	72.9029	75.0447	80.3311	83.7641	88.2262	91.1443	93.3882
Pure Honey	30.8388	35.9350	43.3712	44.9406	53.2579	57.7180	63.3159	67.5928	71.5135	75.6534	80.6100	84.3725	87.0041	89.4922

Table F3 Greyscale values of different types of liquid at thickness 7.5 cm

Type of Liquid	X-ray Energy, kVp													
	70	80	90	100	110	120	130	140	150	160	170	180	190	200
Gasohol 91	42.0946	47.1900	55.9551	62.0728	70.7119	75.9486	81.9482	87.1897	91.7818	97.1109	101.1479	106.4800	110.2825	113.8804
Ethanol 20	40.9998	45.8049	55.0079	60.7437	69.1277	74.2380	80.3285	85.2967	90.2233	95.4040	98.4296	106.3264	108.4139	112.0391
Ethanol	39.9310	44.4872	53.4573	59.1562	67.0519	71.9214	77.8528	83.3552	87.6266	92.7931	96.6424	102.8749	105.1857	109.4480
Cooking Oil	36.3507	40.8443	48.9882	54.0227	61.4384	65.5425	72.3220	77.2106	81.8865	87.0132	90.0923	96.2821	99.5483	102.6933
Water	30.0702	34.3972	41.7601	46.1320	53.4349	56.8151	62.5476	67.7450	72.2863	76.4147	79.0181	85.8053	86.7803	89.6302
Shampoo	26.6028	31.1209	38.0096	42.4196	48.5726	51.9756	56.9519	63.0545	67.6479	70.8845	75.0020	80.2556	82.0036	85.0659
Concentrated Soda	22.4638	26.4426	31.6622	35.5396	41.0118	43.6965	48.4157	52.8207	56.9598	60.7106	63.7342	68.6324	69.9639	73.3248
Pure Honey	21.1967	25.0876	30.2761	33.7117	39.1152	41.2022	45.7471	50.2049	53.6950	57.3221	60.5772	65.3584	66.5746	69.0720

APPENDIX G

Estimation of Standard Deviation and the Percentage Error of the System

The estimation of standard deviation and the percentage error was calculated from the equations below. This is required to set the range of the estimation of error on the density read out by the system. The testing was done with water at X-ray energies of 70 kVp and 200 kVp. The results are tabulated in Table G.

$$\sigma = \sqrt{\frac{\sum(x_i - \bar{x})^2}{n}} \quad (\text{Equation 1})$$

where,

σ = Standard deviation

x_i = Individual transmitted intensity/greyscale

\bar{x} = Mean of transmitted intensity/greyscale

n = Number of samples tested

$$\text{Percentage error (\%)} = \frac{\sigma}{\bar{x}} \times 100 \quad (\text{Equation 2})$$

Table G Calculated standard deviation for estimation of percentage error

Thickness, cm	X-ray energy, kVp	Mean, \bar{x}	$\sum(x_i - \bar{x})^2$	Standard deviation, σ	Percentage error, %
4.5	70	45.1982	0.7954	0.3153	0.6976
	200	107.1514	0.7655	0.3093	0.2887
6.5	70	37.6838	0.7798	0.3122	0.8285
	200	111.0513	4.4231	0.7436	0.6696
7.0	70	31.1309	3.8397	0.6928	2.2254
	200	93.5981	4.4231	0.7436	0.6696

APPENDIX H

Comparison of the Calibrated Data between LScan2015 and LScanInsitu

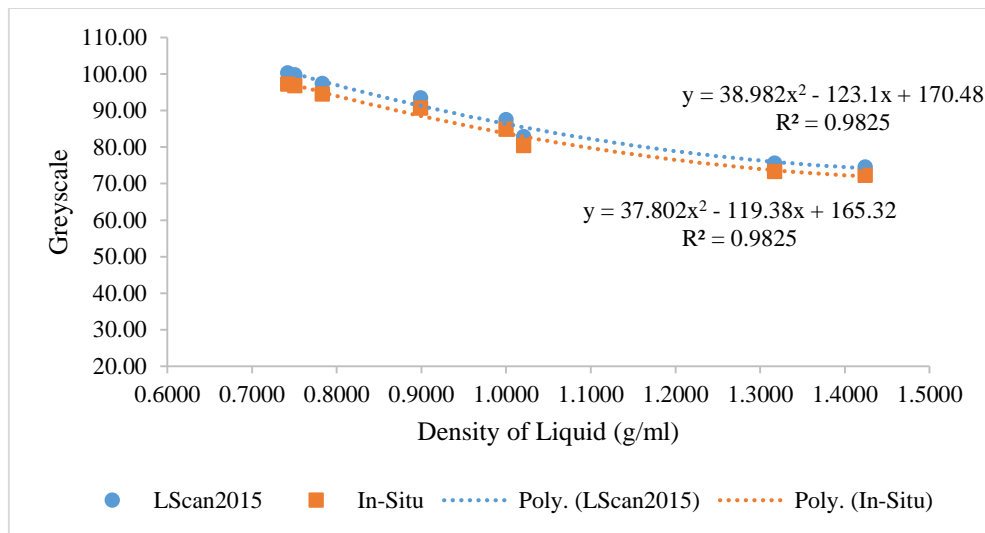


Figure H1 Graph of greyscale versus density of liquid obtained for liquid thickness 4.5 cm at 140 kVp

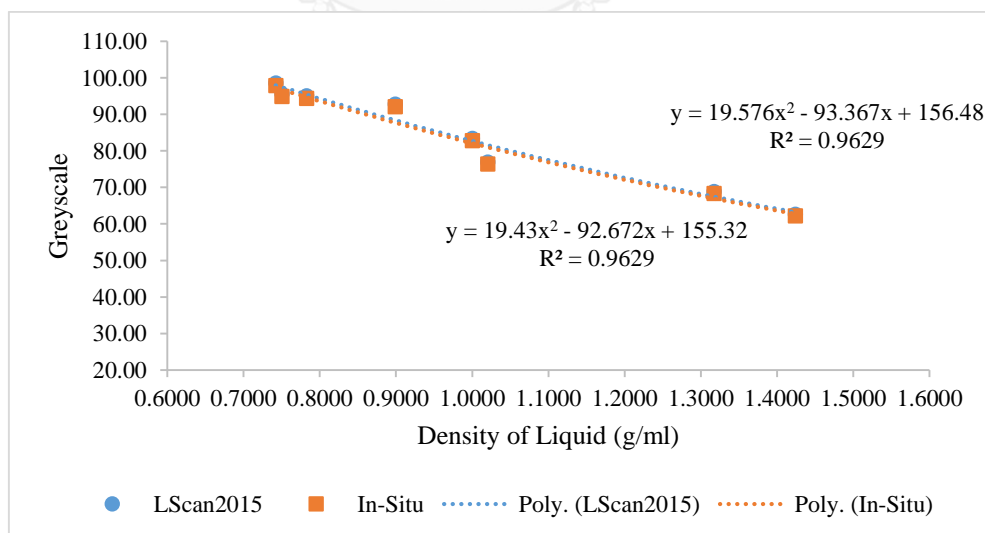


Figure H2 Graph of greyscale versus density of liquid obtained for liquid thickness 6.0 cm at 140 kVp

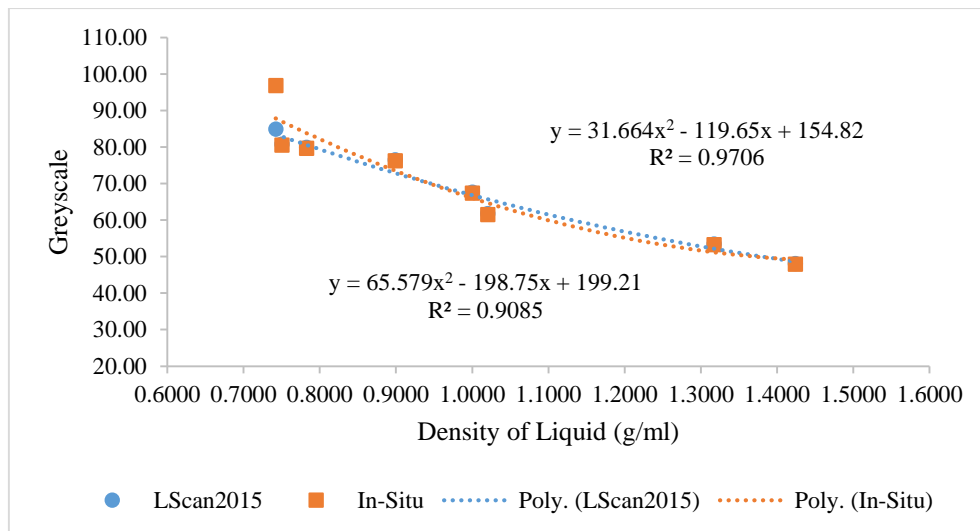


Figure H3 Graph of greyscale versus density of liquid obtained for liquid thickness 7.5 cm at 140 kVp

VITA

Miss Nurhani binti Sulaiman was born on April 1, 1991 in Kuala Lumpur, Malaysia. After completing secondary school in 2008, Nurhani went on to The University of Malaya for her foundation studies in Physics in 2009. She then entered The National University of Malaysia in Selangor, Malaysia in 2010 where she studied for her Bachelor's Degree and received a Bachelor of Science (Hons) in Nuclear Science in October 2013. During the following two years, she further extent her knowledge by pursuing her studies in Master of Science Programme in Nuclear Technology majoring in Nuclear Security and Safeguards at Chulalongkorn University, Thailand.



